SP-1259

ESA's Report to the 34th COSPAR Meeting

Houston, USA
October 2002

European Space Agency
Agence spatiale européenne

SP-1259
August 2002

ESA's Report to the 34th COSPAR Meeting

Houston, USA
October 2002

European Space Agency
Agence spatiale européenne

Contributors

This report on the scientific missions of the European Space Agency was written by:

P. Benvenuti
A. Chicarro
P. Escoubet
F. Favata
M. Fehringer
B. Fleck
B. Foing
M. Fridlund
A. Gimenez
R. Grard
Y. Jafry
F. Jansen
P. Jakobsen
O. Jennrich
J.P. Lebreton
R. Marsden
L. Metcalfe
A. Parmar
M. Perryman
G. Pilbratt
R. Reinhard
J. Romstedt
T. Sanderson
G. Schwehm
J. Tauber
C. Winkler

The authors acknowledge the use of published and unpublished material supplied by experimenters, observers and colleagues.

The report was completed on 15 July 2002.

Communications should be addressed to the scientific editor:

Dr B. Foing
ESA Research and Scientific Support Department
European Space Research and Technology Centre (ESTEC)
Postbus 299
NL-2200 AG Noordwijk
The Netherlands
Telephone: +31 71 565-5647
E-mail: Bernard.Foing@esa.int

Cover:
The Infrared Space Observatory (ISO) found abundant carbonates in the Red Spider Nebula, which is seen in this Hubble Space Telescope image, and which harbours one of the hottest stars in the Universe. The discovery of large quantities of carbonates in two planetary nebulae questioned the traditional assumption that the presence of carbonates was an indicator of the previous action of liquid water. The discovery, which was also the first detection of carbonates outside the Solar System, re-opened questions about the presence of liquid water in the early Solar System. (ESA / G. Mellema, Leiden Univ.)

Edited by: A. Wilson
Production by: I. Kenny
Printed in The Netherlands
Published and distributed by: ESA Publications Division
ESTEC, Noordwijk, The Netherlands

ISBN 92-9092-636-8
ISSN 0379-6566
Price: €40

Contents

1. Introduction

Table 1.1. ESRO/ESA scientific spacecraft.

	Launch date	*End of operational life*	*Mission*
Launched			
ESRO-II	17 May 1968	9 May 1971	Cosmic rays, solar X-rays
ESRO-IA	3 October 1968	26 June 1970	Auroral and polar-cap phenomena, ionosphere
HEOS-1	5 December 1968	28 October 1975	Interplanetary medium, bow shock
ESRO-IB	1 October 1969	23 November 1969	As ESRO-IA
HEOS-2	31 January 1972	2 August 1974	Polar magnetosphere, interplanetary medium
TD-1	12 March 1972	4 May 1974	Astronomy (UV, X- and γ-ray)
ESRO-IV	26 November 1972	15 April 1974	Neutral atmosphere, ionosphere, auroral particles
Cos-B	9 August 1975	25 April 1982	Gamma-ray astronomy
Geos-1	20 April 1977	23 June 1978	Dynamics of the magnetosphere
ISEE-2	22 October 1977	26 September 1987	Sun/Earth relations and magnetosphere
IUE	26 January 1978	30 September 1996	Ultraviolet astronomy
Geos-2	24 July 1978	October 1985	Magnetospheric fields, waves and particles
Exosat	26 May 1983	9 April 1986	X-ray astronomy
FSLP	28 November 1983	8 December 1983	Multi-disciplinary
Giotto	2 July 1985	23 July 1992	Comet Halley and Comet Grigg Skjellerup encounters
Hipparcos	8 August 1989	15 August 1993	Astrometry
Hubble Space Telescope	24 April 1990		UV/optical/near-IR astronomy
Ulysses	6 October 1990	30 September 2004	Heliosphere
Eureca	31 July 1992	24 June 1993	Multi-disciplinary
ISO	17 November 1995	8 April 1998	Infrared astronomy
SOHO	2 December 1995	March 2007	Sun (including interior) and heliosphere
Huygens/Cassini	15 October 1997		Titan probe/Saturn orbiter
XMM-Newton	10 December 1999	March 2006	X-ray spectroscopy
Cluster	16 July/9 August 2000	December 2005	3D space plasma investigation
Planned launches			
Integral	October 2002		Gamma-ray astronomy
SMART-1	March 2003		Navigation with solar-electric propulsion
Rosetta	January 2003		Comet rendezvous
Mars Express	May 2003		Mars exploration
Venus Express	November 2005		Venus exploration
STEP	2005		Test of Equivalence Principle
SMART-2	2006		LISA Technology Package
Planck	2007		Cosmic microwave background
Herschel	2007		Far-infrared and submillimetre astronomy
Eddington	2007-2008		Search for extra-solar planets
NGST	2010		Next Generation Space Telescope
LISA	2011		Search for gravitational waves
BepiColombo	2011-2012		Mission to Mercury
Solar Orbiter	2011-2012		Sun (inc. polar regions) and inner heliosphere
GAIA	≤ 2012		Galaxy mapper

1. Introduction

This report to the 34th COSPAR Meeting covers the missions of the Scientific Programme of ESA in the areas of astronomy, Solar System exploration and fundamental physics. In addition, the meeting coincides with the planned launch of the Integral mission from Baikonour Cosmodrome. Integral is a large high-energy observatory that will provide images and spectra of astrophysical sources in the gamma-ray domain of unprecedented sensitivity and resolution. Then, in rapid succession, ESA will launch three more missions to explore our Solar System: Rosetta, SMART-1 and Mars Express.

In January, Rosetta will depart from Kourou on an Ariane-5 towards a rendezvous with a comet after visiting several asteroids. Following the cometary orbital phase, a lander will perform *in situ* investigations of the nucleus. The first Small Mission for Advanced Research in Technology, SMART-1, is a technology mission to demonstrate navigation through the Solar System using electric propulsion. Its trajectory, leading to a lunar orbit, will also permit new observations of our only natural satellite. Finally, by the middle of next year, Mars Express, based on Rosetta heritage, will be launched to become the first European mission to orbit Mars and to land on its surface. Such a suite of challenging missions launched within 6 months of the meeting in Houston illustrates the high level of activity by ESA's Scientific Programme.

In the meantime, missions in orbit have continued to provide excellent scientific results. XMM-Newton, launched in 1999, is providing a new view of our Universe at X-ray energies thanks to its large photon-collecting capability and throughput. After a phase of commissioning, verification and calibration, XMM-Newton entered a successful phase of routine scientific operations as an observatory. At lower energies, the Hubble Space Telescope continues to generate exciting results even in areas that were unimagined during its design, e.g. the study of extra-solar planets. Recently, the last servicing mission to HST brought back to Earth the European Faint Object Camera after it was replaced by a state-of-the-art instrument, the Advanced Camera for Survey. The NICMOS infrared camera was improved by the addition of a cooling system, allowing it to deliver the original science and beyond.

In the Solar System area, the space infrastructure for the Solar-Terrestrial Science Programme (STSP) was completed with the launch in summer 2000 of the four Cluster spacecraft that replaced the original mission. The 3-D results obtained so far have given important physical information for understanding the magnetosphere and the connection between the behaviour of plasma and the Sun. To this end, the extension of the operations of the successful SOHO observatory, studying the Sun in great detail, have been very useful. SOHO continues its sophisticated and comprehensive surveillance of the Sun's interior and outer atmosphere, as well as the solar wind. For exploring the heliosphere beyond the ecliptic, the Ulysses mission has continued its journey over the polar regions of the Sun. A second passage over the northern polar region was completed at the end of 2001, this time during a solar maximum, which allows comparison with the previous passage at a minimum. The spacecraft is now heading back towards the ecliptic, which it will cross relatively close to the orbit of Jupiter in 2004. Cassini/Huygens continues its journey towards Saturn, after visiting Jupiter. After arrival at the planet in 2004, ESA's Huygens probe will be released into the atmosphere of Titan to investigate its physical nature and conditions that are expected to provide important information for understanding the early evolution of Earth's atmosphere.

Meanwhile, work continues on missions that have entered their post-operational phase, after switch-off of the spacecraft, aimed at obtaining a full homogeneous recalibration of the observations and the delivery of a final archive to the scientific

community. In the case of the IUE ultraviolet explorer, the final archive was delivered some time ago and handed over to national organisations. For the ISO infrared observatory, we are now within the active archive phase, increasing the quality and accessibility of the data by improving the previous global pipeline analyses that populated the existing archive.

Concerning missions under development, the main activity now concentrates on preparing for two astronomy missions: Planck, to investigate the fine spatial variation of the cosmic background radiation, and Herschel, as a powerful far-IR and sub-millimetre observatory. They will be launched together in 2007 and delivered to the L2 Lagrangian point on the Earth-Sun line for their operational phases.

Missions are now also in their study or definition phases. Some are planned for launches between 2010 and 2012, such as the European contribution to the Next Generation Space Telescope, the LISA gravitational waves observatory, the Bepi-Colombo mission to Mercury, and the GAIA mission to produce an unprecedented high-quality 3-D map of our Galaxy's stars. Beyond that, missions such as Darwin, to characterise extra-solar planets, and XEUS, a very large X-ray observatory deployed using the International Space Station, are under study. There have been some additions during recent updates of the programme for missions with launches before 2010. SMART-2 will test the technologies for LISA and, if possible, also those for Darwin, Venus Express or Eddington (stellar oscillations and search for Earth-like planets). Details on all these missions are given in this report.

The main task of the Science Directorate recently has been to maintain a comprehensive space science programme in ESA, preserving the flexibility to incorporate new missions in a short timeframe, even under the pressure of reduced overall budgets. The long-term planning of the programme has proved to be robust and adaptable to new challenges and uncertainties. But, after the Ministerial Conference in Edinburgh (UK) in November 2001, when the proposed expansion of the programme was not confirmed, a full revision of our approach was necessary.

The challenge then was to maintain as much as possible of the missions demanded by European scientists while keeping to a realistic budget within the approved boundaries. Avoiding the temptation to concentrate all efforts on the Cornerstone missions, the aim was to keep an average launch rate close to one mission per year. Mission extensions were, of course, favoured to maximise the scientific return per investment. The reuse of standard platforms was necessary, as well as the need to procure smarter, more system-integrated spacecraft. International cooperation was also maintained and fostered whenever possible. Finally, the concept of 'production groups' was introduced: not only are the platforms reused but also the engineering teams, budget and schedule are tailored for optimimum use of all the available resources for a given group of missions. Thus Eddington is now grouped with the already-paired Herschel and Planck, and Venus Express is included with Mars Express and Rosetta.

Given the changes introduced to the long-term plan of ESA's Scientific Programme – the missions themselves but mainly the way of working – the former 'Horizons 2000' has been replaced by the new global name of 'Cosmic Vision'.

2. Current and Completed Missions

2.1 Hubble Space Telescope

Introduction

The Hubble Space Telescope (HST) was rejuvenated in early 2002 by a highly successful refurbishing mission, which saw the installation of the new Advanced Camera for Surveys (ACS) and the return to scientific operations of the telescope's only existing IR capability, the Near-IR Camera and Multi-Object Spectrometer (NICMOS). ACS belongs to the third-generation of instruments aboard HST. It has three independent cameras to provide wide-field, high-resolution and UV imaging, respectively, with a broad assortment of filters designed to address a large range of scientific goals. Additional coronographic, polarimetric and grism capabilities make ACS a versatile and powerful instrument.

NICMOS was installed in 1997, but a technical problem halted its use at the beginning of 1999. Dormant since then, NICMOS has been brought back to life with the installation of a mechanical cryocooler to maintain its detectors at the low temperature required for IR operations.

ACS has obtained the first Early Release Observations (EROs), a set of astronomical images designed to show that it is performing as expected. Indeed, the images confirm that the combination of detector area and quantum efficiency provides a factor ten improvement over the previous HST optical imaging capabilities. They provide a spectacular preview of the scientific potential of ACS.

The 2002 servicing mission also took care of a number of subsystems. New solar arrays were installed, power conditioning units were replaced, a reaction wheel was exchanged and multi-layer insulating material was repaired.

Science achievements

During the past year, the Hubble Space Telescope (HST) has continued to be a leading observatory in the exploration of the universe. Observations with HST have impacted every area of current astronomical research. A few highlights of the results obtained during the year 2001 are presented here.

Solar System

Observations with HST and the Mars Global Surveyor (MGS) have revealed the biggest global dust storm seen on Mars in several decades (Figure 2.1.1). While HST does not provide continuous Mars coverage, it captured the whole planet in a single snapshot, showing the full range of dust activity from sunrise to sunset. The combined observations show the storm to be the result of a planet-wide series of events that was triggered in and around the Hellas Basin and propagated rapidly across the equator. These extreme climate events provide important clues on how climate changes operate on Mars.

In another collaborative effort, HST and the Deep Space-1 (DS1) spacecraft provided invaluable information on the short-period comet 19P/Borrelly. In particular, DS1 confirmed the size of the nucleus previously determined by HST to be 8x4 km, with approximately 8% of the surface area being active. This is extremely important in proving HST's ability to measure the sizes and shapes of cometary nuclei. In addition, HST observations one day before and one day after the DS1 flyby suggest that the gas around the comet had a highly asymmetric distribution, similar to that of the dust.

The intriguing lives of stars

HST continued to provide fascinating details about the lives of stars, from birth to death, and their effects on the interstellar environment. Images of the inner region of 30 Doradus show 'second generation' star formation – the intense stellar winds from the cluster R136 are compressing neighbouring gas and dust and triggering star formation 10-15 pc from the cluster. The dense regions that are shielded from radiation

For further information, see http://ecf.hq.eso.org/

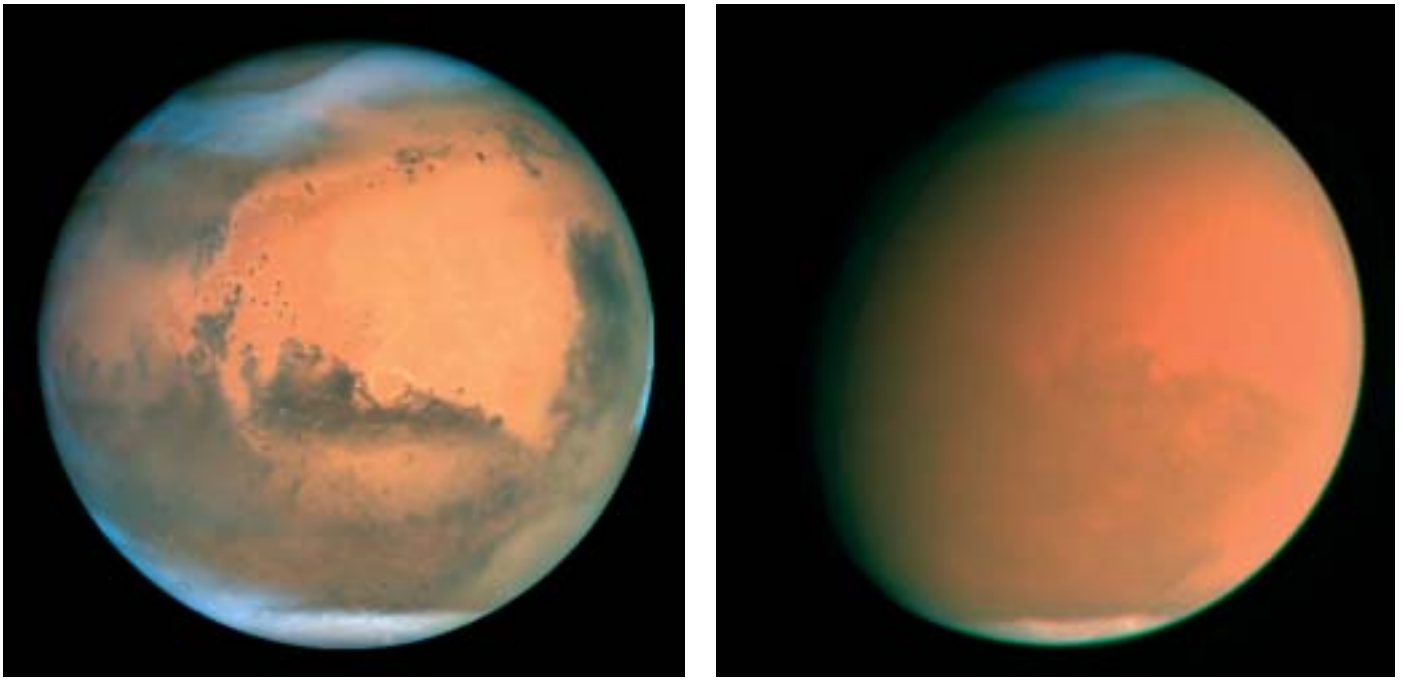

Figure 2.1.1. Observations with HST revealed the biggest global dust storm seen on Mars in several decades. While HST does not provide continuous Mars coverage, it captured the whole planet in a single snapshot, showing the full range of dust activity from sunrise to sunset. Left: 26 June 2001; right: 4 September 2001. WFPC2. J. Bell (Cornell Univ.), M. Wolff (Space Science Inst.) and the Hubble Heritage Team (STScI/AURA).

and winds remain as awe-inspiring pillars, similar to those in the Eagle Nebula. HST has shown that in many star-forming regions there are dust pillars pointing toward massive stars or star clusters. The powerful winds and radiation from the stars erode much of the dust and molecular gas, leaving only the densest regions as narrow pillars.

HST also provided an incredibly detailed image of the evolution of the remains of a famous stellar death: Cassiopeia-A, which is the youngest known Galactic supernova remnant. The spatially-resolved composition of the ejecta (oxygen-burning products in high-velocity ejecta, slower He- and N-rich clumps, and N-rich high-velocity outer ejecta) suggest that the progenitor Wolf-Rayet star experienced substantial mass loss before exploding. HST was able to resolve knots on a scale of $1\text{-}2\text{x}10^{16}$ cm. The morphology of some finger-like ejecta structures and the detection of high-velocity shears (~1000 km/s) suggest the operation of Rayleigh-Taylor instabilities where the reverse shock front encounters the clumped ejecta.

Clusters

HST detected an event that may be the first gravitational microlensing event through a globular cluster. Using the Wide-Field Planetary Camera WFPC2, three fields of bulge stars were observed through the globular cluster M22. Since the distances and the kinematics of the lenses and sources are known, the masses of the lenses could be determined directly. The mass of the potential lens detected is 0.13 $M_{\odot}$. A 30-day modulation shows that the source is a binary system. This observation (if the nature of the event is fully confirmed) shows that microlensing offers the opportunity to determine the mass function of the globular cluster down to planetary masses.

HST has also considerably advanced the study of young clusters. The combination of high resolution and sensitivity is allowing astronomers for the first time to perform an accurate census of the stellar members and investigate in detail the stellar population content.

Figure 2.1.2. HST Observations of the double cluster NGC 1850, an unusual double cluster in the bar of the Large Magellanic Cloud, a satellite galaxy of our own Milky Way. The two components of the cluster are both relatively young and consist of a main, globular-like cluster in the centre and an even younger, smaller cluster, seen below and to the right, composed of extremely hot, blue stars and fainter red T-Tauri stars. The main cluster is about 50 Myr old; the smaller cluster is only 4 Myr old. (M. Romaniello, ESO, Germany).

NGC 1850, imaged with WFPC2 (Figure 2.1.2), is an unusual double cluster in the bar of the Large Magellanic Cloud (LMC). After the 30 Doradus complex, it is the brightest star cluster in the LMC, and is representative of a special class of objects, young, globular-like star clusters, that have no counterpart in our Galaxy.

NGC 1850 splits into NGC 1850A (centre of Figure 2.1.2) and NGC 1850B (lower right), which are both young (50 and 4 Gyr, respectively), but are quite distinct in stellar mass and spatial distribution. Supernova explosions of NGC 1850A massive stars appear to have triggered star formation in the younger NGC 1850B. This latter contains several hundreds of Sun-type stars in such an early evolutionary stage that they still display their original gaseous cocoons.

The ability to resolve clusters into individual stars allows for an accurate determination of their Initial Mass Function (IMF) and the study of the cluster formation mechanism. The IMF was derived for NGC 330, the richest young star cluster in the Small Magellanic Cloud, from deep broadband V and I images obtained with WFPC2. Stars were individually counted and the IMF determined, down to a stellar mass of 0.8 $M_{\odot}$, as a function of radial distance from the centre. For this cluster, the HST observations showed that the IMF becomes steeper at increasing distances from the cluster centre, with the number of massive stars (>5 $M_{\odot}$)

Figure 2.1.3. HST observations of the galaxy group Stephan's Quintet. Most of the star clusters visible in the image were formed in the tidal tail of NGC 7319 and in the tidal debris of the interacting pair NGC 7318B/A (S. Gallagher, Pennsylvania State University, et al.).

decreasing from the core to the outskirts of the cluster five times more rapidly than the lighter objects. This phenomenon is called mass segregation, and it is usually of dynamical origin. For NGC 330, given that the age of the cluster is ten times shorter than the expected relaxation time, the observed mass segregation is likely to be of primordial nature. This is one of the first instances in which primordial mass segregation is directly observed in a young cluster.

Galaxies

HST performed the equivalent of an anatomical dissection of starburst galaxies NGC 1512 and NGC 5248. The data (taken with FOC, WFPC2 and NICMOS) provide a very wide wavelength coverage (from 2300 Å to 1.87 µm), and are particularly well suited for the study of stellar populations.

The ages of a few hundred clusters identified in each galaxy are consistent with continuous star formation in the circumnuclear rings over the past 300 Myr, and the cluster mass functions were found to follow a power law distribution similar to that in the Antennae galaxies. This may indicate that the anatomy of all starbursts is

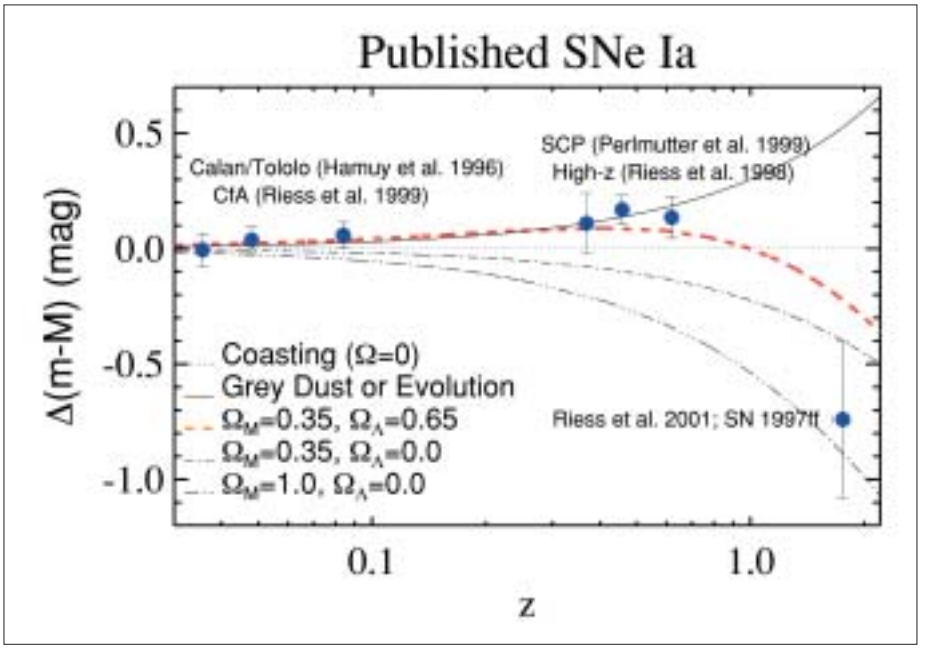

Figure 2.1.4. SN 1997ff was discovered by a re-observation of the Hubble Deep Field. The host of the SN is an elliptical galaxy, implying that SN 1997ff very probably is an SN Ia. The redshift was determined to be 1.7. SN 1997ff supports an accelerating Universe (A. Riess, STSci, et al.)

similar. In addition, the UV emitted by young clusters and the line-emitting gas were found to have different spatial distributions. This indicates that any census of star formation that is based only on total UV light or on total line emission (as often done for distant starbursts) gives an incomplete count.

HST uncovered spectacular details in the galaxy group Stephan's Quintet (Figure 2.1.3). In particular, 115 star clusters were identified, as well as 13 dwarf galaxies. Most of these clusters formed in the tidal tail of NGC 7319 and in the tidal debris of the interacting pair NGC 7318B/A. The observations suggest that there were several epochs of star formation, on timescales ranging from 2 Myr to 500 Myr, and that both star clusters and dwarf galaxies can form in tidal debris.

HST also observed the first case of a quasar lensed by an almost face-on spiral galaxy. Optical and near-IR HST and Gemini-North adaptive optics images, further improved through deconvolution, were used to explore the gravitationally lensed radio source PKS 1830-211. The line of sight to the quasar at $z = 2.507$ appears to show the presence, within 0.5 arcsec from the source, of a possible galactic main-sequence star, a faint red lensing galaxy visible only in H-band and a new object whose colours and morphology match those of an almost face-on spiral. The V-I colour and faint I magnitude of the latter suggest that it is associated with the molecular absorber seen towards PKS 1830-211, at $z = 0.89$ rather than with the $z = 0.19$ HI absorber previously reported in the spectrum of PKS 1830-211.

Cosmology

HST made a dramatic contribution to cosmology by discovering the most distant supernova ever observed. Since 1998, observations of Type Ia supernovae (SNe Ia) suggested that the expansion of the Universe is accelerating, propelled by some form of 'dark energy'. This interpretation was based on the fact that SNe Ia at redshifts $z \sim 0.5$ were found to be dimmer than expected by ~0.3 magnitudes. However, in order to accept this interpretation, we must exclude alternative explanations – that

SNe Ia at high redshifts could be dimmer as a result of pervasive grey dust, or because of evolutionary effects.

SN 1997ff was discovered by a re-observation of the Hubble Deep Field. Serendipitously, the same field was observed by the NICMOS Guaranteed Time Observation team within hours of the SN discovery, and again 25 days later. The host of the SN is an elliptical galaxy, implying that SN 1997ff very probably is an SN Ia. The redshift has been determined to be $z \sim 1.7$.

The key finding was that the SN appears brighter than expected! The brightness is consistent with the SN being in the decelerating phase in a cosmology with $\Omega_M \sim 0.35$ and $\Omega_L \sim 0.65$ (Figure 2.1.4). More importantly, the observations are inconsistent with models in which a monotonic behaviour of dimming by dust or luminosity evolution are assumed. Consequently, SN 1997ff supports an accelerating Universe.

2.2 Ulysses

Introduction

Ulysses is an exploratory mission being carried out jointly by ESA and NASA. Its primary objective is to characterise the uncharted high-latitude regions of the heliosphere within 5 AU of the Sun, under a wide range of solar activity conditions. Ulysses has, for the first time, permitted *in situ* measurements to be made away from the plane of the ecliptic and over the poles of the Sun (Figure 2.2.1). Its unique trajectory (Figure 2.2.2) has taken the spacecraft into the unexplored third dimension of the heliosphere.

The European contribution to the Ulysses programme consists of the provision and operation of the spacecraft and about half of the instruments. NASA provided the launch aboard the Space Shuttle (plus the kick-stage) and the spacecraft power generator, and is responsible for the remaining instruments. NASA also supports the mission using its Deep Space Network (DSN).

The broad range of phenomena being studied by Ulysses includes the solar wind, the heliospheric magnetic field, solar radio bursts and plasma waves, solar and interplanetary energetic particles, galactic cosmic rays, interstellar neutral gas, cosmic dust, and gamma-ray bursts. A summary of the nine instrument sets making up the spacecraft payload is presented in Table 2.2.1.

While the main focus of the mission is clearly concerned with latitudinal variations, other investigations carried out by Ulysses have included detailed interplanetary-physics studies during the in-ecliptic Earth-Jupiter phase (October 1990 to February 1992), and measurements in the jovian magnetosphere during the Jupiter encounter. The spacecraft and ground telecommunication systems have been used to conduct radio-science investigations into the structure of the corona and a search for gravitational waves. Last, but not least, Ulysses continues to make important contributions to our knowledge of the Local Interstellar Medium, and to topics of a broad astrophysical nature.

In addition to the science teams selected at the start of the project, the group of scientists directly associated with the mission comprises nine European Guest Investigator (GI) teams, a similar number of NASA Guest Investigators, and the European Interdisciplinary Investigators who were selected together with the hardware teams.

Status

Ulysses was launched by the Space Shuttle on 6 October 1990, using a combined IUS/PAM-S upper stage to inject the spacecraft into a direct Earth/Jupiter transfer orbit. A gravity-assist manoeuvre at Jupiter in February 1992 placed Ulysses in its final Sun-centred out-of-ecliptic orbit, which has a perihelion distance of 1.3 AU and an aphelion of 5.4 AU. The orbital period is 6.2 yr.

The mission is well into its 12th year, and all spacecraft systems and the nine instrument sets are in excellent health. Between December 2000 and December 2001 spacecraft operations (conducted by the joint ESA-NASA Mission Operations Team at JPL) were complicated by the re-appearance of the nutation-like disturbance that affects the spinning spacecraft when the axial boom is partially illuminated by the Sun. The measures that were developed in 1994-95 to control this disturbance were successfully employed once again, and the impact on science data return was minimal. Indeed, the 24 h/day tracking that is required to monitor and control nutation has benefited the overall data return, which remains well above 95% on average.

Details of the polar passes (defined to be the parts of the trajectory when the spacecraft is above 70° heliographic latitude in either hemisphere) and other key mission milestones are presented in Table 2.2.2. Ulysses arrived over the Sun's south polar regions for the second time in November 2000, followed by the rapid transit from maximum southern to maximum northern helio-latitudes that was completed in

For further information, see http://helio.estec.esa.nl/ulysses/

Table 2.2.1. The Ulysses scientific payload.

Expt. Code	*Investigation*	*Scientific Acronym*	*Principal Investigator*	*Collaborating Institutes*
HED	Magnetic field	VHM/FGM	A. Balogh,Imperial College London (UK)	JPL (USA)
BAM	Solar wind plasma	SWOOPS	D.J. McComas, Los Alamos National Lab (USA)	Ames Research Center (USA); JPL (USA); HAO Boulder (USA) Univ of Boston (USA); MSFC (USA); MPAe Lindau (D)
GLG	Solar wind ion composition	SWICS	J. Geiss, ISSI (CH); G. Gloeckler, Univ of Maryland (USA)	Univ of New Hampshire (USA); GSFC (USA); TU Braunschweig (D); MPAe Lindau (D); Univ of Michigan (USA)
STO	Unified radio and plasma waves	URAP	R.J. MacDowall, GSFC (USA)	Obs de Paris Meudon (F); Univ of Minnesota (USA); CETP Velizy (F)
KEP	Energetic particles and interstellar neutral gas	EPAC/GAS	N. Krupp, MPAe Lindau (D)	Imperial College (UK); Swedish Inst Space Physics Kiruna & Umeå (S); Aerospace Corp (USA); Univ of Bonn (D); MPE Garching (D); Polish Acad Sciences (P)
LAN	Low-energy ions and electrons	HI-SCALE	L.J. Lanzerotti, Bell Laboratories (USA)	APL Laurel (USA); UC Berkeley (USA); Univ of Kansas (USA); Obs de Paris Meudon (F), Univ of Thrace (Gr); Univ of Birmingham (UK)
SIM	Cosmic rays and solar particles	COSPIN	R.B. McKibben, Univ of Chicago (USA)	Imperial College (UK); ESA Research & Scientific Support Dept (NL); NRC Ottawa (Can); Univ of Kiel (D); CEN Saclay (F); Danish Space Research Inst (DK); NCR Milan (I); MPK Heidelberg (D); Univ of Maryland (USA); MPAe Lindau (D)
HUS	Solar X-ray and cosmic gamma-ray bursts	GRB	K. Hurley, UC Berkeley (USA) M. Sommer (retired), Samerberg (D)	CESR Toulouse (F); SRON Utrecht (NL); Obs de Paris Meudon (F); GSFC (USA)
GRU	Cosmic dust	DUST	H. Krüger, MPK Heidelberg (D)	Univ of Canterbury (UK); ESA Space Science Dept (NL); MPE Garching (D); JSC (USA); Univ of Florida (USA)

October 2001. Solar activity reached its maximum in 2000, so that Ulysses experienced a very different high-latitude environment from the one it encountered during the first high-latitude passes. The spacecraft is now heading away from the Sun towards aphelion at the end of June 2004.

At its meeting in June 2000, ESA's Science Programme Committee approved the continuation of the mission until September 2004, when Ulysses will have completed two full out-of-ecliptic orbits of the Sun. Based on the positive recommendation of the Sun Earth Connections Senior Review held in mid-2001, NASA has also confirmed its support for mission operations until 2004.

Figure. 2.2.1. Artist's impression of Ulysses' exploratory mission.

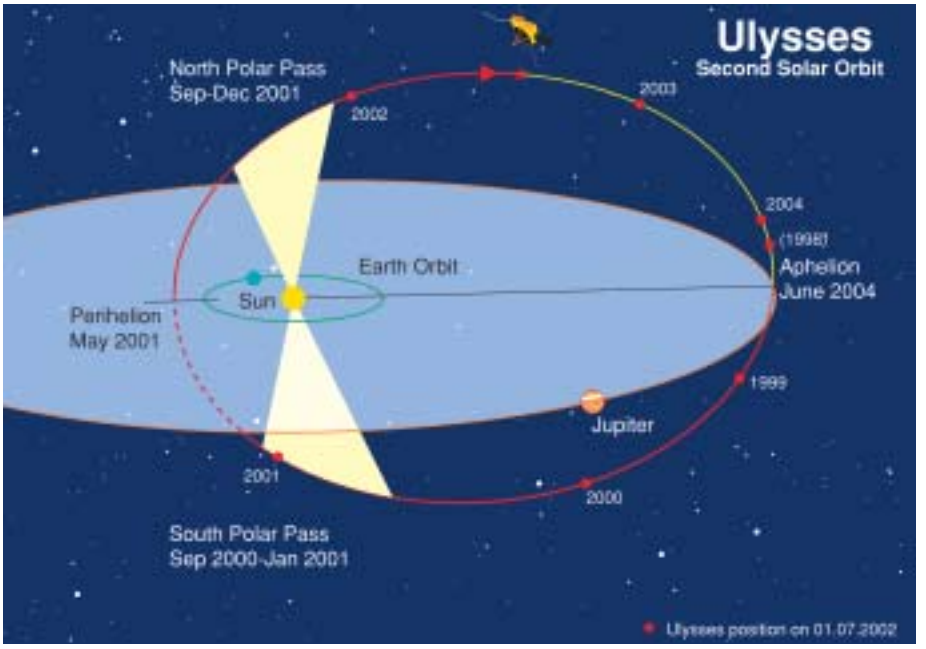

Figure. 2.2.2. The Ulysses orbit viewed from 15 degrees above the ecliptic plane. Dots mark the start of each year.

Table 2.2.2. Key dates in the Ulysses mission.

Events	*Date*
Launch	1990 10 06
Jupiter flyby	1992 02 08
start	1994 06 26
maximum latitude (80.2°, 2.3 AU)	1994 09 13
end	1994 11 05
1st Perihelion (1.34 AU)	1995 03 12
2nd Polar Pass (north)	
start	1995 06 19
maximum latitude (80.2°, 2.0 AU)	1995 07 31
end	1995 09 29
Start of Solar Maximum Mission	1995 10 01
Aphelion (5.40 AU)	1998 04 17
3rd Polar Pass (south)	
start	2000 09 06
maximum latitude (80.2°, 2.3 AU)	2000 11 27
end	2001 01 16
2nd Perihelion (1.34 AU)	2001 05 23
4th Polar Pass (north)	
start	2001 08 31
maximum latitude (80.2°, 2.0 AU)	2001 10 13
end	2001 12 12
Jupiter approach (0.8 AU)	2004 02 04
Aphelion	2004 06 30
End of Mission	2004 09 30

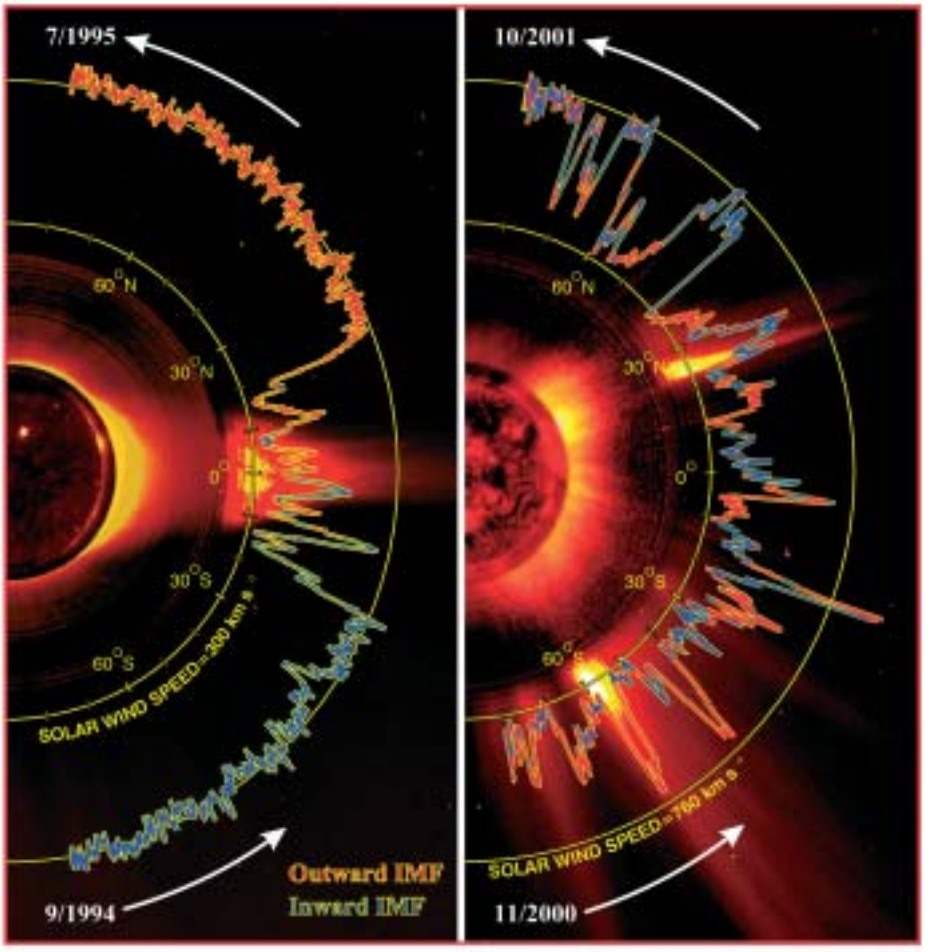

Figure. 2.2.3 A comparison of solar wind observations during the fast-latitude scans near solar minimum (left panel) and around solar maximum (right panel). (Courtesy D.J. McComas)

Scientific highlights

With the completion of the second northern polar pass in December 2001, Ulysses has provided the first, and for the forseeable future only, survey of the high-latitude heliosphere within 5 AU of the Sun over the full range of solar activity conditions. The results from the first set of polar passes, in 1994-95, have been described extensively in the scientific literature, in earlier COSPAR reports, and in particular in the recent book *The Heliosphere Near Solar Minimum: the Ulysses Perspective*. Preliminary results from the polar passes at solar maximum are summarised in the proceedings of the 34th ESLAB Symposium, 'The 3-D Heliosphere at Solar Maximum'. Some recent highlights are given below.

In order to provide context for some of the other results, the solar wind and magnetic field observations are discussed first. The exploration of the latitude dependence of solar wind characteristics (speed, temperature, composition) during maximum solar activity has revealed an entirely different configuration of the 3-D heliosphere compared with that observed near solar minimum. At solar minimum, Ulysses found a heliosphere dominated by the fast wind from the southern and northern polar coronal holes. In contrast, during solar maximum, the large polar coronal holes had disappeared, and the heliosphere appeared much more symmetric. The solar wind flows measured throughout the south polar pass, and much of the rapid transit from south to north, showed no systematic dependence on latitude. The

wind itself was generally slower and much more variable than at solar minimum at all latitudes (Figure 2.2.3). Nevertheless, when Ulysses reached high northern latitudes in late 2001, it witnessed the formation and growth of a new polar coronal hole. This clearly marked the return to more stable conditions following activity maximum. The solar wind recorded at Ulysses became commensurately faster and more uniform, resembling the flows seen over the poles at solar minimum.

The development of the solar wind characteristics was matched by the magnetic field observations. One of the questions that has been investigated is how the high solar activity level affected the structure and dynamics of the heliospheric magnetic field. Although the solar magnetic field, corona and solar wind were highly variable, the magnetic field at Ulysses (~1.5-2.5 AU from the Sun) maintained a surprisingly simple, dipole-like structure. In contrast to the situation at solar minimum, however, the equivalent magnetic poles were located at low latitudes rather than in the polar caps. This is consistent with the presence of coronal holes (the source of the open field carried out with the solar wind to form the heliospheric magnetic field) near the equator, and their absence at the poles. In turn, the spreading out of the field lines from these equatorial sources to high latitudes caused the solar wind to be deflected poleward.

Another phenomenon of great interest was the Sun's magnetic polarity reversal during the polar passes. It was found that the process is a complex one that takes place over a period of several months while the corona evolves to reflect the changes occurring at the level of the photosphere. The coronal evolution is reflected, in turn, in complex dynamic structures in the heliospheric magnetic field. Nevertheless, the previous finding of Ulysses concerning the heliolatitude-independence of the radial component of the magnetic field at solar minimum is found to be valid even in the more disturbed conditions at solar maximum. This therefore appears to be a fundamental property of the distribution of magnetic flux carried in the solar wind.

One of the key discoveries made during the high-latitude passes at solar minimum was the unexpected ease with which energetic particles, accelerated at low-to-middle latitudes, were able to gain access to the polar regions of the heliosphere. Recurrent increases in particle intensity, with a period of ~26 days (i.e. close to the solar rotation period), were observed up to the highest latitudes even though the source of these particles, corotating interaction regions (CIRs), were confined to much lower latitudes. This discovery prompted theorists to reassess existing models of the heliospheric magnetic field, leading ultimately to new suggestions regarding the source of the solar wind itself. An obvious question, then, when Ulysses returned to high latitudes at solar maximum, was: do energetic particles have the same easy access when the heliosphere is much more chaotic? The observations provided an unequivocal answer: yes. Clearly, the source of energetic particles at solar maximum is not CIR-related, since the stable fast-slow solar wind stream structures that are responsible for CIRs do not exist during this phase of the solar cycle. Transient shock waves that are driven by fast coronal mass ejections (CMEs) give rise to the numerous large increases in particle flux that are characteristic of solar maximum. The Ulysses data from the recent high-latitude passes, in addition to confirming the presence of large fluxes of energetic particles over the poles, have revealed that the absolute intensity of these particles in many events is comparable to that measured simultaneously in the ecliptic near 1 AU. This has lead to the idea of the inner heliosphere near solar maximum acting as a 'reservoir' for solar energetic particles.

The precise mechanism by which the particles are transported in latitude and longitude to fill this reservoir is still being debated. The process is certainly different from that in operation at solar minimum, whereby systematic changes to the

underlying Parker spiral magnetic field configuration permit particles accelerated at low-latitude CIRs to propagate to an observer at high latitudes. As noted above, at solar maximum, magnetic pressure acting on open magnetic field lines originating in near-equatorial coronal holes may push them poleward, thereby providing the necessary magnetic connection to high latitudes. Whatever the mechanism, Ulysses has shown that energetic charged particles can gain access to the high-latitude regions of the heliosphere at all phases of the solar cycle far more easily than expected.

On a different topic, Ulysses has for the first time directly observed how the magnetic field of the Sun changes the amount of extrasolar material entering the Solar System. The dust detector has counted an increasing number of interstellar grains since the beginning of 2000. This increase follows a depletion of interstellar grains observed by Ulysses after mid-1996 that was attributed to the deflection of the interstellar dust stream by the highly ordered, solar-minimum heliospheric magnetic field. According to model calculations of the electromagnetic interaction of small interstellar dust grains with the heliospheric plasma, the return of interstellar dust to the Solar System is the result of large-scale disturbances of the heliospheric magnetic field that occur during solar maximum. The model calculations also show that the configuration of the heliospheric magnetic field will cause the number of interstellar dust grains in the Solar System to increase steadily until the next solar maximum.

Ulysses data archive

Data from the Ulysses investigations and flight project are being archived and made accessible to the public through two channels: the ESA Ulysses Data Archive at ESTEC, and NASA's National Space Science Data Center (NSSDC). The ESA archive provides an online facility to browse and download selected measurements made by the scientific instruments. The user is able to view 26-day and 1-year summary plots of the main parameters measured, and (if of interest) download ASCII data files and accompanying documentation for further analysis. The ESA archive is accessible via the Ulysses homepage.

2.3 SOHO

Introduction

Since the launch of the Solar and Heliospheric Observatory (SOHO) in 1995, the joint ESA/NASA mission has provided an unparalleled breadth and depth of information about the Sun, from its interior, through the hot and dynamic atmosphere, to the solar wind and its interaction with the interstellar medium. Research using SOHO observations has revolutionised our understanding of the Sun, and science teams from around the world have made great strides towards a better understanding of 'the big three' areas of research that SOHO set out to tackle: the structure and dynamics of the solar interior, the heating of the solar corona, and the acceleration of the solar wind. However, much remains to be done. The findings have been documented in an impressive and growing body of scientific literature and popular articles. At the same time, SOHO's easily accessible, spectacular data and basic science results have captured the imagination of the space science community and the general public alike.

SOHO enjoys a remarkable 'market share' in the worldwide solar physics community: more than 1100 papers in refereed journals and more than 1500 papers in conference proceedings and other publications, representing the work of more than 1500 scientists.

A summary of SOHO's 12 instruments, which represent the most comprehensive set of solar and heliospheric instruments ever developed and placed on the same platform, is presented in Table 2.3.1.

Mission status

SOHO was launched by an Atlas IIAS from Cape Canaveral on 2 December 1995 and inserted into a halo orbit around the L1 Lagrangian point on 14 February 1996, 6 weeks ahead of schedule. An extension of the SOHO mission for a period of 5 years beyond its nominal lifetime, i.e. until March 2003, was approved in 1997. A further extension until March 2007 was approved by ESA's Science Programme Committee in February 2002. Based on the positive recommendation of the Sun Earth Connections Senior Review held in mid-2001, NASA has also approved its funding for the next 4 years.

An unexpected loss of contact occurred on 25 June 1998. Fortunately, the mission was completely recovered in one of the most dramatic rescue efforts in space, and normal operations were resumed in mid-November 1998 after the successful recommissioning of the spacecraft and all instruments. When the last onboard gyro failed on 21 December 1998, SOHO went into Emergency Sun Reacquisition (ESR) mode. In a race against time – the ESR thruster firings were consuming an average of about 7 kg of hydrazine per week – engineers at ESTEC and Matra Marconi Space developed software to exit the ESR mode without a gyro and allow gyroless operation of the spacecraft. The first gyroless reaction wheel management and stationkeeping manoeuvre was performed on 1 February 1999, making SOHO the first 3-axis spacecraft to be operated without a gyro. A new Coarse Roll Pointing (CRP) mode, which uses the reaction wheel speed measurements to monitor and compensate for roll rate changes, was successfully commissioned in September 1999. The CRP mode is almost two orders of magnitude more stable than using gyros. It also acts as an additional safety net between the normal mode and ESR mode, making SOHO perhaps more robust than ever. Conservative estimates of propellant usage yields a remaining lifetime of more than 10 years.

Operations

The SOHO Experiment Operations Facility (EOF), at NASA's Goddard Space Flight Center (GSFC), is the focal point for mission science planning and instrument operations. At the EOF, the experiment teams receive real-time and playback telemetry, process them to determine instrument commands, and send commands

For further information, see http://soho.estec.esa.nl

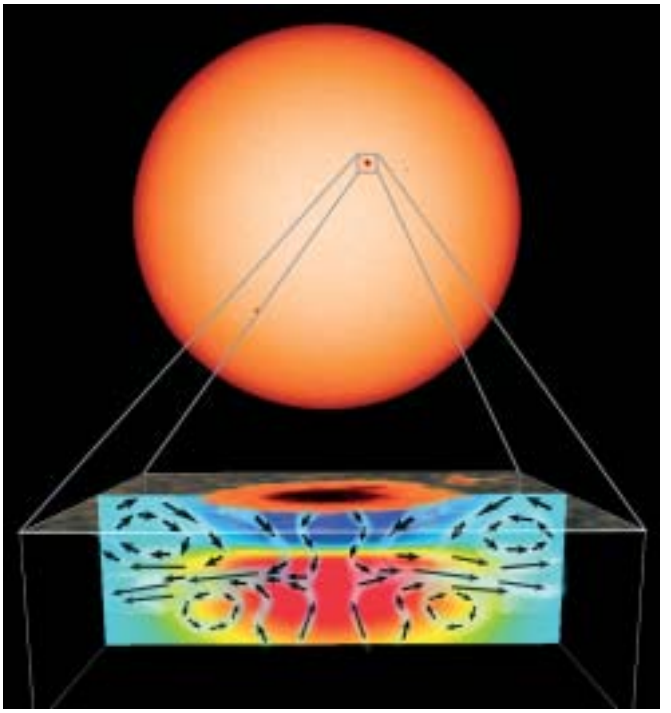

Figure 2.3.1. SOHO's MDI reveals subsurface inflows beneath a sunspot. A cross-section going down 12 000 km below the surface of the Sun in the vicinity of a sunspot shows a convergence of cool gas (blue) near the surface. This inflow concentrates the magnetic field and suppresses hot gas (red) trying to rise from below. The analysis also revealed that sunspots are surprisingly shallow, changing from cooler to hotter than the surroundings only 5000 km below the surface.

directly from their workstations through the ground system to their instruments, both in near real-time and for delayed execution.

From the very beginning much of the observing time has been devoted to coordinated campaigns. As of late March 2002, the SOHO campaign database (*http://sohowww.nascom.nasa.gov/cgi-bin/soho_campaign_search*) lists a total of 830 coordinated campaigns. Of these, 272 involved ground-based observatories, 109 involved Yohkoh, and 278 TRACE. With the successful launch of RHESSI (Reuven Ramaty High Energy Solar Spectroscopic Imager) mission on 5 February 2002, long-established plans for SOHO-RHESSI collaborations were activated. Daily target selections by a solar flare research group (the 'Max Millennium group') are used for day-to-day co-observations. The special Joint Observing Program "Major Flare Watch – Regions Likely to Produce Major Flares" allows for off-hours notification for some instruments (plus TRACE) through the Science Operations Coordinators. An automated system is in place to alert them and instrument personnel about ongoing solar energetic particle events, allowing instruments to minimise detector wear by turning down high voltages.

Special operations performed since 2000 include both an off-point and a 360º roll manoeuvre, for instrument calibration, flat-fielding and special observation purposes.

Scientific highlights

The near-uninterrupted data from the Michelson Doppler Imager (MDI) yield oscillation power spectra with an unprecedented signal-to-noise ratio that allow the determination of the frequency splittings of the global resonant acoustic modes of the Sun with exceptional accuracy. MDI data revealed 'zonal bands' in the northern and southern hemispheres where currents flow at ~5 m/s relative to each other. The zonal bands migrate towards the equator with time, and penetrate to a depth of at least 56 Mm.

Table 2.3.1. Instruments in the SOHO payload.

Investigation	*Principal Investigator*	*Collaborating Countries*	*Measurements*	*Technique*
Helioseismology				
Global Oscillations at Low Frequencies (GOLF)	A. Gabriel, IAS, Orsay, F	F, ESA, DK, D, CH, UK, NL, E, USA	Global Sun velocity oscillations (l=0-3)	Na-vapour resonant scattering cell, Doppler shift and circular polarisation
Variability of solar IRradiance and Gravity Oscillations (VIRGO)	C. Fröhlich, PMOD/WRC, Davos, CH	CH, N, F, B, ESA, E	Low-degree (l =0-7) irradiance oscillations and solar constant	Global Sun and low-resolution (12-pixel) imaging and active cavity radiometers
Michelson Doppler Imager (MDI)	P.H. Scherrer, Stanford Univ, California, USA	USA, DK, UK	Velocity oscillations high-degree modes (up to l=4500)	Doppler shift with Fourier tachometer, 4 and 1.3 arcsec resolution
Solar Atmosphere Remote Sensing				
Solar UV Measurements of Emitted Radiation (SUMER)	W. Curdt, MPAe, Lindau, D	D, F, CH, USA	Plasma flow characteristics (temperature, density, velocity); chromosphere through corona	Normal-incidence spectrometer, 50-160 nm, spectral resolution 20000-40000, angular resolution 1.2-1.5 arcsec
Coronal Diagnostic Spectrometer (CDS)	R.A. Harrison, RAL, Chilton, UK	UK, CH, D, USA, N, I	Temperature and density: transition region and corona	Normal and grazing-incidence spectrometers, 15-80 nm, spectral resolution 1000-10000, angular resolution 3 arcsec
Extreme-ultraviolet Imaging Telescope (EIT)	J-P Delaboudinière, IAS, Orsay, F	F, USA, B	Evolution of chromospheric and coronal structures	Full-disc images (1024×1024 pixels in 42×42 arcmin) at lines of HeII, FeIX, FeXII, FeXV
Ultraviolet Coronagraph Spectrometer (UVCS)	J.L. Kohl, SAO, Cambridge, MA, USA	USA, I, CH, D	Electron and ion temperature densities, velocities in corona (1.3-10 $R_\odot$)	Profiles and/or intensity of selected EUV lines between 1.3 and 10 $R_\odot$
Large Angle and Spectrometric COronagraph (LASCO)	R. Howard NRL, Washington DC, USA	USA, D, F UK	Structures' evolution, mass, momentum and energy transport in corona (1.1-30 $R_\odot$)	One internally and two externally occulted coronagraphs. Spectrometer for 1.1-3 $R_\odot$
Solar Wind ANisotropies (SWAN)	J.L. Bertaux, SA Verrières-le-Buisson, F	F, FIN, USA	Solar wind mass flux anisotropies. Temporal variations	Scanning telescopes with hydrogen absorption cell for Lyman-alpha
Solar Wind 'in situ'				
Charge, ELement and Isotope Analysis System (CELIAS)	P. Bochsler, Univ. Bern, CH	CH, D, USA, Russia	Energy distribution and composition. (mass, charge, charge state) (0.1-1000 keV/e)	Electrostatic deflection, time-of-flight measurements and solid-state detectors
Comprehensive SupraThermal Energetic Particle analyser (COSTEP)	H. Kunow Univ. Kiel, D	D, USA, J, F, E, ESA, IRL	Energy distribution of ions (p, He) 0.04-53 MeV/n and electrons 0.04-5 MeV	Solid-state detector telescopes and electrostatic analysers
Energetic and Relativistic Nuclei and Electron experiment (ERNE)	J. Torsti, Univ. Turku, SF	FIN, UK	Energy distribution and isotopic, composition of ions (p-Ni) 1.4-540 MeV/n and electrons 5-60 MeV	Solid-state and plastic scintillation detectors

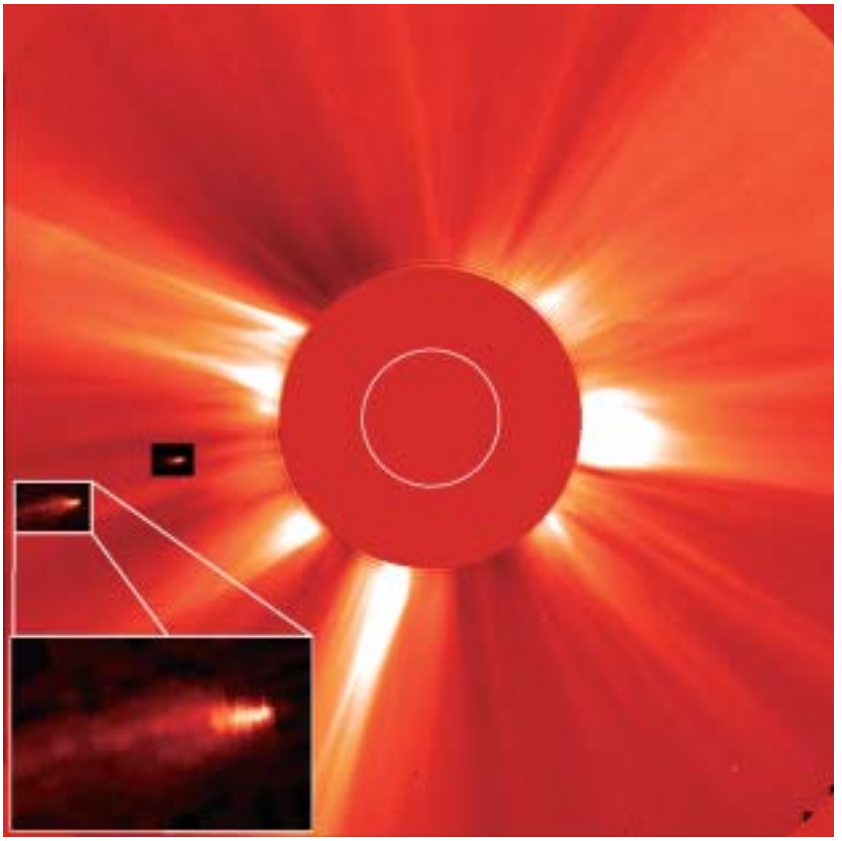

Figure 2.3.2. Composite of a LASCO C2 white-light image and two UVCS Ly-alpha images, showing Comet C/2001 C2 (also known as SOHO-294) as it approaches the Sun on 6-7 February 2001. These observations enabled estimates of the outgassing rate and the size of the comet to be made, as well as the local density of the solar wind.

A longstanding problem in solar physics has been to explain how sunspots can last for several weeks without flying apart. Theories have been developed that require inward flows of material that stabilise the structure. The problem: material often appears to be flowing out of sunspots! The 'time distance helioseismology' or 'acoustic tomography' – a very exciting technique for probing the 3D structure and flows beneath the solar surface – has helped to shed light on this problem: just below the surface, the required inward flows are present. We now have the first clear picture of what lies beneath sunspots, the enigmatic, planet-sized dark areas on the surface of the Sun; and have peered inside the Sun to see swirling flows of plasma that create a self-reinforcing cycle that holds a sunspot together (Figure 2.3.1).

A far-UV and extreme-UV spectral atlas of the Sun between 670 Å and 1609 Å, derived from observations obtained with the SUMER spectrograph, identifies more than 1100 distinct emission lines, of which more than 150 had not been recorded or identified before. The atlas contains spectra of the average quiet Sun, a coronal hole and an active region on the disc, providing a rich source of new diagnostic tools to study the physical parameters in the chromosphere, transition region and corona. In particular, the wavelength range below 1100 Å as observed by SUMER represents a significant improvement over the spectra produced in the past.

UVCS observations show that solar-maximum equatorial coronal holes exhibit 3-5 times lower outflow speeds than solar-minimum polar coronal holes. Since wind speeds observed at 1 AU are similar in the two cases, the bulk of the acceleration must occur outside the region observed by UVCS, i.e. above 3 solar radii.

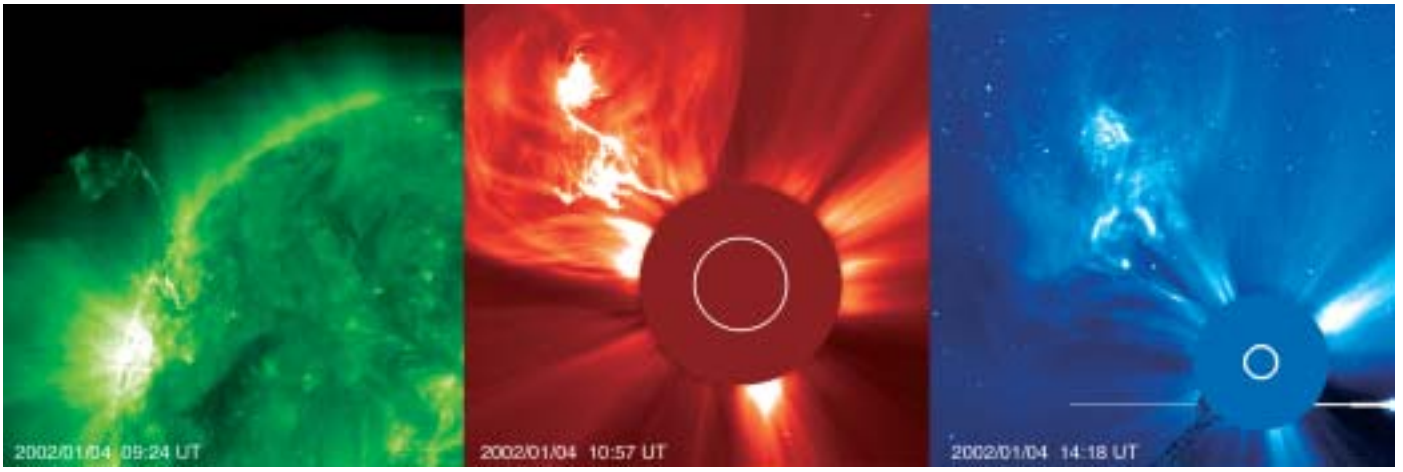

Figure 2.3.3. A spectacular Coronal Mass Ejection (CME) taking off from the Sun on 4 January 2002, starting off as a filament eruption seen by EIT in Fe XII 195 Å. The complexity and structure of the CME as it passed through the LASCO C2 and C3 fields of view amazed even experienced solar physicists at the SOHO operations centre.

LASCO has discovered infalling matter at coronal heights. These inflows show a strong correlation with non-polar coronal holes and the Sun's non-axisymmetric open flux, but only a broad long-term correlation with conventional indicators of solar activity.

SOHO is providing new measurements not only of the Sun: it had discovered more than 385 comets by April 2002, most of them belonging to Sun-grazing comets of the Kreutz family. Thanks to rapid communication from the LASCO group and SOHO's near-realtime observing capabilities, UVCS made spectroscopy measurements of several comets (Figure 2.3.2). Comet C/2000 C6 was observed by the UVCS instrument in Ly-α emission. From the the Ly-α intensity and its rate of fading owing to H I ionisation the streamer density at 4.56 solar radii was estimated to be 0.68×10^5 particles/cm^3.

The outgassing rates at various heights, which in turn give an estimate of the diameter of the cometary nucleus (12 m), was also determined. In addition, a sudden brightening was observed between 5.7 and 4.6 solar radii, interpreted as a fragmentation of the nucleus.

The break-up of Comet LINEAR was monitored by the SWAN instrument. The total amount of water vapour observed by SWAN from 25 May to 12 August 2000 was estimated at 3.3×10^6 t. Only about 1% of this was left on 6 August, when observations by the Hubble Space Telescope of the dying comet's fragments gave an estimate of the total volume of the fragments. Combining the two numbers gives a remarkably low value for the density – about 15 kg/m^3, compared with 917 kg/m^3 for familiar non-porous ice. Even allowing for an equal amount of dust grains, 30 kg/m^3 is far less than the 500 kg/m^3 often assumed by cometary scientists.

The VIRGO instrument measures both total solar irradiance (TSI) and spectral irradiance, extending the record of TSI measurements into solar cycle 23. EUV irradiance measurements are being made on a regular basis by the CELIAS/SEM and CDS instruments. These measurements represented the only total solar EUV spectral irradiance observations available until the launch of TIMED in 2002. Owing to its influence on the terrestrial atmosphere, the solar EUV variability may constitute a significant source of climate changes. Tracking the long-term variations of the solar spectral irradiance is therefore of critical importance.

2.4 Cassini/Huygens

Introduction

Huygens is the element contributed by ESA to Cassini/Huygens, the joint NASA/ESA planetary mission to the Saturnian system. Titan, the largest moon of Saturn, is a central target of the mission. The Saturn Orbiter is provided by NASA, while the Italian Space Agency (ASI) has contributed its high-gain antenna and other radio subsystem equipment under a bilateral NASA/ASI agreement. The Jet Propulsion Laboratory (JPL, Pasadena, California) is managing the mission for NASA. The overall mission is named after the French/Italian astronomer Jean-Dominique Cassini, who discovered several Saturnian satellites and ring features, including the Cassini division, during 1671-1685. ESA's probe is named after Dutch astronomer Christiaan Huygens, who discovered Titan in 1655.

The Cassini/Huygens spacecraft was launched at 08:43 UT on 15 October 1997 by a Titan IVB-Centaur rocket from Cape Canaveral Air Force Station in Florida. The 5.6 t spacecraft was too heavy to be injected into a direct trajectory to Saturn, so the interplanetary voyage of about 6.7 years includes gravity-assist manoeuvres at Venus, Earth and Jupiter (Figure 2.4.1). Upon arrival at Saturn, the spacecraft will be inserted into orbit around Saturn. At the end of the third revolution around Saturn, the Orbiter will deliver the Huygens Probe to Titan. After completion of the Probe mission, the Orbiter will carry out its exploration of the Saturnian system during 75 orbits around Saturn over 4 years. It will make repeated close flybys of Titan, both for data gathering about the moon and for gravity-assist orbit changes that will permit it to make a tour of Saturn's satellites, reconnoitre the magnetosphere and obtain views of Saturn's higher latitudes. During its 4-year nominal mission, Cassini will make detailed observations of Saturn's atmosphere, magnetosphere, rings, icy satellites and Titan.

The Huygens Probe was selected by ESA's Science Programme Committee in November 1988 as the first medium-size mission of the Horizon 2000 long-term scientific programme. NASA received approval for the start of Cassini in 1990.

Scientific objectives

The Cassini/Huygens mission is designed to explore the Saturnian system and all its elements: the planet and its atmosphere, rings and magnetosphere, and a large number of its moons, particularly Titan and the icy satellites. Titan is the second largest moon in the Solar System after Jupiter's Ganymede. Its atmosphere resembles that of the

Figure 2.4.1. Left: the interplanetary trajectory of the Cassini/Huygens spacecraft. Right: the trajectory upon arrival at Saturn; the Probe is released towards the end of the initial orbit around Saturn.

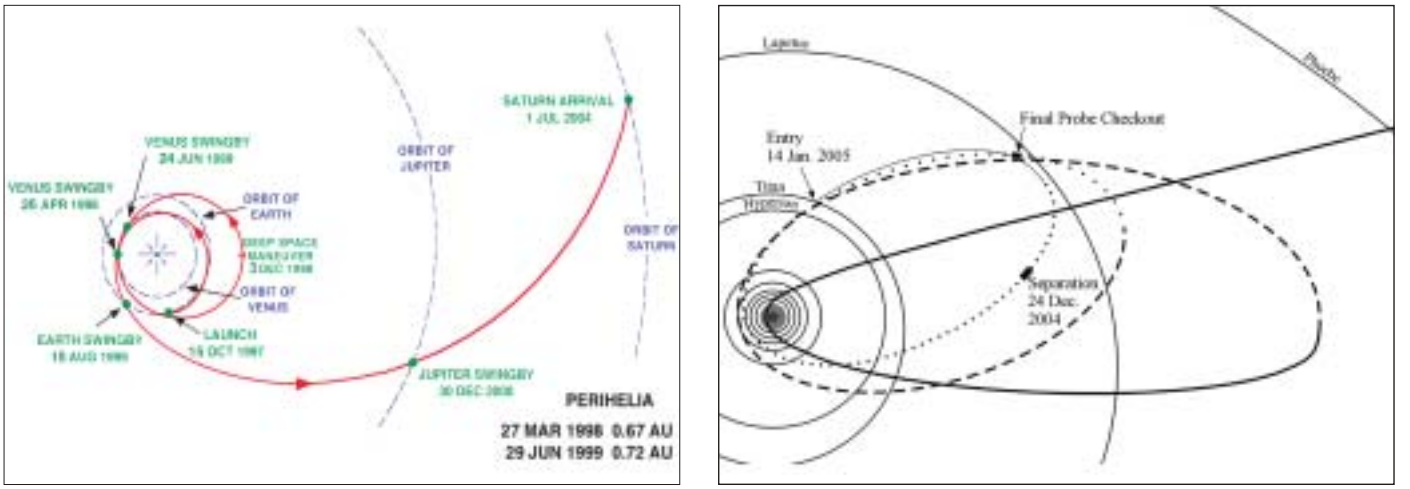

For further information, see http://sci.esa.int/huygens

Table 2.4.1. The principal characteristics of the Huygens payload.

Instrument/PI	*Science objectives*	*Sensors/measurements*	*Mass (kg)*	*Power (typical/ peak, W)*	*Participating countries*
Huygens Atmospheric Structure Instrument (HASI) M. Fulchignoni, University Paris 7/ Obs. Paris-Meudon (France)	Atmospheric temperature and pressure profile, winds and turbulence Atmospheric conductivity. Search for lightning. Surface permittivity and radar reflectivity.	*T*: 50-300K, *P*: 0-2000 mbar γ: 1 μ*g*-20 m*g* AC *E*-field: 0-10 kHz , 80 dB at 2 μV/m Hz DC *E*-field: 50 dB at 40 mV/m Conductivity 10^{-15} Ω/m to ∞ Relative permittivity: 1 to ∞ Acoustic: 0-5 kHz, 90 dB at 5 mPa	6.3	15/85	I, A, D, E, F, N, SF, USA, UK, ESA/SSD, IS
Gas Chromatograph Mass Spectrometer (GCMS) H.B. Niemann, NASA/GSFC, Greenbelt (USA)	Atmospheric composition profile. Aerosol pyrolysis products analysis.	Mass range: 2-146 dalton Dynamic range: $>10^{8}$ Sensitivity: 10^{-10} mixing ratio Mass resolution: 10^{-6} at 60 dalton GC: 3 parallel columns, H_2 carrier gas Quadropole mass filter 5 electron impact sources Enrichment cells (×100-×1000)	17.3	28/79	USA, A, F
Aerosol Collector and Pyrolyser (ACP) G.M. Israel, SA/CNRS Verriéres-le-Buisson (France)	Aerosol sampling in two layers – pyrolysis and injection to GCMS	2 samples: 150-40 km; 23-17 km 3-step pyrolysis: 20°C, 250°C, 600°C	6.3	3/85	F, A, USA
Descent Imager/Spectral Radiometer (DISR) M.G. Tomasko, University of Arizona, Tucson (USA)	Atmospheric composition and cloud structure. Aerosol properties. Atmospheric energy budget. Surface imaging.	Upward and downward (480-960 nm) and IR (0.87-1.64 μm) spectrometers, res. 2.4/6.3 nm. Downward and side looking imagers. (0.660-1 μm), res. 0.06-0.20° Solar Aureole measurements: 550±5 nm, 939±6 nm. Surface spectral reflectance with surface lamp.	8.1	13/70	USA, D, F
Doppler Wind Experiment (DWE) M.K. Bird, University of Bonn (Germany)	Probe Doppler tracking from the Orbiter for zonal wind profile measurement.	(Allan Variance) : 10^{-11} (1 s); 5×10^{-12} (10 s); 10^{-12} (100 s) Wind measurements 2-200 m/s Probe spin, signal attenuation	1.9	10/18	D, I, USA
Surface Science Package (SSP) J.C. Zarnecki, University of Kent, Canterbury (UK)	Titan surface state and composition at landing site. Atmospheric measurements.	γ: 0-100 *g*; tilt ±60°; *T*: 65-110K; T_{th}: 0-400 mW m^{-1} K^{-1} Speed of sound: 150-2000 m s^{-1}, Liquid density: 400-700 kg m^{-3} Refractive index: 1.25-1.45 Acoustic sounding, liquid relative permittivity	3.9	10/11	UK, F, USA, ESA/SSD, PL

Table 2.4.2. The Huygens interdisciplinary scientists.

Scientist/Affiliation	*Field of Investigation*
ESA Selection	
D. Gautier, Obs. de Paris, Meudon, F	Titan aeronomy
J.I. Lunine, Univ. of Arizona, Tucson, USA	Titan atmosphere/surface interactions
F. Raulin, LPCE, Univ. Paris 12, Creteil, F	Titan chemistry and exobiology
NASA Selection	
M. Blanc, Observatoire Midi-Pyrénées, Toulouse, F	Plasma circulation and magnetosphere/ ionosphere coupling
J. Cuzzi, NASA Ames Research Center, Moffett Field, USA	Rings and dust within Saturnian system
T. Gombosi, Univ. of Michigan, Ann Arbor, USA	Plasma environment in Saturn's magnetosphere
T. Owen, Inst. for Astronomy, Honolulu, USA	Atmospheres of Titan and Saturn
J. Pollack (deceased), NASA Ames Research Center, Moffett Field, USA	Origin and evolution of Saturnian system
L. Soderblom, US Geological Survey, Flagstaff, USA	Satellites of Saturn
D. Strobel, Johns Hopkins University, Baltimore, USA	Titan's and Saturn's atmospheric aeronomy

Earth more closely than that of any other Solar System body. Nitrogen is the major constituent, at a surface pressure of 1.5 bar, compared with 1 bar on Earth. Other major constituents are methane (a few percent) and hydrogen (0.2%). It is speculated that argon could also be present (the most recent models suggest an upper limit of 1%), although it has not yet been detected. Another resemblance to Earth is that Titan's surface could be partially covered by lakes or even oceans of methane and ethane mixtures. The photolysis of methane in the atmosphere, owing mainly to the solar UV radiation but also to cosmic rays and precipitating energetic magnetospheric particles, gives rise to a complex organic chemistry. Chemical reactions taking place in the continuously evolving atmosphere provide possible analogues to some of the prebiotic organic chemistry that was at work on the primitive Earth, before the appearance of life some 3.8 Gyr ago.

Huygens will carry out a detailed *in situ* study of Titan's atmosphere and to characterise the surface of the satellite near the Probe's landing site. The objectives are to make detailed *in situ* measurements of the atmosphere's structure, composition and dynamics. Images and spectroscopic measurements of the surface will also be made during the atmospheric descent. Since it is hoped that the Probe will survive after the impact for at least a few minutes, the payload includes the capability for making *in situ* measurements for a direct characterisation of the surface at the landing site.

The payload

On 10 October 1989, NASA and ESA simultaneously released coordinated Announcements of Opportunity (AOs) calling respectively for investigations to be performed with the Saturn Orbiter and the Huygens Probe. The NASA AO called for four types of proposals:

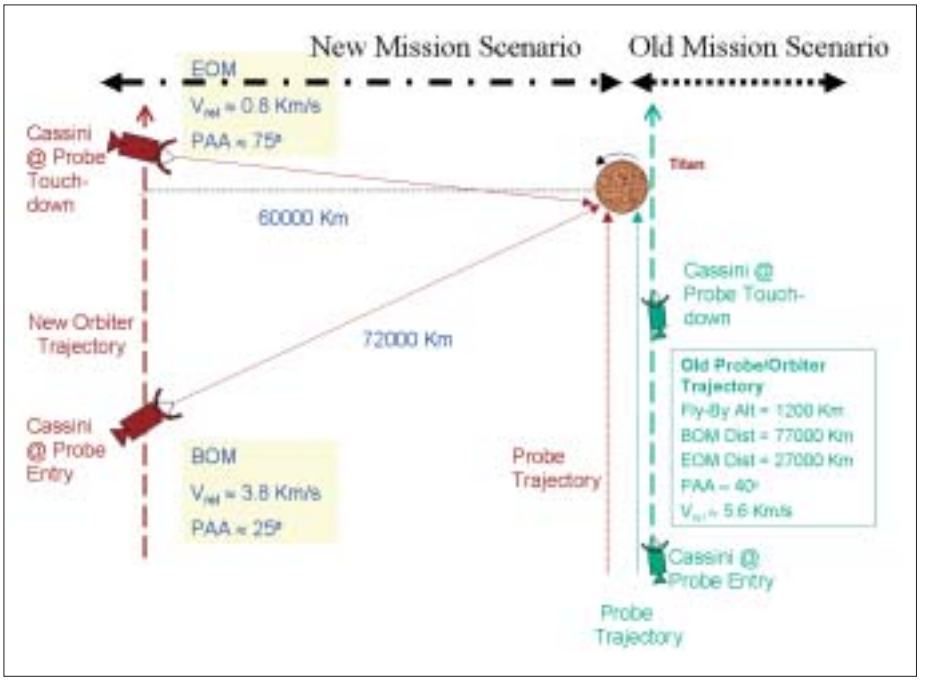

Figure 2.4.2. The revised approach strategy for Huygens at Titan.

— Principal Investigator (PI) Instruments;
— Orbiter facility team leader (TL);
— Orbiter facility team member (TM);
— Interdisciplinary Scientist (IDS) investigation.

The ESA AO called for two types of proposals:
— PI Instrument;
— Interdisciplinary Scientist investigation.

The ESA Huygens selection, which comprises six PI Instruments (Table 2.4.1) and three IDS investigations (Table 2.4.2), was announced in September 1990. The NASA Saturn Orbiter selection, which comprised seven PI Instruments, four Team Leaders, 52 Team Members and seven IDS investigations, was announced in November 1990. During the selection process, NASA included an additional facility instrument on the Orbiter, the Ion and Neutral Mass Spectrometer (INMS), for which a call for Team Leader and Team Member investigation proposals was released in August 1991. The INMS investigation selection was announced in February 1992. The NASA-selected IDS is shown in Table 2.4.2 and the Orbiter Payload in Table 2.4.3.

Cassini/Huygens mission overview

The Cassini/Huygens spacecraft will arrive at Saturn in late June 2004. The Saturn Orbit Insertion (SOI) manoeuvre will be executed while the spacecraft is crossing the ring plane on 1 July 2004. This manoeuvre will place the spacecraft in a 90-day orbit, which includes the first targeted Titan flyby. The second (48-day) orbit, which also includes a targeted Titan flyby, will shape the trajectory so that the Huygens mission can be carried out on the third (32-day) orbit using an Orbiter flyby altitude of 60 000 km. The Huygens mission trajectory was changed in 2001 to accommodate a new geometry requirement during the Probe relay phase that reduces the Doppler shift

Table 2.4.3. Saturn Orbiter payload.

Instrument *PI*	*Measurement*	*Technique*	*Mass (kg)*	*Power (W)*	*Countries*
Optical Remote Sensing					
Composite Infrared Spectrometer (CIRS) V. Kunde, NASA/GSFC, USA	High-resolution spectra, 7-1000 μm	Spectroscopy using 3 interferometric spectrometers	43	43.3	USA, F, D, I, UK
Imaging Science Subsystem (ISS) C. Porco, U. Arizona, USA	Photometric images through filters, 0.2-1.1 μm	Imaging with CCD detectors; 1 wide-angle camera (61.2 mrad FOV); 1 narrow-angle camera (6.1 mrad FOV)	56.5	59.3	USA, F, D, UK
Ultraviolet Imaging Spectrometer (UVIS) L. Esposito, U. Colorado, Boulder, USA	Spectral images, 55-190 nm; occultation photometry, 2 ms; H and D spectroscopy, 0.0002 μm resolution	Imaging spectroscopy, 2 spectrometers; hydrogen-deuterium absorption cell	15.5	14.6	USA, F, D
Visible and Infrared Mapper Spectrometer (VIMS) R. Brown, U. Arizona, Tucson, USA	Spectral images, 0.35-1.05 μm (0.073 μm resolution); 0.85-5.1 μm (0.166 μm resolution); occultation photometry	Imaging spectroscopy; 2 spectrometers	37.1	24.6	USA, F, D, I
Radio Remote Sensing					
Cassini Radar (RADAR) C. Elachi, JPL, USA	Ku-band radar images (13.8 GHz); radiometry, <0.5K resolution	Synthetic aperture radar; radiometry with a microwave receiver	43.3	108.4	USA, F, I, UK
Radio-Science Instrument (RSS) A. Kliore, JPL, USA	Ka/S/X-bands; frequency, phase, timing and amplitude	X/Ka-band uplink; Ka/X/S-band downlink	14.4	82.3	USA, I
Particle Remote Sensing & In-Situ Measurement					
Magnetospheric Imaging Instrument (MIMI) S.T. Krimigis, Johns Hopkins Univ, Baltimore, USA	1. Image energetic neutrals and ions at <10 keV to 8 MeV per nucleon; composition. 2. 10-265 keV/e ions; charge state; composition; directional flux; 3. mass range: 20 keV to 130 MeV ions; 15 keV to >11 MeV electrons; directional flux	1. Particle detection and imaging; ion-neutral camera (time-of-flight, total energy detector); 2. charge energy mass spectrometer; 3. solid-state detectors with magnetic focusing telescope and aperture-controlled ~45° FOV	29	23.4	USA, F, D
In-Situ Measurement					
Cassini Plasma Spectrometer (CAPS) D.T. Young, SWRI, San Antonio, USA	Particle energy/charge: 1. 0.7-30 000 eV/e; 2. 1-50 000 eV/e 3. 1-50 000 eV/e	Particle detection and spectroscopy: 1. electron spectrometer; 2. ion-mass spectrometer; 3. ion-beam spectrometer	23.8	19.2	USA, SF, F, H, N, UK
Cosmic Dust Analyser (CDA) E. Gruen, MPI Heidelberg, D	Directional flux and mass of dust particles in the range 10^{-16}-10^{-6} g; chemical composition	Impact-induced currents	16.8	19.3	D, CZ, F, ESA/SSD, N, UK, USA
Dual Technique Magnetometer (MAG) D. Southwood, IC, UK	B: DC to 4 Hz up to 256 nT; scalar field DC to 20 Hz up to 44 000 nT	Magnetic field measurement; flux gate magnetometer; vector-scalar magnetometer	8.8	12.4	UK, D, USA
Ion and Neutral Mass Spectrometer (INMS) J.H. Waite, SWRI, San Antonio, USA	Fluxes of +ions and neutrals in mass range 2-66 amu	Mass spectrometery; closed source and open source	10.3	26.6	USA, D
Radio and Plasma Wave Science (RPWS) D. Gurnett, U. Iowa, USA	E: 10 Hz-2 MHz; B: 1 Hz-20 kHz; plasma density and temperature	Radio frequency receivers; 3 electric monopole antennas; 3 magnetic search coils; Langmuir Probe	37.7	17.5	USA, A, F, S, UK, N

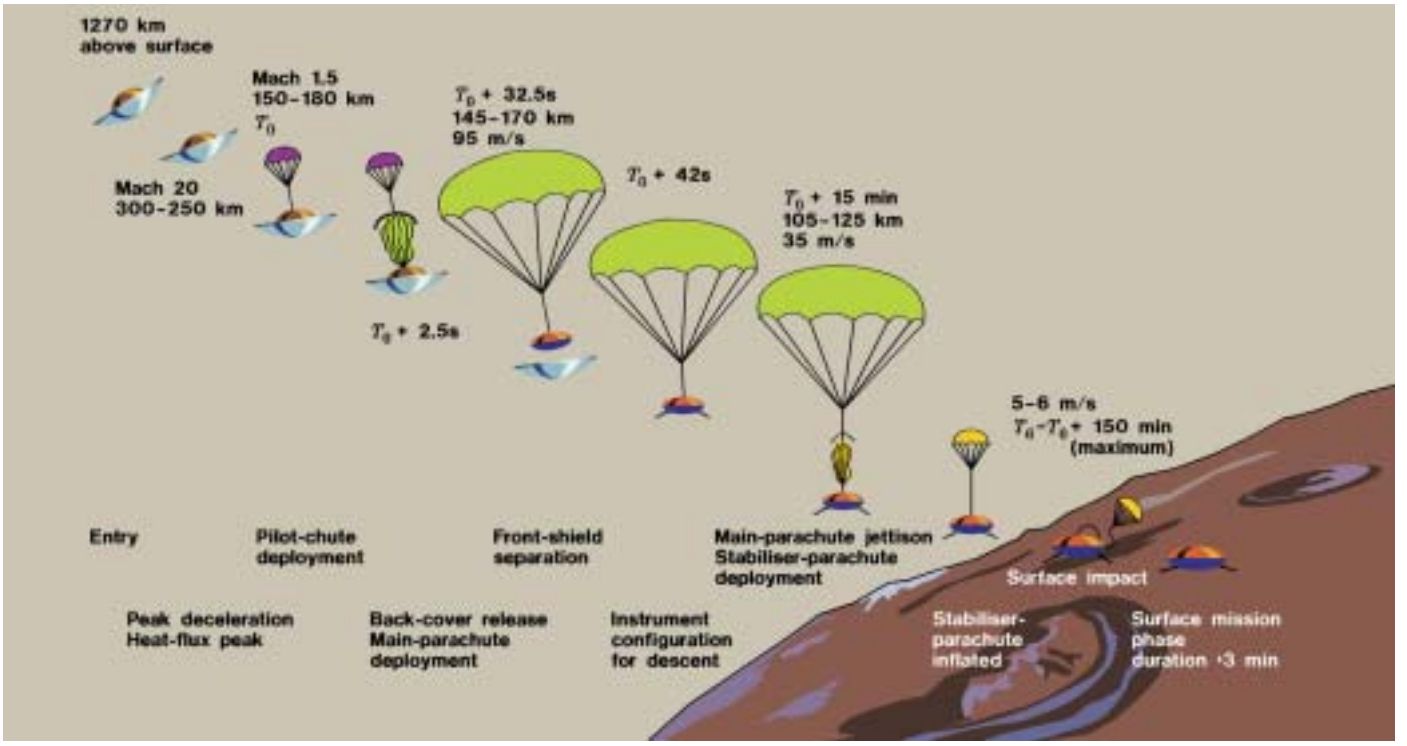

Figure 2.4.3. The entry and descent sequence for the Huygens Probe.

of the radio signal received by the Orbiter (Figure 2.4.2). This change was necessary to cope with a design flaw of the Huygens radio receiver discovered during inflight testing in 2000. The Probe will be released on 24 December 2004, 22 days before Titan encounter. Five days after release, the Orbiter will perform a deflection manoeuvre in order to avoid impacting Titan. This manoeuvre will also set up the Probe-Orbiter radio communication geometry for the Probe descent phase. Huygens' entry into Titan's atmosphere is planned for 14 January 2005. The Orbiter will act as a relay during the Huygens mission, receiving the data on its High Gain Antenna (HGA). This configuration does not allow the Probe mission to be conducted with a real-time link between the Orbiter and Earth. The Probe data will be stored aboard the Orbiter in the two solid-state recorders for later transmission to Earth after completion of the Probe mission. The main events of the Probe entry and descent are illustrated in Figure 2.4.3.

After completion of the Probe mission, the Orbiter will begin its 4-year satellite tour of the Saturnian system. This consists of 75 Saturn-centred orbits, connected by Titan gravity-assist flybys or propulsive manoeuvres. The size of these orbits, their orientation to the Sun/Saturn line and their inclination to Saturn's equator are dictated by the various scientific requirements, which include: Probe and landing site ground-track coverage, icy-satellite flybys, Saturn, Titan or ring occultation, magnetosphere coverage, orbit inclinations and ring-plane crossings. Titan is also a principal target for the Orbiter; it will be observed during each of the 44 targeted Titan flybys.

The Orbiter science instruments are mounted on two body-fixed platforms: the remote-sensing pallet and the particle & field pallet; the magnetometer is mounted at the tip of an 11 m-long boom; the magnetic and electric antennas of the RPWS experiment are mounted on the body; both the radar and the radio-science instrument

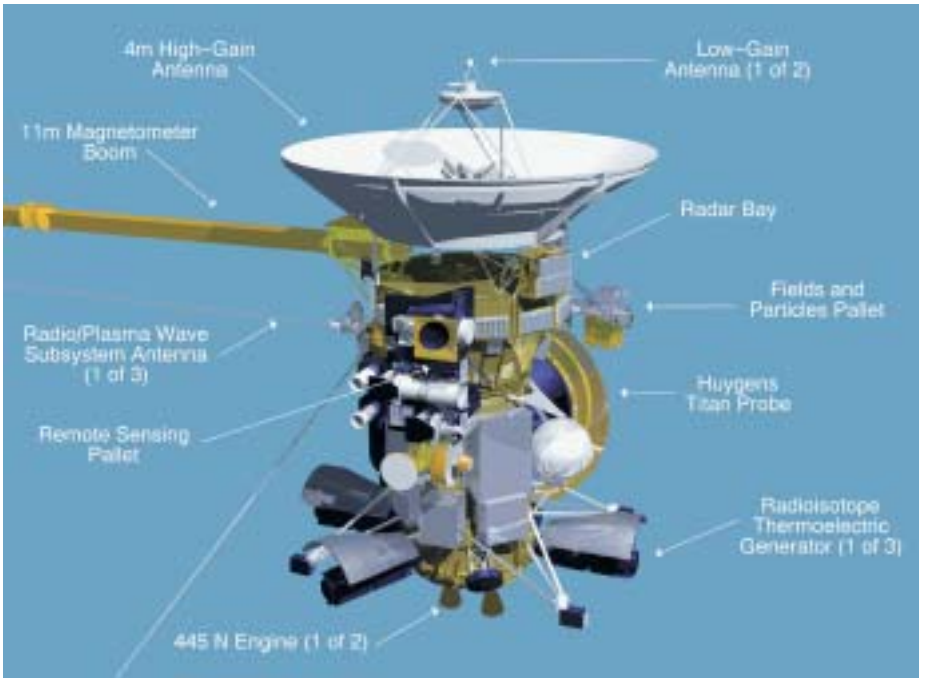

Figure 2.4.4. The Cassini/Huygens spacecraft and its principal features.

Table 2.4.4. Mass breakdown of the Cassini/Huygens spacecraft.

Orbiter (dry, inc. payload)	2068 kg
Probe (inc. 44 kg payload)	318 kg
Probe Support Equipment	30 kg
Launch adaptor	135 kg
Bipropellant	3000 kg
Monopropellant	132 kg
Launch mass	5683 kg

use the HGA. The main elements of the Cassini/Huygens spacecraft are illustrated in Figure 2.4.4. The mass budget of the spacecraft is shown in Table 2.4.4.

Huygens flight operations

After separation from the Orbiter, the Probe will operate autonomously, the radio relay link to the Orbiter being one-way for telemetry only. Up to that point, telecommands can be sent via an umbilical link from the Orbiter, but this facility will be used only during the cruise and Saturn orbit phases for monitoring the health of the subsystems and calibrating the instruments during the 6-monthly checkouts. Huygens does not perform scientific measurements before arrival at Titan and for most of the cruise the Probe is switched off. It is activated only for a 3 h period for the biannual checkouts. During the 22-day coast phase after separation from the Orbiter, only a timer will operate to activate the Probe shortly before the predicted entry into Titan's atmosphere. Loading the value of this timer's duration and depassivating the batteries that power the Probe after separation will be the last activities initiated by command from the ground.

The Probe flight operations, and the collection of telemetered data, are controlled from a dedicated control room, the Huygens Probe Operations Centre (HPOC) at ESOC (Darmstadt, Germany). Here, command sequences are generated and transferred by dedicated communication lines to the Cassini Mission Operations Center at JPL. There, the Probe sequences are merged with commands to be sent to other subsystems and instruments of the Orbiter for uplink via NASA's Deep Space Network (DSN). Probe telecommands are stored onboard the Orbiter and forwarded to the Probe Support Equipment (PSE) at specified times (time tags) for immediate execution. Because of the great distance of Saturn from Earth (requiring up to 2.5 h for round-trip radio communication) real-time operations are not possible during the Probe descent.

Data collected by the Probe and passed to the PSE via the umbilical (during the

cruise) or the relay link (during the descent) will be formatted by the PSE and forwarded to the Orbiter's Command and Data Subsystem (CDS). The Orbiter stores all data on solid-state recorders for transmission to Earth at times when it is visible from one of the DSN ground stations. From the ground station, the data are forwarded to JPL, where Probe data are separated from other Orbiter data before being stored on the Cassini Project Database (PDB). HPOC operators access the PDB to retrieve Probe data via a Science Operations and Planning Computer (SOPC), supplied to ESOC by JPL under the terms of the interagency agreement.

Probe subsystem housekeeping data are used by ESOC to monitor the performance of the Probe, while data from the science instruments are extracted for forwarding to the investigators. During the cruise phase, these data are shipped to the scientists' home institutes by public data line or on CD-ROMs. After analysis of these data, the investigators meet the operations team to review the results of the previous checkout and to define the activities for the following checkout period. During the Saturn orbit and Probe mission phases, the investigators will be located at HPOC to expedite their access to the data and facilitate interaction with their colleagues and the Probe operators. Accommodation will be provided for the ground support equipment they need to reduce and interpret their data.

All in-flight Probe activities are prepared very carefully as any mistake could endanger its mission performance. Each checkout sequence is tested on the Probe Simulator and then on the Engineering Model (EM), installed in HPOC. The EM has been retrofitted with flight spare computers and the instrument interfaces have been upgraded to flight standard. If required, the EM Probe will be used as a testbed to validate any modification to the Probe's onboard software.

Status

Venus, Earth and Jupiter encounters

Unique science observations were made during the second Venus encounter (24 June 1999), the Earth encounter (18 August 1999) and the 6-month Jupiter flyby campaign (October 2000 to March 2001). Results were published in 'First Results from Cassini: Venus and Earth Swing-Bys', *J. Geophys. Res.*, vol. 106, Dec. 2001, and in *Nature* 'Cassini at Jupiter', 28 Feb. 2001.

Saturn Orbiter

After the very successful launch and injection of Cassini/Huygens on its interplanetary trajectory, Cassini/Huygens performed four nominal planet flybys: Venus-1 (26 April 1998), Venus-2 (24 June 1999), Earth (18 August 1999) and Jupiter (30 December 2000). The flight performances of the spacecraft are excellent. The Orbiter software for the two critical sequences, the SOI manoeuvre and the Probe Relay Link mission, is under design.

Huygens Probe

Nine inflight checkouts have been conducted. The payload and subsystem performance have been as expected. An end-to-end test of the Probe relay link was carried out in February 2000, using a DSN antenna to transmit a simulated Probe radio signal. This test uncovered a malfunction in the Huygens radio receivers. After intensive investigations supported by further inflight and ground tests, it was found that, owing to a design flaw, the bandwidth of the bit synchroniser of the Huygens radio receivers was too narrow. It could not cope with the expected Doppler shift from the relative displacement between the two spacecraft during the Probe mission. It would have led to significant Huygens data loss, but a change in the Orbiter trajectory and other changes in Probe operations will allow recovery of the full Probe mission.

2.5 XMM-Newton

Introduction

The XMM-Newton observatory, formerly known as the high-throughput X-ray spectroscopy mission, was successfully launched on 10 December 1999 from Kourou, French Guiana on the first commercial Ariane-5 (V504). The mission is now routinely producing high-quality data and will complete the guaranteed time and open time observations (from AO-1) by end-2002. The mission, which was originally approved for operations until end-March 2002, was approved for a further 4 years of operations by ESA's Scientific Programme Committee in December 2001.

Status

The initial operational efficiency for XMM-Newton was fairly low. This was mostly driven by instrument operations overheads, and the lack of full orbital coverage of the spacecraft's telemetry. Following a large number of changes in the mission's ground segment at the end of 2000 and in early 2001, the operations efficiency rapidly increased to its current value of almost 70% (the maximum achievable). Simultaneously with the increase in operations efficiency, the generation and shipment of data and standard data products picked up speed.

European Photon Imaging Camera (PI: M. Turner, Leicester University, UK)
A European Photon Imaging Camera (EPIC) detector is positioned behind each of the three X-ray mirror modules. Two MOS-CCD cameras share the mirrors with the grating array, while the PN-CCD detector is located behind the fully open telescope position. The in-orbit performance of the EPIC cameras is excellent. The degradation of the camera from irradiation by (mostly solar) protons is as predicted pre-launch. The EPIC cameras are particularly powerful for weak extended X-ray emission sources, such as clusters of galaxies, and many exciting results are already available. As an illustration of the collecting power of XMM-Newton observatory, Figure 2.5.1 shows the results from a 100 ks observation of the Lockman Hole. Besides a wealth of previously unknown point sources and extended emission, it also illustrates XMM-Newton's ability for performing X-ray spectroscopy on fairly faint sources.

Reflection Grating Spectrometer (PI: J. Kaastra, SRON, The Netherlands)
The Reflection Grating Spectrometer (RGS) is a powerful, large-area detector that allows XMM-Newton to take X-ray spectra with an E/ΔE of 300-700 (1st order) in the 5-35 Å (0.35-2.4 keV) soft X-ray band. The effective area for the two grating arrays is in the range 40-200 cm^2 over this wavelength band. The instrument's in-orbit performance is as predicted, although two of the 18 detector readout chains failed early on in the mission, leaving the throughput in two limited energy bands a factor of two lower than predicted. However, the RGS wavelength range has not been compromised, and excellent results are being obtained.

Optical Monitor (PI: K. Mason, Mullard Space Science Laboratory, UK)
The Optical Monitor (OM) is a powerful telescope in the 170-600 nm wavelength band, able to detect sources down to 24th magnitude in a few thousand seconds (depending on spectral type). This camera is powerful enough, both in sensitivity and positional accuracy, to identify the optical counterparts of many of the new X-ray sources be detected by XMM-Newton.

The analysis of XMM-Newton data is supported by the Science Analysis System (SAS) software package that is released twice a year and that allows users to derive reliable calibrated results for further analysis with standard X-ray astronomy spectral analysis packages. The derivation of accurate calibration data, and the proper incorporation of this knowledge into the SAS software is a continuous process. The status

For further information, see http://sci.esa.int/xmm

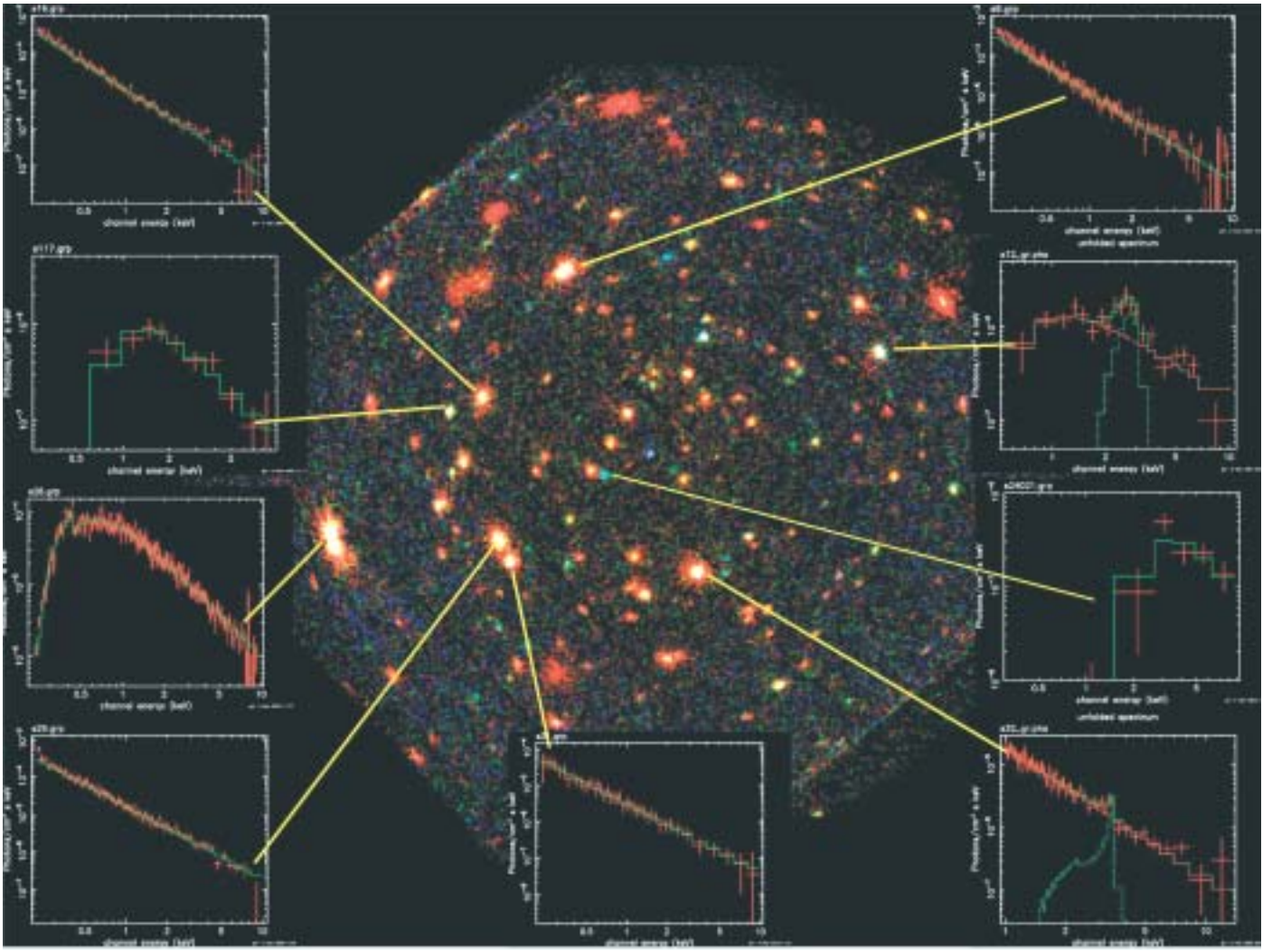

Figure 2.5.1. The Lockman Hole, showing excellent spectra, even for faint sources.

of the calibration is now such that most (spectral) parameters can be derived to an absolute accuracy better than 5%.

Science results

XMM-Newton results are already impacting many areas of science. Its ability to enable progress in many fields of astrophysics is illustrated below.

Active Galactic Nuclei

The high spectral resolution and throughput of RGS made it possible to map the gas in the violent environment of Active Galactic Nuclei (AGN). XMM-Newton has seen the signatures of the accreting gas very close to the central black hole and demonstrated, in some cases, that the space-time around the black hole is rapidly rotating. The warm wind emanating from the central regions was found to contain significantly less gas than previously thought to be present in many of these galaxies. These winds show a very broad range of variation in ionisation and dynamical state amongst different AGN. XMM-Newton has just begun to explore this parameter

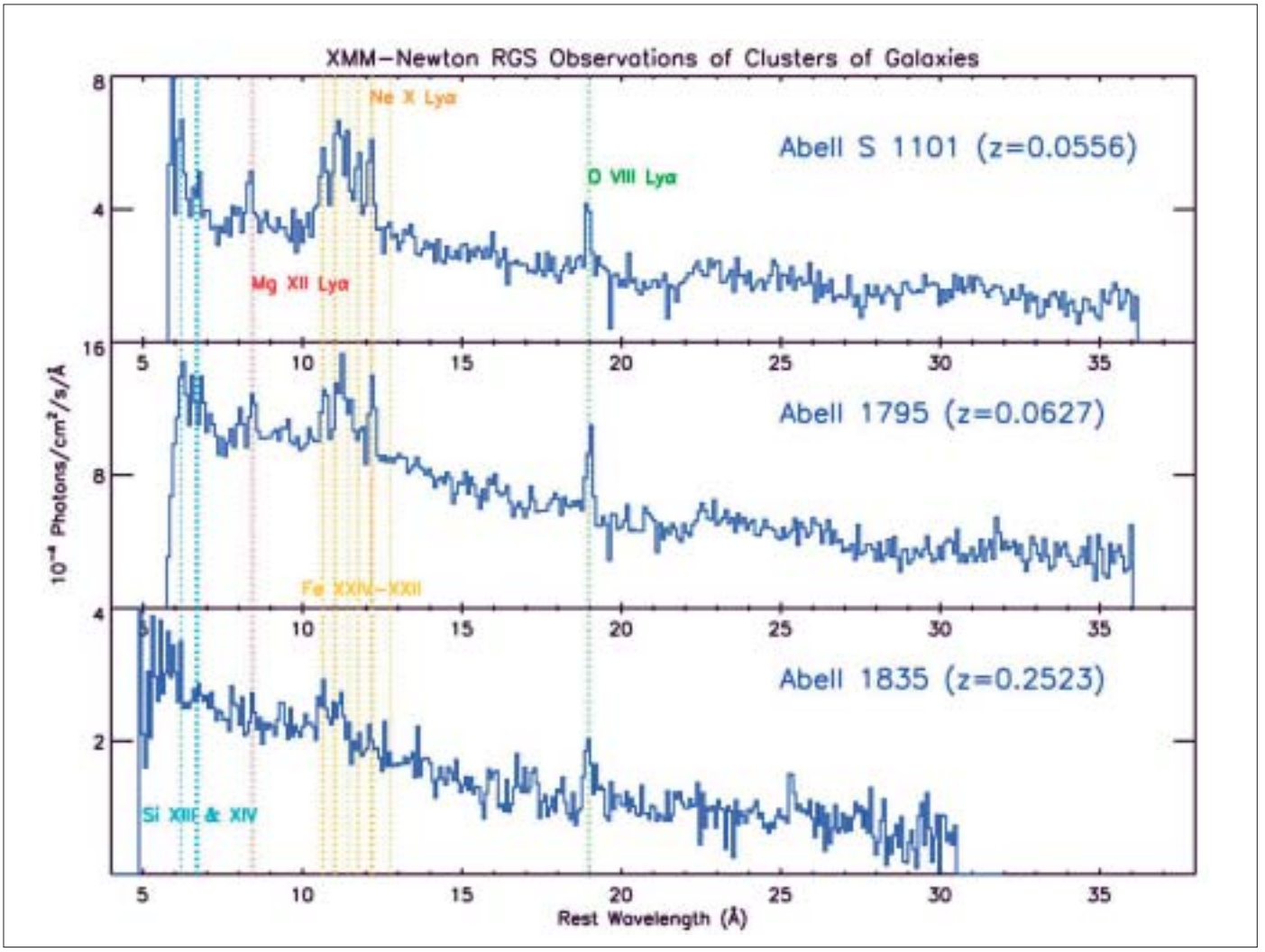

Figure 2.5.2. RGS spectrum of three 'cooling flow' clusters, illustrating the absence of cool material.

space and has shown its ability to resolve the wind into components with different ionisation and dynamical states, thereby significantly contributing to the unravelling of the complex astrophysics around black holes.

Clusters of galaxies

The high spectral resolution and sensitivity offered by XMM-Newton has broadened our knowledge about clusters of galaxies in several ways. Using the imaging spectroscopy provided by the EPIC instruments, it is now possible to resolve the radial abundance and temperature gradients in the outer parts of clusters, thereby tracing the chemical and dynamical history of these clusters. At the same time, the temperature drop in the centre of clusters can now be studied with high spectral resolution via RGS. Most of the cooling-flow clusters studied so far have no significant emission from Fe XVII and Fe XVIII ions in their X-ray spectra (Figure 2.5.2). This implies a deficit of cool gas in comparison with simple isobaric cooling flow models.

Figure 2.5.3. Coma cluster mosaic.

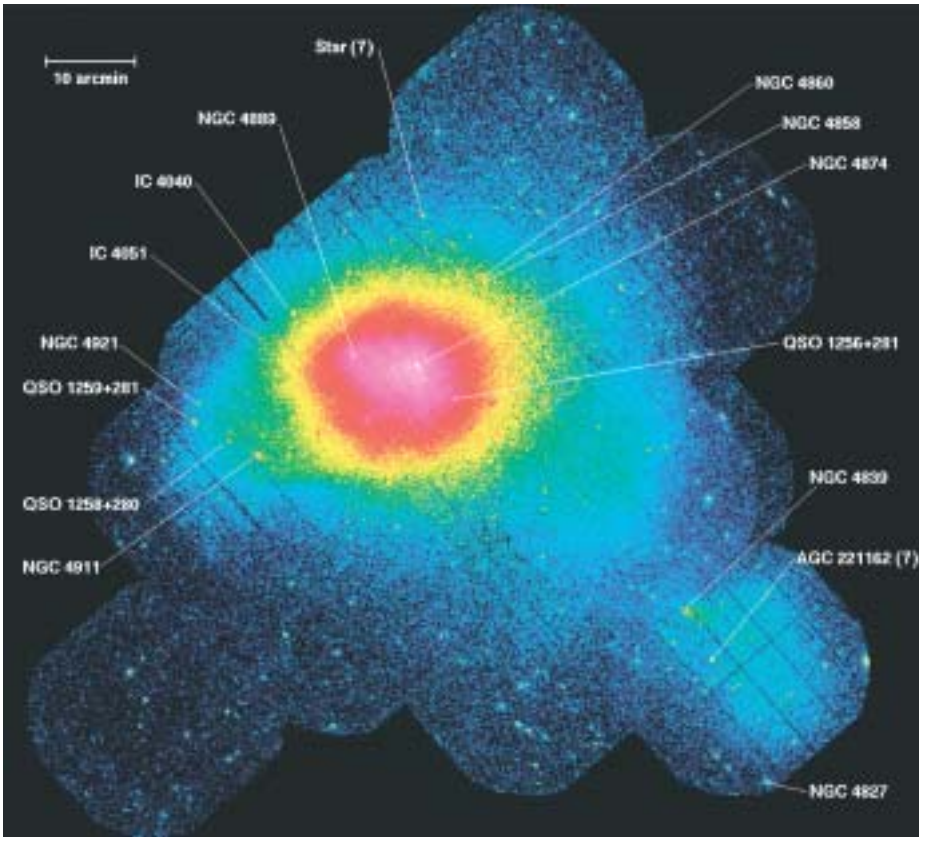

Another example of XMM-Newton's contribution to cluster physics comes from a set of mosaic-like observations of the Coma cluster, using the power of the EPIC cameras – a combination of high-throughput with medium spatial resolution (Figure 2.5.3). The images reveal structures associated with galaxies (or galaxy groups) being drawn into the cluster core by the cluster's gravitational potential well, and permit the determination of parameters such as matter density and infall velocity.

XMM-Newton will observe more clusters, at the faint and cosmologically distant side of the spectrum, in order to significantly further our understanding of the formation and evolution of clusters.

Supernova remnants

The combination of medium spectral resolution imaging by EPIC with high-resolution spectroscopy by RGS is extremely useful for the study of supernova remnants. For the first time, it is possible to resolve simultaneously the most important line complexes for all chemical elements from the CNO group up to argon, calcium and iron. This allows the detailed study of the precursor of the supernova as well as its surroundings. In several supernova remnants, not only have the spatial distribution and kinematics of the shocked gas been explored but also, thanks to XMM-Newton's sensitivity, the distribution of non-thermal radiation has been traced in detail (Fig. 2.5.4). During the coming years, XMM-Newton will study and resolve the state, composition and distribution of the shocked gas in many more remnants. It

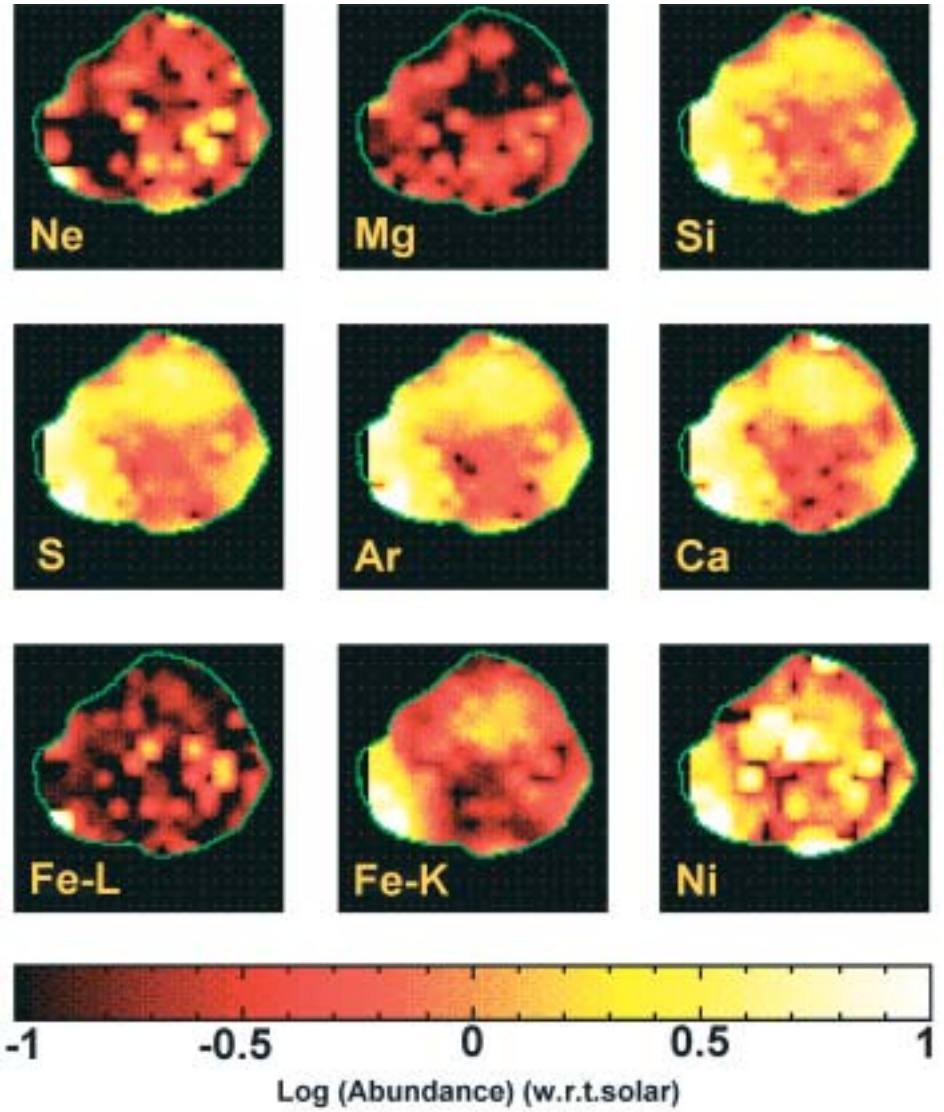

Figure 2.5.4. Cas-A elemental abundance maps.

will thus deepen our understanding of the end products of stellar evolution as well as the dynamical interaction of these products with the interstellar medium.

X-ray background

The background glow of X-rays from all over the sky has puzzled astrophysicists since its discovery in 1962. The ROSAT observatory found that the *soft* X-ray background is made up of Active Galactic Nuclei (massive black holes at the centres of galaxies), but did not solve the main problem because most of the energy comes from harder X-rays. XMM-Newton has finally found the answer. With unrivalled sensitivity at these energies, it has shown that the harder X-ray background actually comprises a mixture of sources. The bulk of the emission comes from black holes, which cannot be seen at the soft X-ray wavelengths of previous observatories. Over the next few years, these studies will investigate the spectra of the many detected

sources in detail, as well the potential for large-scale structure in the log N–log S distribution.

Science highlights

A number of papers on XMM-Newton results were of such importance that they were also issued as press releases, drawing the attention of the international media.

On 22 October 2001, ESA/NASA issued a press release on an XMM-Newton observation of the bright Seyfert 1 galaxy MCG-6-30-15, where the broad Fe Ka line at ~6 keV and the associated reflection continuum were shown to originate from the inner accretion disc. The observed reflection features are extremely broad and red-shifted, indicating they originate from the innermost regions of the accretion disc. It seems likely that this source was observed in the 'deep minimum' state. The implied central concentration of X-ray illumination is difficult to understand in any pure accretion disc model. The paper suggested that we are witnessing the extraction and dissipation of rotational energy from a spinning black hole by magnetic fields connecting the black hole or plunging region to the accretion disc.

On 4 April 2002 a paper was published in *Nature* describing the results of an XMM-Newton observation of a gamma-ray burst (GRB). Since their identification with cosmological distances, GRBs have been recognised as the most energetic phenomena in the Universe, with an isotropic energy as high as 10^{54} erg. However, the progenitors responsible for the bursts remain elusive, with favoured models ranging from a neutron-star binary merger to the collapse of a massive star. Crucial to understanding the origins of GRBs is the study of the afterglow emission, where spectroscopy can reveal details of the environment of the burst. Following an XMM-Newton observation of the X-ray afterglow of GRB 011211, it was shown that the X-ray spectrum reveals evidence for emission lines of magnesium, silicon, sulphur, argon, calcium and possibly nickel, arising in enriched material with an outflow velocity of order 0.1 c. This was the first direct measurement of outflowing matter in a gamma-ray burst. This observation strongly favours models where a supernova explosion from a massive stellar progenitor precedes the burst event and is responsible for the outflowing matter.

2.6 Cluster

Introduction

The four Cluster spacecraft were launched in pairs by two Russian Soyuz rockets on 16 July and 9 August 2000. On 14 August, the second pair joined the first in highly eccentric polar orbits, with apogees of 19.6 Earth radii and perigees of 4 Earth radii. The highly accurate orbital injection and low propellant consumption meant that spacecraft operations can continue for 3 years after the nominal 2-year mission.

This is the first time that Earth's magnetic field and its environment is being explored by a constellation of four identical spacecraft (Figure 2.6.1). Preliminary results show that with four spacecraft we can obtain a detailed, 3-D view of the Sun-Earth connection processes taking place at the interface between the solar wind and Earth's magnetic field. Cluster is one of the two missions (the other being SOHO) constituting the Solar Terrestrial Science Programme (STSP), the first Cornerstone of ESA's Horizons 2000 Programme. With the successful launches of the rebuilt Cluster satellites, the STSP Cornerstone is complete and it is possible to exploit these two missions scientifically in order to study the full chain of processes from the Sun's interior to the Earth.

At its meeting in February 2002, ESA's Science Programme Committee (SPC) approved the extension of the mission for a period of 35 months (up to end-2005). In addition, the SPC agreed to double the amount of data acquired along the orbit using a second ground station. This allows continuous coverage and promises to enhance greatly the scientific output of the mission.

Status

Once in orbit, a lengthy verification phase of all spacecraft subsystems and the payload of 44 instruments (Table 2.6.1) began. The 16 solid booms, eight for the magnetometers and eight for communications, were deployed. A few days later, the

Figure 2.6.1. The four Cluster spacecraft each carry 11 instruments. ASPOC (1), CIS (2), EDI (3), FGM (4), PEACE (5), RAPID (6), DWP (7), EFW (8), STAFF (9), WBD (10), WHISPER(11).

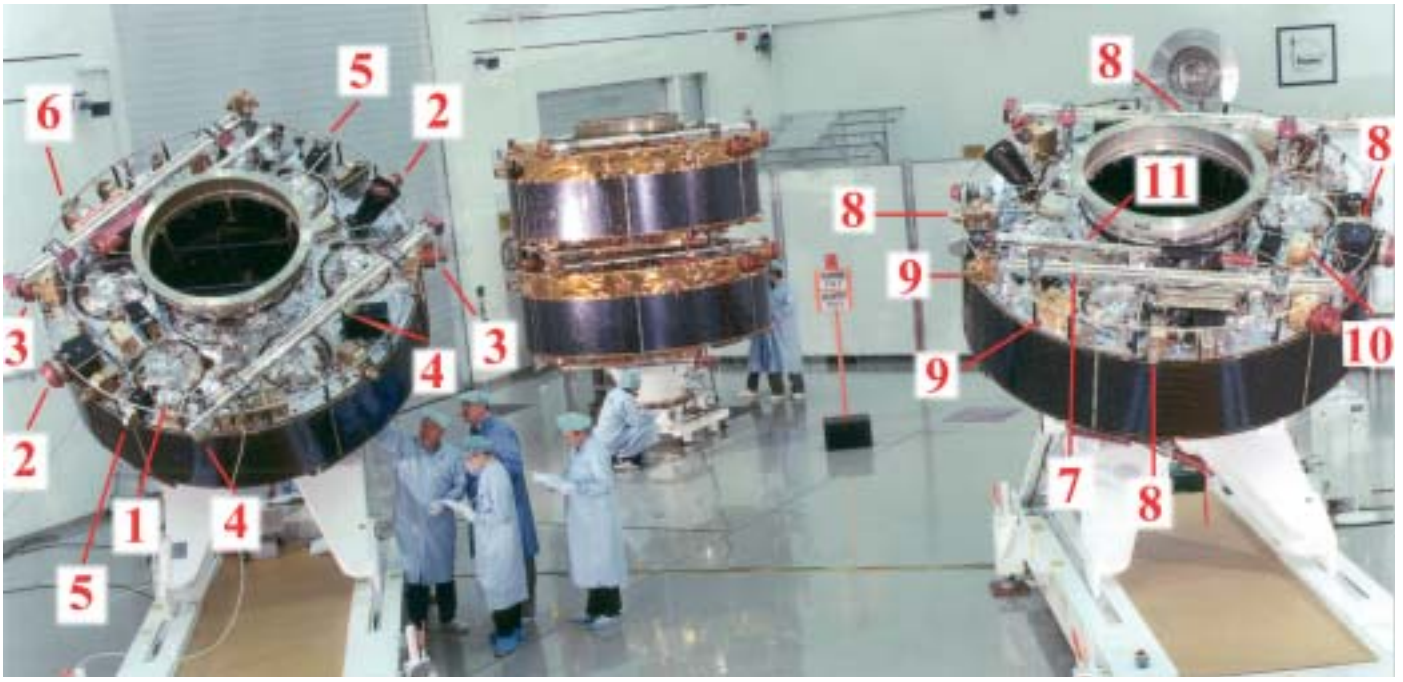

For further information, see http://sci.esa.int/cluster

Table 2.6.1. The Cluster payload.

Acronym/Instrument	*Principal Investigator*
FGM/Fluxgate Magnetometer	A. Balogh (IC, UK)
STAFF*/Spatio-Temporal Analysis of Field Fluctuation experiment	N. Cornilleau-Wehrlin (CETP, France)
EFW*/Electric Field and Wave experiment	M. André (IRFU, Sweden)
WHISPER*/Waves of High Frequency and Sounder for Probing of Electron density by Relaxation	P. M. E. Décréau (LPCE, France)
WBD*/Wide Band Data	D.A. Gurnett (Iowa U., USA)
DWP*/Digital Wave Processing experiment	H. Alleyne (Sheffield U., UK)
EDI/Electron Drift Instrument	G. Paschmann (MPE, Germany)
CIS/Cluster-II Ion Spectrometry	H. Rème (CESR, France)
PEACE/Plasma Electron and Current Experiment	A. Fazakerley (MSSL, UK)
RAPID/Research with Adaptive Imaging Particle Detectors	P. Daly (MPAe, Germany)
ASPOC/Active Spacecraft Potential Control	K. Torkar (IWF, Austria)

* Members of the Wave Experiment Consortium (WEC)

spacecraft had to survive the first long eclipses, with up to 4 h of darkness, which they did with very good performance from the batteries. Then the verification phase for the 11 sets of instruments started. This phase was complicated by the fact that, in order to perform their measurements, some instruments had to deploy very long wire antennas. These 44 m-long antennas altered the spin rate of the spacecraft, which was incompatible with the particle instruments that needed a fixed spin rate. Altogether, more than 1100 individual tasks were performed on the instruments. At the end of this phase, in early December 2000, a 2-week interference campaign was conducted to test potential interference between the instruments. After successfully testing all the instruments, the nominal operations phase started on 1 February 2001.

After a year of nominal mission, the spacecraft and instruments are in good shape to continue the collection of data. During the first half-year, the inter-spacecraft distance was chosen to be 600 km to study small-scale structures in the polar cusp and bow shock regions. Then the spacecraft thrusters were fired to change the orbits slightly to increase the inter-spacecraft distance to 2000 km. This allowed the investigation of the magnetotail at larger scales. In January 2002, the separation was reduced to 100 km to study the cusp and bow shock at very small scales (this will be the smallest distance achieved by Cluster). Figure 2.6.2 shows the inter-spacecraft distances planned for the 2-year nominal mission and the 35-month extension, varying from 100 km to 20 000 km.

Science highlights

The prime scientific objective of Cluster is to derive physical quantities, such as the electric current density and electron density gradients, that can be obtained only by combining measurements from the four spacecraft. A first example where this has been achieved was obtained in a Flux Transfer Event (FTE) close to the external boundary of the Earth's magnetic field (Figure 2.6.3). An FTE is a magnetic flux tube

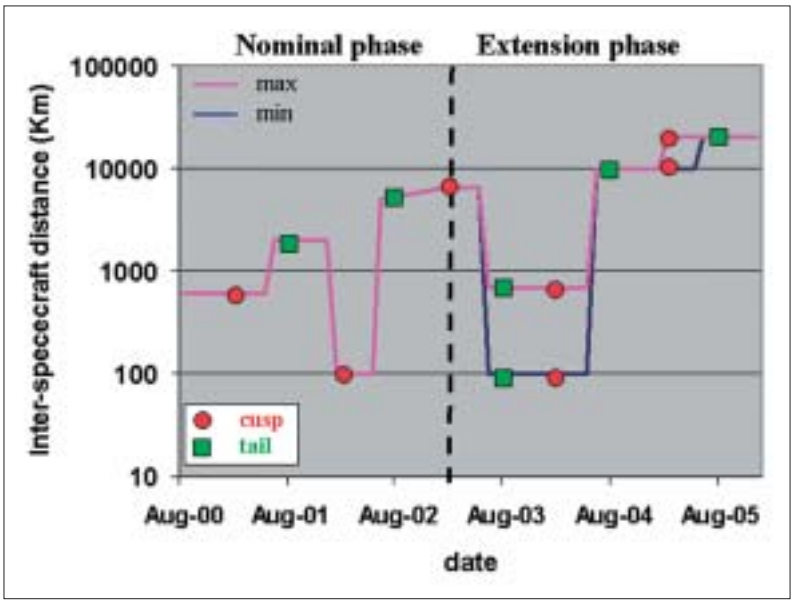

Figure 2.6.2 (above). Spacecraft separation during the nominal and extended mission. The minimum and maximum are indicated. The exact distance will be determined about 9 months before the event.

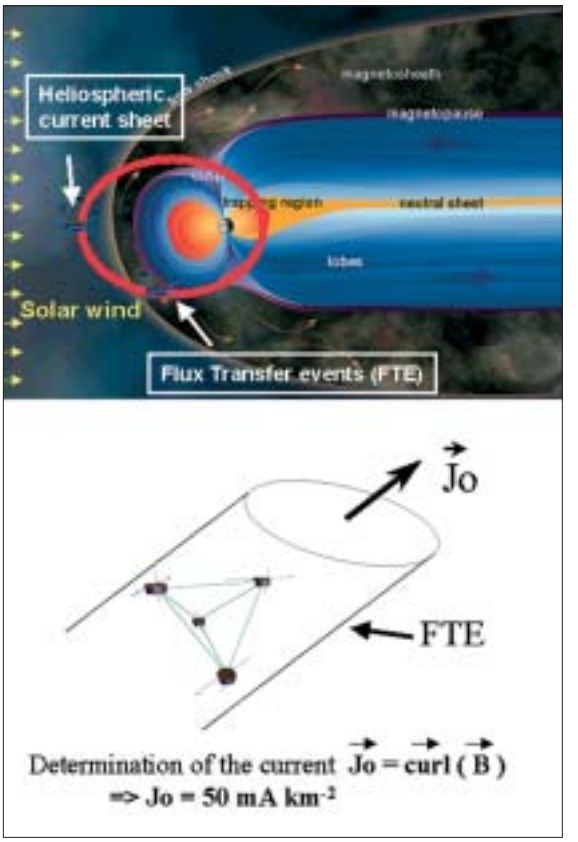

Figure 2.6.3 (right). Top panel: the Cluster orbit in the magnetosphere. The position along the orbit where the electric current was calculated is indicated. Bottom panel: sketch of a flux transfer event (FTE) and the four Cluster measuring the magnetic field.

that is connected, by magnetic reconnection, on one side to the Earth and on the other side to the solar wind. The 4-point magnetic field measurements have given a maximum electric current density of 50 mA km^{-2} in the flux tube. Never before have these currents been measured with such precision and without any assumption about the current structure. This new finding has important implications for modelling these structures, and how energy flows from the solar wind to the magnetosphere. Another example was obtained in the heliospheric current sheet, which is the large-scale surface dividing the heliosphere into two hemispheres of oppositely directed magnetic fields. There, a maximum current density of 10 mA km^{-2} was obtained. Finally, the plasma density has been measured with the four spacecraft during the crossing of the magnetopause, allowing the gradient of density to be deduced. It was observed that the vector of the gradient density was opposite to the magnetopause motion. All these methods will be applied to other regions of space and will further our understanding of the complex mechanisms involved in the Sun-Earth relation.

A unique feature of the Cluster mission is the possibility for measuring structures in three dimensions. The external boundary of Earth's magnetic field – the magnetopause – is the place were the solar wind interacts with Earth's environment. The solar wind is blowing on Earth's magnetic field like the wind on a lake, creating waves on the surface. Such waves detected by Cluster are shown in Figure 2.6.4. The waves travel through space much faster than the Cluster spacecraft. As they sweep past the four closely-spaced satellites, instruments detect changes in the magnetic and

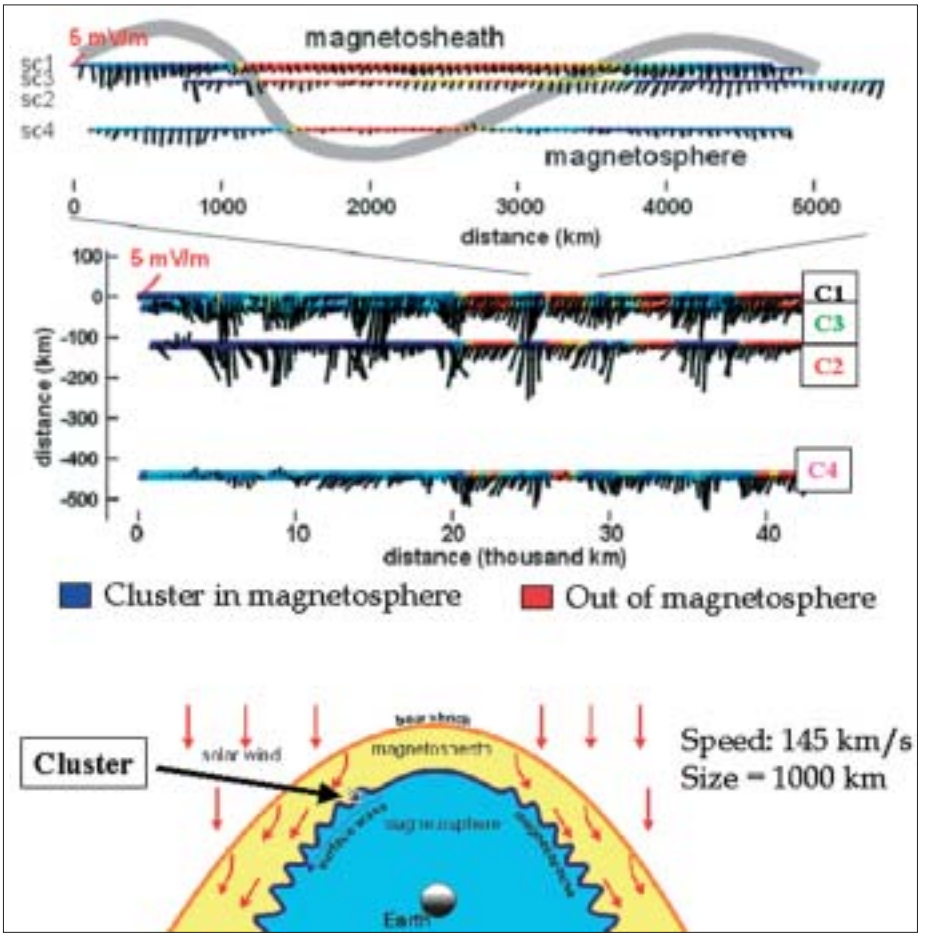

Figure 2.6.4. The electric field measured by four spacecraft and the shapes of waves. Here, the colour of the four horizontal lines on each panel shows the potential of the electric field detected by each spacecraft. Red corresponds to plasma in the magnetosheath (shocked solar wind) region and blue to plasma inside the magnetosphere. The grey curved line shows schematically the size and shape of the waves. The short black lines show the electric field measurements. The top panel is a more detailed view of part of the overall observations, covering a horizontal distance of about 5000 km. The lower panel shows observations over a horizontal distance of about 40 000 km. Note that, during the observation, the satellites moved only about 550 km. (It is the wave that passes the satellites). The bottom panel is a sketch of the waves propagating along the magnetopause. (Figure courtesy of M. Andre and A. Vaivads, Uppsala, S).

electric fields. These regular changes show that a series of 'steep' waves is sweeping past the spacecraft. The measurements indicate that the waves are about 500 km across and travel through space at about 145 km/s.

Close to perigee, the four spacecraft do not forming a tetrahedron but follow each other like a 'string of pearls'. In that configuration, we can observe *in situ*, for the first time, the evolution of auroral structures. The evolution of the electric field structure responsible for the black aurora, a kind of anti-aurora, was observed for the first time with the four spacecraft following each other at 100 s intervals (Figure 2.6.5). The structure was observed to be growing over a time scale of 3 min and then disappearing. Understanding the development and growth of dynamic structures associated with the aurora is a major goal of the Cluster mission, and something that cannot be solved by single-satellite measurements.

Other science highlights include:

Short Large Amplitude Magnetic Pulsations (SLAMPs) have been observed at the parallel bow shock. Despite both theoretical and previous timing-inferred estimates of SLAMP sizes above 3000 km, the 4-spacecraft resolution reveals considerable spatial variability on scales below 600 km.

The thickness of the magnetopause current layer was estimated to be about

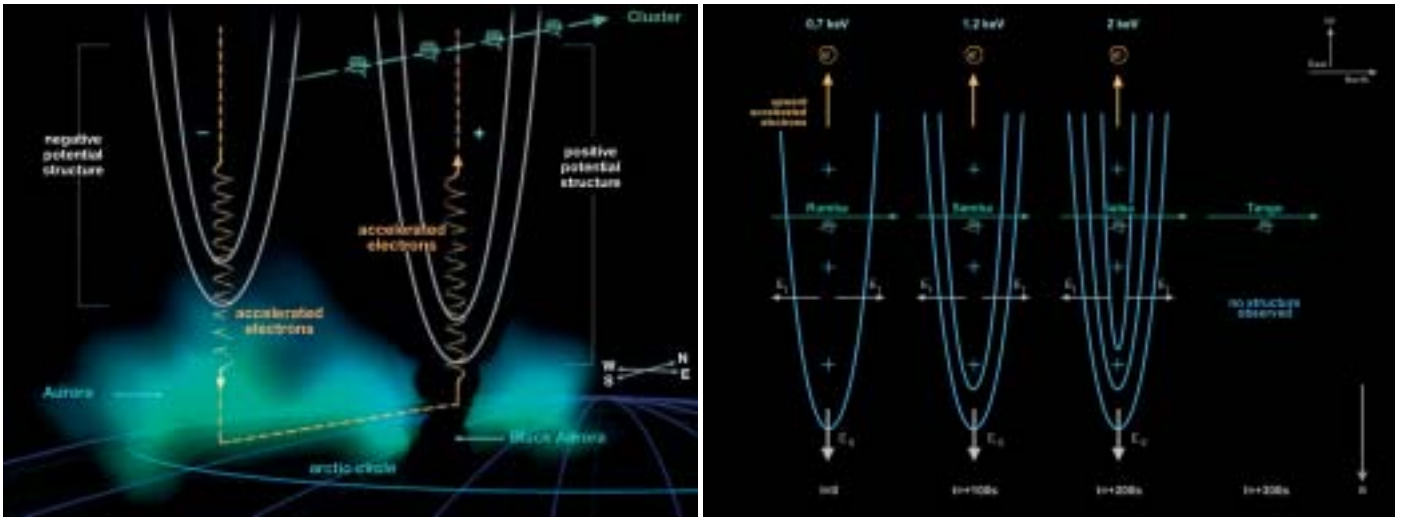

Figure 2.6.5. The black aurora observed by Cluster. Left: the data show that black aurorae represent holes in the ionosphere. Here, negatively charged electrons are being accelerated upwards into space inside regions known as positively charged electric potential structures. This is the opposite process to that which creates visible aurorae, where electrons spiral down from space into the atmosphere within similar, negatively charged, structures. Right: Cluster observed the electric field structure responsible for the black aurora growing in time and disappearing (from Marklund et al., *Nature*, 2001).

200 km. One surprising result on an individual crossing showed that the magnetopause was impermeable to the solar wind at that location. On another occasion, the magnetopause was observed to be associated with plasma jets, indicating magnetic reconnection. The fact that jets were detected each time a spacecraft crossed the magnetopause indicates that reconnection must have happened continuously, although not necessarily at a fixed rate.

Above the northern and southern pole, the polar cusps are the windows through which the solar wind can enter directly and reach Earth's ionosphere. They are characterised by a minimum in the magnetic field, plasma injections and strong turbulence. The four spacecraft measured for the first time the motion of the cusps at around 90 km/s. At mid-altitude, the cusps could also be observed by Cluster with the spacecraft following each other. There, an interesting phenomenon was observed: three spacecraft detected a normal cusp, while the fourth found a double cusp.

The tail of the magnetosphere, where geomagnetic substorms are initiated, was studied with a spacecraft separation of 2000 km. Ion flows and magnetic dipolarisation play a key role in substorms. For the first time, Cluster observed that the main direction of the flow was along the dipolarisation plane.

Another aurora result was obtained using very long baseline interferometry with the four spacecraft. For the first time, the source of the acceleration of electrons in the aurora could be located. It was shown to match perfectly a bright spot on the aurora images obtained by the Polar spacecraft.

Finally, the plasmasphere, an inner region of the magnetosphere, has been observed with Cluster in unprecedented details. The Cluster spacecraft, in a string-of-pearlss configuration, showed that the structures at its boundary are remarkably stable and that wave emissions are observed very close to the magnetic equator in low-density cavities.

Cluster Science Data System

The Cluster Science Data System (CSDS) is designed as a distributed system consisting of eight nationally funded and operated data centres. It makes possible the joint scientific analysis of data from all 44 instruments (four sets of 11). The general approach is to have national data centres near the Principal Investigators (PIs) and thus near the expertise required for processing the data. CSDS also serves to some

extent as the infrastructure for the Joint Science Operations Centre (JSOC), which is a staffed facility located at the Rutherford Appleton Laboratory (UK), to support the scientific payload operations.

The data centres produce data products on behalf of the national PI teams. Members of the Cluster science community wishing to access CSDS do so via their national data centre. In those countries not served by a national data centre, members of the Cluster community may contact the relevant PI to determine which data centre should be contacted. It should be noted that all data centres offer the same data products. Scientists from outside the Cluster community also have access to CSDS, according to the policy on data rights as agreed by the PIs. Full access can be granted to the Summary Parameters and CSDSweb.

One of the major tasks of CSDS is to offer, as a routine, a variety of products:

Prime Parameter Data Base (PPDB): 65 parameters are contained in this database. The data files are written in the Common Data Format (CDF) and are held in physical units with an exhaustive set of ancillary information (or metadata). The PPDB holds data from all four spacecraft with a time resolution of 4 s. The data set is accessible by all Principal and Co-Investigators.

Summary Parameter Data Base (SPDB): 86 parameters are contained in this data base. These files are also written in the Common Data Format and are held in physical units with an exhaustive set of ancillary information. The SPDB only holds data from one of the four spacecraft with a time resolution of about 60 s. Aaccess is not restricted.

Summary Plots: plots of summary parameters with 1 min resolution used to search for interesting events. The German Data Centre produces these plots as Postscript files centrally and distributes them to the other data centres. The plot information is encoded in a compact form for sending it over the network.

CSDSWeb: quicklook plots of the latest data (a few hours to a few days after acquisition) are provided from one spacecraft, including particle and wave spectrograms, as gif files. The plots cover 6 h and a full orbit (2.5 days). These data are available to the general science community.

The CSDS was opened on 1 February 2001. The access to data started with a download rate of 700 Mbytes/month and increased steadily at an average rate of about 150 Mbytes per month. The CSDSweb plots download rate has increased smoothly, indicating that users regularly download these products. The summary and prime parameters data access shows peaks before major events, e.g. one in September 2001 before a Cluster workshop held at ESTEC and one in November 2001 before the American Geophysical Union meeting. More information and data access can be found at *http://sci2.estec.esa.nl/cluster/csds/csds.html*

3. Missions in Post-Operations/Archival Phase

3.1 ISO

Introduction

By May 1998, at the end of its 2.5-year operational life, ESA's Infrared Space Observatory (ISO) had made nearly 30 000 scientific observations, employing its four sophisticated and versatile scientific instruments to provided astronomers with diverse data of unprecedented sensitivity at IR wavelengths of 2.5-240 µm. By covering this wavelength range, ISO was able to explore regions of the Universe obscured in visible light. IR light penetrates the obscuring dust that hides much of the Universe from inspection at visible wavelengths, and light of these wavelengths originates from bodies and material that are cool and distinct from the energetic sources of visible light, like stars. But these cool sources are of fundamental importance. A rich variety of atomic, ionic, molecular and solid-state spectral features trace the chemistry and evolution of the cold gas and dust from which the stars form, and which they in turn enrich with the heavy elements produced during their nuclear burning and terminal phases. New generations of stars and planets form from the enriched interstellar medium, revealing their presence first through the IR emission associated with proto-stellar and proto-planetary sources. Most of the star formation in the history of the Universe is revealed through the IR emission of the heated dust clouds which would otherwise hide it from our view.

The two spectrometers, a camera and an imaging photo-polarimeter jointly covered wavelengths from 2.5 µm to around 240 µm with spatial resolutions ranging from 1.5 arcsec (at the shortest wavelengths) to 90 arcsec (at the longer wavelengths). All went very smoothly in orbit and, at a wavelength of 12 µm, ISO was a thousand times more sensitive and had a hundred times better angular resolution than IRAS. Routine scientific operations began in February 1996 and continued until April 1998, with limited operations continuing through May. All data were reprocessed with the end-of-mission calibration to populate the first homogeneous ISO Data Archive, which opened to the community in December 1998. By August 1999, all data had entered the public domain.

Through the ensuing 4 years of the post-operations phase, ESA's ISO Data Centre developed and refined the ISO Data Archive to offer the ISO data to the worldwide astronomical community and, together with the several National Data Centres in various member states and in the US (see footnote p52), worked to fill the archive with the best systematically processed and calibrated data products that could be achieved for the huge ISO database. These products allow users to select from the archive data sets of interest for deeper study with interactive analysis tools. ISO's Legacy Archive, containing this reference product set, was released at the end of February 2002.

During ISO's Active Archive Phase, which will run from January 2002 to December 2006, the ISO Data Centre will continue to work with active National Data Centres in The Netherlands, Germany and the UK to support the community in its use of the ISO data and to leave behind a homogeneous archive as a legacy to future generations of astronomers, especially those preparing and interpreting Herschel observations. Particular emphasis will be placed on the opportunity represented by the growing mass of published ISO data to gather into the archive the refined data products upon which astronomers have based their published work. In this way, we will fill the archive with immediately reusable refined data products, so preparing the ISO archive for its role as part of a system of interoperable archives forming the 'virtual observatories' of the future.

ISO science

ISO broke new ground on all scales. Through new asteroid counts and improved asteroid thermophysical models, along with important advances in Solar System chemistry, it returned a striking body of results addressing our planetary system. ISO permitted comparison of stellar spectra with cometary spectra, which revealed

For further information, see http://www.iso.vilspa.esa.es

Figure 3.1.1 (left). ISO found abundant carbonates in the Red Spider Nebula, which is seen in this HST image, and which harbours one of the hottest stars in the Universe. Planetary nebulae are the glowing embers of ordinary stars, such as our Sun. At the end of their lives, these stars expel most of their material into space, often forming a double-lobed structure, as in the case of the Red Spider. The discovery of large quantities of carbonates in this and another planetary nebula (the Bug Nebula/NGC 6302) called into question the traditional assumption that the presence of carbonates was an indicator of the previous action of liquid water. The discovery, which was also the first detection of carbonates outside the Solar System, re-opened questions about the presence of liquid water in the early Solar System. (ESA & G. Mellema, Leiden Univ., The Netherlands)

Figure 3.1.2 (right). M16, the Eagle nebula. This image was produced by combining images obtained as part of the ISOGAL programme, retrieved from the ISO Archive and reprocessed with the most recent calibration files. The false-colour image was constructed from a 7.7 µm IR exposure (shown as blue) and a 14.5 µm exposure (shown as red).

parallels between the chemical composition of dust in our Solar System and dust around other stars. Taken together with results on the occurrence and stability of discs of material around nearby stars, these results cast new light on the birth of our Solar System and point to fundamental similarities with other star systems. Figure 3.1.1 shows a Hubble Space Telescope image of the Red Spider Nebula. ISO detected abundant carbonates in this stellar remnant – too much to have relied on the presence of liquid water for their formation. This observation broke the theoretical link that had associated the presence of carbonates with the action of liquid water, and called into question one of the previously important diagnostics for tracing the action of liquid water in the early Solar System.

Numerous important facts concerning the chemistry of the interstellar medium have been uncovered by ISO, such as the ubiquity of water (notwithstanding the result mentioned above) and of the probably organic substances that give rise to broad features in IR spectra of a huge range of astronomical objects, from protostars to galaxies. Figure 3.1.2 shows the Eagle Nebula, M16, in a combined 7.7 µm and 14.5 µm false colour map that traces the emissions of organic dust grains and heated silicate dust in a region of star formation. The large systematic body of data on galactic stars gathered by ISO has permitted fascinating advances in the characterisation of important aspects of stellar evolution.

Investigations of nearby normal galaxies complement template specimens of dusty, star-forming, interacting galaxies. The disrupted, star-forming galaxies in turn serve to exemplify evolutionary processes that formed and reformed galaxies in the early Universe, giving rise to a huge burst of dust-obscured star formation at redshifts just below 1. This global surge of star formation, revealed by the surveys of ISO, serves to explain a diffuse background of IR light that had previously puzzled astronomers, and represents a major advance in charting the global history of star formation in the Universe, and a major advance in determining the relative importance in the Universe of energy generation by stars and energy generation by processes of accretion of matter onto black holes. This wide sweep of discovery affirms ISO's place at the forefront of successful spaceborne astronomy missions.

At the end of ISO's post-operations phase in December 2001, nearly 4 years after the depletion of the cryogen that marked the end of its orbital operations, a sustained

Table 3.1.1. Principal characteristics of the ISO instruments.

Instrument/ PI	*Participating countries*	*Main function*	*Wavelength (μm)*	*Spectral resolution*	*Spatial resolution*	*Outline description*
ISOCAM (C. Cesarsky, CEN-Saclay, F)	F, GB, I, S, USA	Camera and polarimetry	2.5-17	Broadband, narrow-band and circular variable filters	Pixels of 1.5, 3, 6 & 12 arcsec	Two channels, each with a 32×32-element detector array
ISOPHOT (D. Lemke, MPI für Astronomie, Heidelberg, D)	D, DK, E, GB, IRL, SF, USA	Imaging photopolarimeter	2.5-240	Broadband and narrowband filters Near-IR grating spectrometer (R~90)	Variable from diffraction-limited to wide-beam	Three subsystems: 1. multi--band, multi-aperture photopolarimeter (3-125 μm) 2. far-IR camera (50-240 μm) 3. spectrophotometer (2.5-12 μm)
SWS (Th. de Graauw, Lab. for Space Research, Groningen, NL	B, D, NL, USA	Short-wavelength spectrometer	2.5-45	1000 across wavelength range and 2×10^4 for 12-44 μm	14×20 and 20×44 arcsec	Two gratings and two Fabry-Perot interferometers
LWS (P. Clegg, Queen Mary College, London, UK	F, GB, I, USA	Long-wavelength spectrometer	43-195	200 and 10^4 across wavelength range	1.65 arcmin	Grating and two Fabry-Perot interferometers

publication rate of about 150 refereed papers per year (entirely comparable with corresponding rates for other successful space science missions) has resulted in publications traceable to about 30% of ISO's science observations. Entering the Active Archive Phase of the mission, 70% of the data remain to be explored and exploited.

Science and spacecraft operations

Operations were conducted from ESA's Villafranca Satellite Tracking Station (Vilspa), near Madrid (E). Two ISO teams were collocated there; one was responsible for the operations of the spacecraft and the other for community support and scientific operations ranging from the Calls for Observing Proposals, through the scheduling and use of the scientific instruments, to the pipeline processing and distribution of the data products.

ISO Data Archive (IDA)

ISO performed around 30 000 science observations. If account is taken of observations made in the parallel and serendipity modes of the instruments (observational modes in which an instrument could observe while another instrument was prime), almost 150 000 data sets were recorded with ISO. Since ISO was operated as an observatory with four complex instruments, the resulting data are highly heterogeneous. The data underwent sophisticated processing, including validation and accuracy analysis.

In total, around 400 GBytes of data are stored on magnetic disks. To serve these data to the user community, a sophisticated archive has been developed by ISO Data Centre, with continuous and fruitful cooperation between users and developers to provide a unique state-of-the art astronomical data archive. In addition to the

Figure 3.1.3. An example illustrating user interaction with the Archive. The upper part of the figure illustrates how a central list of observations can spawn many sub-screens containing quick-look data products, details of corresponding publications, and maps of each target field extracted from other archives and databases. The lower part of the figure illustrates the diversity of background information and details that can be called up about any ISO observation through interoperability with other archives.

observational data products, the archive also contains satellite housekeeping data, software tools, documentation, and externally derived products.

The IDA is based on an open and flexible 3-tier architecture comprising the Data Products and Database, the Business Logic and the User Interface. An important consideration was to separate the stored data from their final presentation to the user. The Business Logic and the User Interface have been developed entirely in JAVA and XML, which allows the IDA to be accessible from any platform and from the most popular web browsers. This has facilitated its re-use for other archive projects, in particular the XMM-Newton Science Archive (http://xmm.vilspa.esa.es/xsa/), significantly reducing development and maintenance costs.

A textual and visual presentation of the data is offered to the users to aid in selecting observations for retrieval through FTP. One of the main features of the ISO Data Archive is the provision of browse products or quick-look data associated with each observation. These products enable users to make informed decisions as to which bservations they want to download for detailed astronomical analysis.

By April 2002, in the first months of ISO's Active Archive Phase, nearly 1250 astronomers had registered as users of IDA. IDA supports easy-to-make but powerful queries against all ISO data. The quick-look images and on-line visualisation tools aid users in the selection of products for data retrieval through a 'shopping basket' mechanism familiar to anyone who has made commercial purchases via the web. After email notification that their request has been serviced, users make fast data retrieval by FTP.

The ISO archive incorporates many, and growing, elements of interoperability with other popular astronomical archives, in anticipation of the 'Virtual Observatories' of the future. Target names entered into the IDA user interface are resolved with searches in the NED or SIMBAD databases. Individual observations in the ISO database are linked to related publications listed in the ADS database maintained by Harvard Univ. ADS in turn links publications to ISO data sets upon which they are based. Searches in the Strasbourg-based CDS/Vizier archive will link targets to any existing ISO data for that target, and at NASA's IPAC tools allow overlap of ISO and IRAS target fields to be visualised. Figure 3.1.3 illustrates the diversity of information that the archive serves to astronomers in support of their usage of the ISO data.

Off-line products

Every ISO observation has been run through an automatic data-analysis pipeline called Off-Line Processing, or OLP, to produce standard data products. The automatic data products passed through several generations, until at the end of ISO Post Operations and in the first months of the Active Archive Phase in early 2002, a final full reprocessing of all ISO data was performed, producing the 'ISO Legacy Archive'. All products were put on hard disk, superseding previous product versions.

Interactive analysis tools

All interactive analysis tools, including a number of software packages offered to the community for reduction and analysis of ISO data, are archived. These include: ISOCAM Interactive Analysis (CIA); ISOPHOT Interactive Analysis (PIA); Observers' SWS Interactive Analysis (OSIA); LWS Interactive Analysis (LIA); and ISO Spectroscopic Analysis Package (ISAP). They are obtainable through the ISO WWW page or directly from the responsible software groups.

Documentation

Extensive explanatory and technical support documentation is archived. This includes

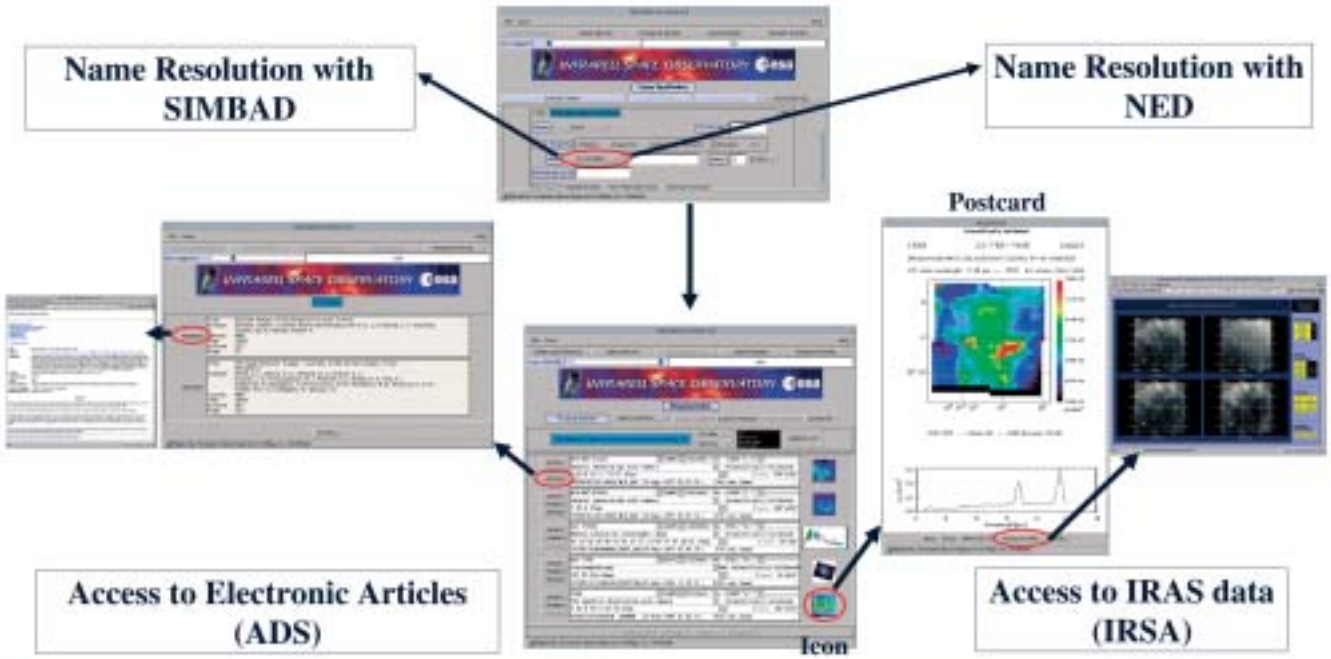
Name Resolution with SIMBAD
Name Resolution with NED
Postcard
Access to Electronic Articles (ADS)
Access to IRAS data (IRSA)
Icon

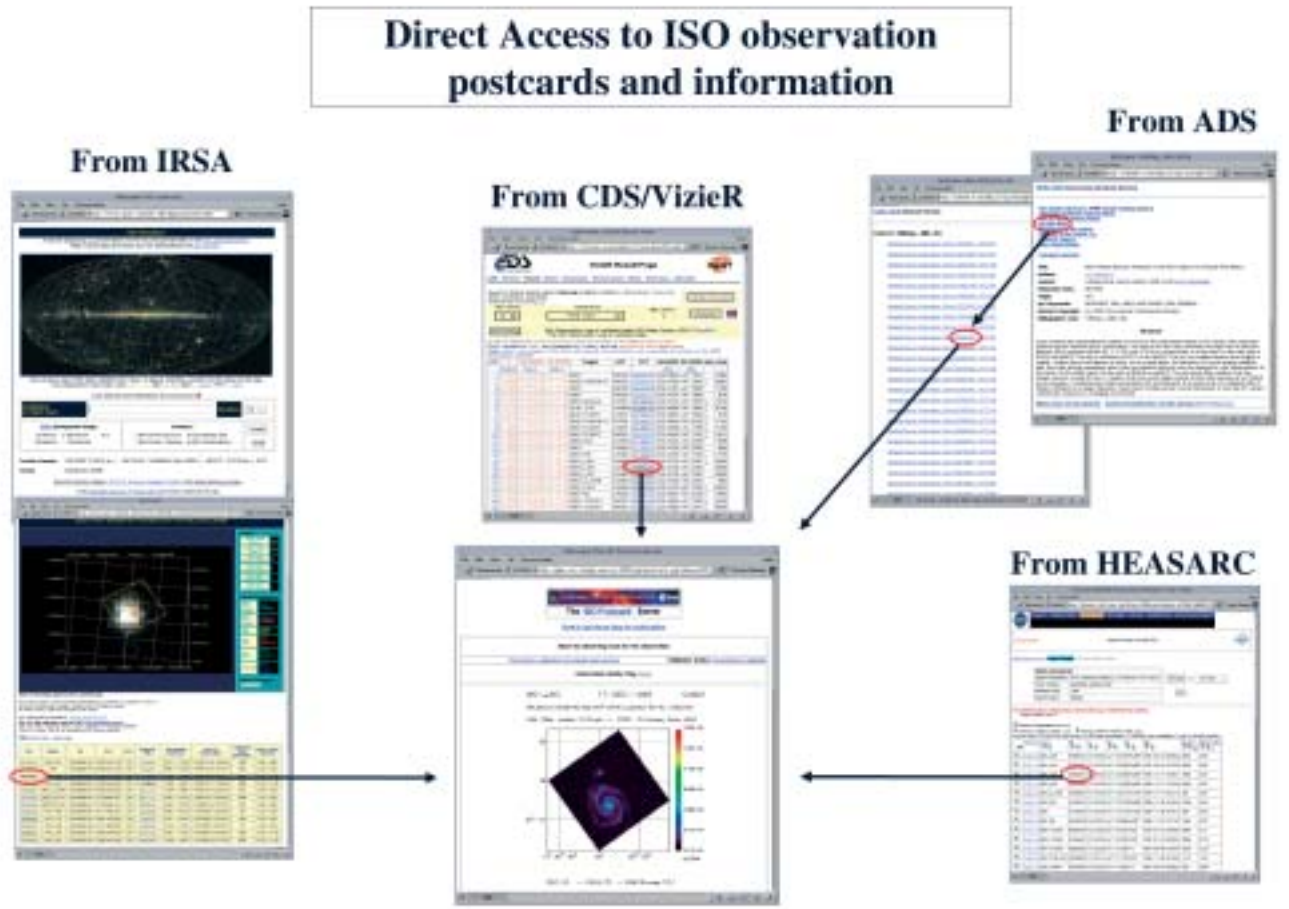
Direct Access to ISO observation postcards and information
From IRSA
From CDS/VizieR
From ADS
From HEASARC

the five volumes of the *ISO Handbook*, and extensive technical documentation tracing and explaining the experience of the instrument teams as they worked to understand the calibration of their instruments. Together with the ISO Data Products, the body of explanatory and support documentation is called the ISO Explanatory Library.

User Reduced Data Products (URDPs)
Users of ISO data are encouraged to make their interactively-reduced ISO data products available to the community through the IDA after their results have been published in the refereed literature. This ensure that data sets that could not be reduced optimally during the automatic bulk processing of the archive may still ultimately become associated with optimum archived data products having had the direct interactive attention of the publishing authors. Instructions and standards for supply of URDPs are given on the ISO web pages.

Virtual observatory

A virtual observatory is a collection of interoperating data archives and software tools that use the internet to form a scientific research environment in which astronomical research programmes can be conducted. In much the same way as a real observatory consists of telescopes, each with a collection of unique astronomical instruments, the virtual observatory consists of a collection of data centres each with unique collections of astronomical data, software systems and processing capabilities. Currently, the development of the ISO Data Archive leads the way towards its future integration into the virtual observatory concept.

Conclusions

ISO has made, and continues to make, ground-breaking contributions to all areas of astronomy, from Solar System studies, to the limits of cosmology and the history of the Universe. The mission itself was technically extremely successful, with several key aspects of the technology substantially outperforming their specifications (e.g. cryostat hold time, attitude and orbit control accuracy and stability, among others). Beyond that, the challenge of serving the huge body of ISO results to the astronomical community in a user-friendly way stimulated the development of an innovative data archive, pioneering many aspects of interoperability, and leading the way towards the virtual observatories of the future.

One of the major keys to success of the active archive phase will be the knowledge, skills and continuity of expertise of the people involved. The ESA ISO Data Centre at Villafranca has built up a unique set of experience around the archive, the data and the related community support, together with the detailed expertise on all four instruments that is necessary to support the general European community. Retention of these core skills and knowledge will continue to enable the community to get the most out of ISO and will, additionally, build a bridge in ESA's planning towards future missions, especially Herschel.

Footnote to p47: the Data Centres responsible for ISO User Support were or are (Centres continuing to operate into the Active Archive Phase are marked with *:

ISO Data Centre at ESA, Vilspa in Spain*
Five Specialist National Data Centres (NDCs) :
French ISO Centres, SAp/Saclay and IAS/Orsay, France; ISOPHOT Data Centre at MPIA, Heidelberg, in Germany*; Dutch ISO Data Analysis Centre at SRON, Groningen, NL*; ISO Spectrometer Data Centre at MPE in Munich, D*; UK ISO Data Centre at RAL, Oxford, UK*
plus, in the USA: ISO Support Center at NASA's IPAC, on CalTech campus.

4. Projects Under Development

4.1 Integral

Introduction

The International Gamma-Ray Astrophysics Laboratory (Integral), planned for launch in October 2002, is dedicated to the fine spectroscopy (energy resolution: $E/\Delta E = 500$) and fine imaging (angular resolution: 12 arcmin FWHM) of celestial gamma-ray sources in the energy range 15 keV to 10 MeV. Integral is an observatory led by ESA with contributions from Russia (Proton launcher) and NASA (Deep Space Network ground station). It will provide to the science community at large an unprecedented combination of imaging and spectroscopy over a wide range of X-ray and gamma-ray energies, including optical monitoring. The scientific instruments and the Integral Science Data Centre (ISDC) have been provided by large collaborations encompassing many scientific institutes in ESA member states, USA, Russia, Czech Republic and Poland, nationally funded and led by Principal Investigators (PIs).

Scientific objectives

Gamma-ray astronomy explores the most energetic phenomena occurring in nature and addresses some of the most fundamental problems in physics and astrophysics. It embraces a great variety of processes: nuclear excitation, radioactivity, positron annihilation, Compton scattering, and an even greater diversity of astrophysical objects and phenomena: nucleosynthesis, nova and supernova explosions, the interstellar medium, cosmic ray interactions and sources, neutron stars, black holes, gamma-ray bursts, active galactic nuclei and the cosmic gamma-ray background. Not only do gamma-rays allow us to see deeper into these objects, but the bulk of the power radiated by them is often at gamma-ray energies.

Integral's scientific goals address the fine spectroscopy with imaging and accurate positioning of celestial sources of gamma-ray emission. The fine spectroscopy over the entire energy range will permit spectral features to be uniquely identified and line profiles to be determined for physical studies of the source region. The fine imaging capability within a large field of view will permit the accurate locating and hence identification of the gamma-ray emitting objects with counterparts at other wavelengths, enable extended regions to be distinguished from point sources and provide considerable serendipitous science – very important for further discoveries.

In the 15 keV - 10 MeV region, line-forming processes such as nuclear excitation, radioactivity, positron annihilation, cyclotron emission and absorption become important. Unique astrophysical information is contained in the spectral shift, line width and line profiles. Detailed studies of these processes require the resolving power ($E/\Delta E = 500$) of a germanium spectrometer such as that employed on Integral. Lower-resolution spectrometers (e.g. SIGMA, OSSE, COMPTEL) did not have sufficient energy resolution to study the parameters of these lines, and the last high-resolution spectrometer, on HEAO-3 in 1979-80, was 100 times less sensitive than Integral's. Solid observational and theoretical grounds already exist for predicting detectable emission from such varied celestial objects as the Galactic Centre region, the interstellar medium, compact objects, novae and supernovae, and a variety of active galactic nuclei.

Scientific payload

The Integral payload consists of two main gamma-ray instruments: Spectrometer SPI and Imager IBIS. Each has spectral and angular resolution, but they are differently optimised in order to complement each other and to achieve overall excellent performance. Recent observations show that line emissions occur on a wide range of angular and spectral extent, i.e. broader lines seem to be emitted from point-like sources and narrower lines from extended sources. These instruments are supported by two monitors that provide complementary observations in the X-ray and optical energy bands.

The spectrometer, imager and X-ray monitor share a common principle of

For further information, see http://astro.estec.esa.nl/Integral/

Table 4.1.1. Principal characteristics of the Integral scientific payload.

	SPI	*IBIS*	*JEM-X*	*OMC*
Energy range	20 keV - 8 MeV	15 keV - 10 MeV	3-35 keV	500-850 nm
Detectors/characteristics	19 Ge (each 6x7 cm) cooled @ 85K	16384 CdTe (each 4x4x2 mm); 4096 CsI (each 9x9x30 mm)	Microstrip Xe-gas detector (1.5 bar)	CCD + V-filter
Detector area (cm^2)	500	2600 (CdTe) 3100 (CsI)	2 x 500	2048 x 1024 pix
Spectral resolution	2.2 keV @ 1.33 MeV	9 keV @ 100 keV	1.3 keV @ 10 keV	–
FOV (fully coded)	16°	9x9°	4.8°	5x5°
Angular res (FWHM)	2°	12 arcmin	3 arcmin	17.6 arcsec/pix
10σ source location	1.3°	< 1 arcmin	< 30 arcsec	6 arcsec
Continuum sensitivity*	10^{-7} @ 1 MeV	$5x10^{-7}$ @ 100 keV	$1.3x10^{-5}$ @ 6 keV	18.2^{m} (10^{-3} s)
Line sensitivity*	$5x10^{-6}$ @ 1 MeV	$2x10^{-5}$ @ 100 keV	$1.7x10^{-5}$ @ 6 keV	–
Timing accuracy (3σ)	129 μs	62 μs - 30 min	122 μs	var. in units of 1 s
Mass (kg)	1309	628	65	17
Power (W)	250	220	52	12
Data rate (kbit/s)	20	57	7	2

*sensitivities are 3σ in 10^6 s, units ph cm^{-2} s^{-1} keV^{-1} (continuum) and ph cm^{-2} s^{-1} (line)

operation: they are all coded aperture mask telescopes. The coded mask technique is the key to gamma-ray imaging, which is all-important in separating and locating sources. It also provides near-perfect background subtraction because, for any particular source direction, the detector pixels can be considered to be split into two intermingled subsets – those capable of viewing the source and those for which the flux is blocked by opaque mask elements. In effect, the latter subset provides an exactly contemporaneous background measurement for the former, made under identical conditions.

Spectrometer SPI

The Spectrometer SPI will perform spectral analysis of gamma-ray point sources and extended regions with an unprecedented energy resolution of 2 keV FWHM at 1 MeV. This will be accomplished using an array of 19 hexagonal high-purity germanium detectors cooled by active Stirling coolers to an operating temperature of about 85K. A hexagonal coded aperture mask is located 1.7 m above the detection plane in order to image large regions of the sky (16° fully coded field of view) with an angular resolution of 2°. In order to reduce background radiation, the detector assembly is shielded by an active scintillator veto system that extends around the bottom and side of the detector and up to the coded mask. The aperture (and hence contribution by cosmic diffuse radiation) is limited to 25°. The SPI collaboration is led by the Co-PIs: J.-P. Roques (CESR, Toulouse/France) and V. Schoenfelder (MPE Garching, D).

Figure 4.1.1. Members of the Integral Science Working Team and the Flight Model spacecraft (April 2002).

Imager IBIS

The IBIS imager provides powerful diagnostic capabilities of fine imaging (12 arcmin FWHM), source identification and spectral sensitivity to both continuum and broad lines over a broad (15 keV - 10 MeV) energy range. A tungsten coded-aperture mask (3.2 m above the detection plane) is optimised for high angular resolution and accurate source location (accuracy ~ 1 arcmin). As diffraction is negligible at gamma-ray wavelengths, the angular resolution obtainable with a coded mask telescope is limited by the spatial resolution of the detector array. The Imager design takes advantage of this by using a detector with a large number of spatially resolved pixels, implemented as physically distinct elements.

The detector uses two planes, a front layer of CdTe pixels, each 4x4x2 mm wxdxh), and a second one of CsI pixels, each 9×9×30 mm. The detector provides the wide energy range and high sensitivity continuum spectroscopy required for Integral. The division into two layers allows the paths of the photons to be tracked in 3-D, as they scatter and interact with more than one element. The aperture is restricted by a lead tube system and shielded in all other directions by an active scintillator veto system. The Imager collaboration is led by the PI P. Ubertini (IAS, Frascati, I).

X-Ray Monitor JEM-X

The Joint European X-Ray Monitor JEM-X supplements the main instruments and plays a crucial role in the identification of the gamma-ray sources and in the analysis

Table 4.1.2. Principal characteristics of the Integral mission.

Launch: 17 October 2002 by Proton into orbit of 72 h, 51.6° inclination, 10 000 km perigee height, 153 000 km apogee height. Start of science operations December 2002 (nominal duration 2 years, extension to 5 years possible).

Science goals: compact objects; extragalactic astronomy; stellar nucleosynthesis; galactic structure; particle processes and acceleration; identification of high-energy sources.

Science operations:
Integral Science Operations Centre (ISOC) at ESTEC;
Integral Science Data Centre (ISDC) in Versoix (CH);
distribution of observing time:
first mission year: 35% guaranteed time, 65% open time (via AO)
second mission year: 30% guaranteed time, 70% open time (via AO)

Spacecraft:
3-axis stabilised (all errors 3σ; instruments point along x-axis, y-axis is along length of solar arrays):
absolute pointing error: 5 arcmin (y,z), 15 arcmin (x)
absolute pointing drift (10^5 s): 0.6 arcmin (y,z), 2 arcmin (x)
relative pointing error (10^3 s) : 0.3 arcmin (y,z), 1 arcmin (x)
absolute measurement error : 1 arcmin (y,z), 3 arcmin (x)
Data rate: 86 kbit/s (science telemetry)
Power (payload): 690 W
Spacecraft size: 3x4x5 m (solar arrays stowed)
Mass: about 4000 kg at launch; 3500 kg dry; 520 kg hydrazine propellant

Operations:
Operations Centre: Mission Operations Centre (Darmstadt, D), ISOC (ESTEC)
Data transmission: S-Band, ground stations: Redu (B), Goldstone (USA)
Mission lifetime: 2 years nominal, up to 5 years technically possible

and scientific interpretation of Integral gamma-ray data. JEM-X will make observations simultaneously with the main gamma-ray instruments and will provide images with 3 arcmin angular resolution in the 3-35 keV prime energy band (extension up to 60 keV possible). The baseline photon detection system consists of two identical high-pressure imaging microstrip gas chambers (xenon at 1.5 bar) each viewing the sky through a coded aperture mask 3.2 m above the detection plane. The JEM-X collaboration is led by the PI N. Lund (DSRI, Copenhagen, DK).

Optical Monitoring Camera OMC

OMC consists of a passively cooled CCD in the focal plane of a 50 mm lens. The CCD (1024×2048 pixels) uses one section (1024×1024 pixels) for imaging, the other for frame transfer before readout. OMC will observe the optical emission from the prime targets of the main gamma-ray instruments and will provide simultaneous optical light curves for the generally highly variable compact gamma-ray sources. OMC offers the first opportunity to make long observations in the optical band simultaneously with those at X-rays and gamma-rays. Variability patterns ranging from 10s of seconds through hours, months and up to years will be monitored. The limiting magnitude will be 18.2 visual magnitudes (3σ, 5×10^3 s), which corresponds to ~42 photons $cm^{-2}\ s^{-1}\ keV^{-1}$ (@ 2.2 eV) in the V-band. Multi-wavelength observations are particularly important in high-energy astrophysics where variability is typically rapid. The wide band observing opportunity offered by Integral is of

unique importance in providing for the first time simultaneous observations over seven orders of magnitude in photon energy for some of the most energetic objects in the Universe. The OMC collaboration is led by the PI M. Mas-Hesse (INTA, Madrid, E).

Status

The Flight Model satellite (Figure 4.1.1) arrived at ESTEC in mid-2001 for final instrument integration and system testing. The payload was exposed to various radioactive sources and X-ray beams during a 2-week science calibration campaign in January 2002. The thermal balance test was carried out in April 2002. The spacecraft will be shipped to Baikonur Cosmodrome in August 2002 for launch on 17 October 2002.

All the instruments were successfully integrated onto the spacecraft and completed their functional tests, calibration programmes, EMC and acoustic tests. Based on scientific calibration measurements at both instrument- and spacecraft-level, the scientific performance is generally according to, or better than, the expectations.

The ground segment, involving the Mission Operations Centre (MOC), the Science Operations Centre (ISOC) and the Science Data Centre (ISDC), is preparing for the commissioning phase and nominal operations according to schedule. A series of end-to-end tests of the entire ground segment including the spacecraft were successful.

The call for open time observing proposals (Announcement of Opportunity, AO-1) was completed in summer 2001. There was an overwhelming response from the worldwide scientific community, with requests for observing time exceeding that available by a factor of 19. The observing programme for the first year of the nominal mission, including open time and guaranteed time observations, is available and is being scheduled by the ISOC mission planners.

4.2 SMART-1

Introduction

SMART-1 is the first of the SMART (Small Missions for Advanced Research in Technology) series introduced in the ESA Scientific Programme to prepare the technology for future Cornerstone missions. SMART-1 (Figure 4.2.1) will demonstrate the use of Solar Electric Primary Propulsion (SEPP) for deep-space missions. SEPP will have applications for the BepiColombo (Cornerstone mission to Mercury) and for Solar Orbiter, to be launched in 2011-2012. Also, the LISA mission (search for gravitational waves) and the Darwin mission (nulling IR interferometry for terrestrial exoplanet finding) will benefit from the timely development of SEPP technology. Several other technologies will be tested on SMART-1, involving spacecraft subsystems, SEPP diagnostics and instruments that will be useful for a wide range of future missions. SMART-1 will also provide an early opportunity for scientific instruments and investigations. The low overall budget for SMART-1 means a low-cost launch and new procurement and management approach.

Mission objectives

The SMART-1 scenario aims at a transfer to the Moon after a cruise to demonstrate SEPP. The mission will be launched in March 2003 as an Ariane-5 piggyback payload into Geostationary Transfer Orbit (GTO). SMART-1 will perform its primary demonstration (the use and navigation of SEPP with a Stationary Plasma Thruster) throughout the whole mission, bringing SMART-1 from GTO into lunar orbit, by expanding the elliptical orbit and making use of lunar resonances during swingbys. SMART-1 will reach the Moon in 15-17 months, entering a polar orbit of 300 x 10 000 km for lunar observations. Depending on the propellant remaining after arrival, the apolune may be lowered. Science operations in lunar orbit are planned for a baseline 6 months, with an extension possible.

In synergy with the technology objectives, the science objectives for the lunar investigations include studies of the origin of the Earth-Moon system, accretional processes that led to the formation of planets, the chemical composition and evolution of the Moon, geophysical processes (volcanism, tectonics, cratering, erosion,

Figure 4.2.1. SMART-1 in lunar orbit.

For further information, see http://sci.esa.int/smart-1/

Table 4.2.1. The SMART-1 payload experiments.

Expt. Code	*Investigation Type*	*Main Investigator*	*Team Co-Is*	*Description of Experiment*
AMIE	Principal Investigator	J.L. Josset (CH)	F, NL, I, ESA	5.3° FOV miniaturised CCD-camera, with 4 fixed filters and micro-Data Processing Unit for Moon multi-band imaging. 1.8 kg, 9 W
Laser-link	Guest Technology Investigator	Z. Sodnik (ESA)		Demonstration of a deep-space laser link with ESA Optical Ground Station; sub-aperturing techniques for mitigating atmospheric distortion. Uses AMIE
OBAN	Guest Technology Investigator	F. Ankersen (ESA)		Validation of On-Board Autonomous Navigation algorithm by planetary bodies tracking. Uses star trackers and AMIE images
SPEDE	Principal Investigator	W. Schmidt (FIN)	FIN, S, ESA, USA	Langmuir probes measure spacecraft potential and plasma environment. Support to Electric Propulsion monitoring. 0.7 kg,1.2 W
RSIS	Guest Science Investigator	L. Iess (I)	USA, D, UK, F, ESA, S	Radio-science experiment monitors the Electric Propulsion. Uses KATE and AMIE
SIR	Technology Investigator	U. Keller (D)	D, UK, CH, I, IRL	Miniaturised near-IR (0.9-2.4 μm) grating spectrometer for lunar surface mineralogy studies. 1.7 kg, 2.5 W
D-CIXS/ XSM	Technology Investigator	M. Grande (UK) J. Huovelin (FIN)	FIN, S, E, I, F, ESA, USA	Compact X-ray spectrometer for mapping lunar chemical and variations of X-ray objects. 3.3 kg, 13 W
EPDP	Technology Investigator	G. Noci (I)	I, ESA, FIN, A	Multi-sensor package for monitoring the Electric Propulsion; plasma environment characterisation. 2.3 kg, 18 W
KATE	Technology Investigator	R. Birkl (D)	ESA, UK	X/Ka-band Telemetry, Tracking & Control package, demonstrates telecommunication and tracking 5.2 kg, 18 W

Table 4.2.2. Principal characteristics of the SMART-1 spacecraft.

Stabilisation: 3-axis, zero momentum
Attitude control: autonomous star tracker, Sun sensor, rate sensor gyro, reaction wheels, reaction control hydrazine system, thruster engine gimbals
Mass: 350 kg at launch
Size: 1 m cube, 14 m from tip-to-tip of solar arrays
Propellants: 70 kg of xenon and 4 kg of hydrazine
Power: two solar wings of three panels each; total area 10 m^2, generating 1950 W @ 1 AU. Supported by 5 Li-ion batteries totalling 600 Wh storage
Telemetry data rate: S-band 62 Kbit s^{-1}, X-band: 2 Kbit s^{-1} (from lunar orbit), Ka-band 120 Kbit s^{-1}
Onboard memory: redundant 4 Gbit solid-state mass memory
Primary propulsion: Stationary Plasma Thruster PPS-1350, nominal 70 mN thrust at 1350 W inlet power and Specific Impulse of 16 000 Ns kg^{-1}

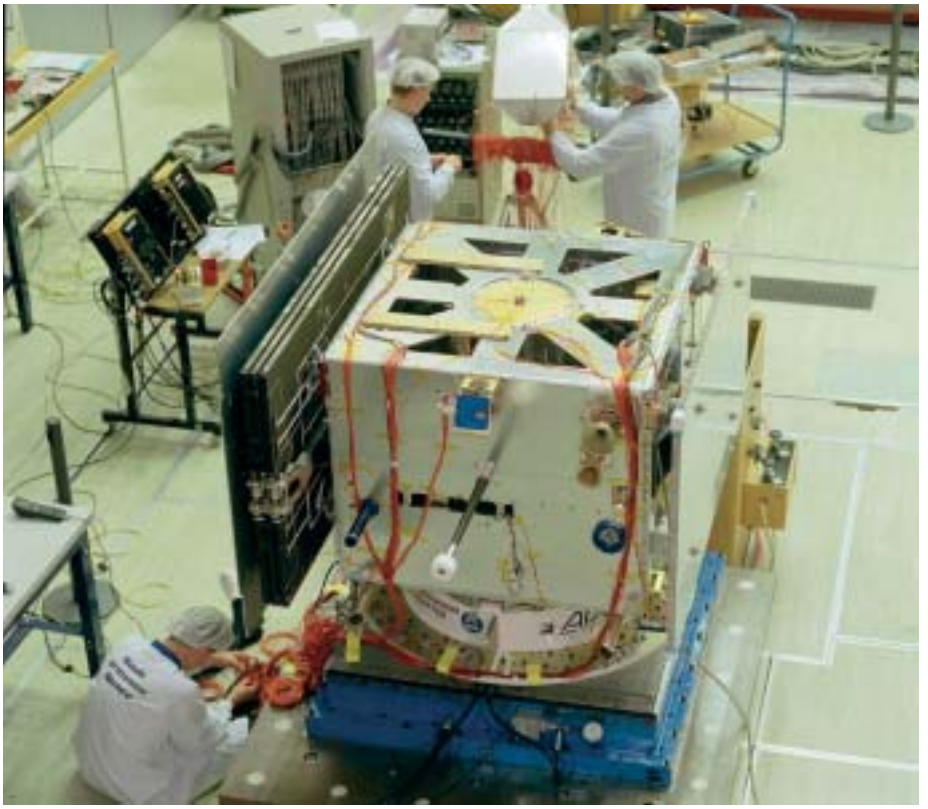

Figure 4.2.2. SMART-1 Structural and Thermal Model at ESTEC.

deposition of ices and volatiles) for comparative planetology, and high-resolution mapping. These studies also prepare for future international lunar and planetary exploration. Astronomy measurements can be made during cruise periods (coast arcs with no ion propulsion during the spiral out from GTO, or around apolune).

Payload

SMART-1 hosts seven instruments (Table 4.2.1) with which 10 experiments will be performed during the whole duration of the mission. Part of the payload will monitor the electric propulsion and the spacecraft environment, and test novel spacecraft and instrument technologies:

— the diagnostic instruments include SPEDE, a spacecraft potential plasma and charged particles detector, to characterise the spacecraft and planetary environment, together with EPDP, a suite of sensors monitoring secondary thrust-ions, charging and deposition effects;
— innovative spacecraft technologies will be tested: lithium batteries and KATE, an experimental X/Ka-band deep-space transponder that will support radio science (RSIS) to monitor the accelerations of the electric propulsion and test the turbo-code technique to improve the return of scientific data;
— RSIS, a set of radio-science and technology investigations, aimed at characterising the X/Ka-band deep space communication channels and demonstrating a method for measuring the libration of a celestial body (the Moon) from its orbit by using high-resolution imaging (AMIE) and accurate orbit determination by tracking in Ka-band (in preparation for BepiColombo).

The remote-sensing instruments for imaging and spectrometry are all highly miniaturised and based on novel technologies:

— D-CIXS, a compact X-ray spectrometer based on novel SCD detectors and micro-collimator optics, to perform lunar geochemistry, by fluorescence mapping of the major rock-forming elements (Mg, Si, Al, O, Fe) and to monitor bright X-ray sources during cruise;
— XSM, an X-ray solar monitor, to observe variations of the Sun owing to activity and flares, and to serve in the calibration of the D-CIXS determination of absolute lunar elemental abundances;
— SIR, a miniaturised quasi-monolithic point-spectrometer, will be the first ever near-IR lunar spectrometer, to survey the distribution of the main minerals in the lunar crust;
— AMIE, a miniature camera based on 3-D integrated electronics, imaging the Moon in four spectral bands defined by thin-film filters, and supporting three guest investigations: LASER-LINK, a demonstration of acquisition of a deep-space laser-link from the ESA Optical Ground Station at Tenerife; OBAN, the demonstration of an autonomous navigation tool; and RSIS for the in-orbit measurement of lunar libration.

Mission timeline and operations

Science and technology will be carried out during the whole mission, with different targets:

— commissioning and early technology demonstration: EPDP, SPEDE and KATE will support characterisation of the electric propulsion; D-CIXS/XSM will regularly monitor solar fluxes; AMIE will image the Earth and make the first measurements for the laser-link and navigation (OBAN) experiment;
— cruise phase: D-CIXS will observe X-ray sources, while SIR perform its calibration. AMIE will support visual observations and continuing imaging and support of the laser-link and OBAN. SPEDE will profile the charged particle and dust environment, concentrating on the effect of the solar wind over the orbit terminator;
— lunar capture: imaging the moon and high-data rate communication via KATE are foreseen;
— lunar observation: this is scientifically the most fruitful phase. D-CIXS will perform elemental global mapping of the Moon; SIR will perform spot spectrometry orbital mapping in 256 NIR bands at 0.9-2.4 μm; AMIE will perform high-resolution imaging of the south pole regions and of the Aitken Basin, plus investigate in four spectral bands the southern hemisphere. SPEDE will explore the space plasma environment and KATE will support RSIS in the demonstration of the libration measurement from orbit.

The mission is supported by a number of Principal and Technology Investigator teams from ESA member states and international collaborators (Table 4.2.1). The SMART-1 characteristics are summarised in Table 4.2.2.

4.3 Rosetta

Introduction

The International Rosetta Mission was approved in November 1993 by ESA's Science Programme Committee as the Planetary Cornerstone Mission in the Agency's Horizon 2000 long-term space science programme. The mission's main goal is a rendezvous with Comet 46P/Wirtanen, but it will also study two asteroids during close flybys enroute to the comet. Rosetta will study the nucleus of Comet Wirtanen and its environment in great detail for almost 2 years, the near-nucleus phase nominally starting at a heliocentric distance of about 3.25 AU, from the onset of activity through to perihelion, close to 1 AU. On its long journey to the comet, the spacecraft will pass close to the asteroids Otawara and Siwa. NASA is collaborating in the mission and is providing three of the Orbiter instruments.

The principal mission milestones are:

Launch	13 January 2003
Mars gravity assist	26 August 2005
Earth gravity assist #1	28 November 2005
Otawara flyby	17 July 2006
Earth gravity assist #2	28 November 2007
Siwa flyby	24 July 2008
Orbit adjust manoeuvre	June 2009
Rendezvous manoeuvre	29 November 2011
Start of near-nucleus operations (3.25 AU from Sun)	July 2012
Perihelion passage (end of mission)	10 July 2013

The prime scientific objective of the mission is to study the origin of comets, the relationship between cometary and interstellar material, and its implications with regard to the origin of the Solar System. The measurements to be made in support of this objective are:

— global characterisation of the nucleus, determination of dynamic properties, surface morphology and composition;
— determination of the chemical, mineralogical and isotopic compositions of volatiles and refractories in a cometary nucleus;
— determination of the physical properties and interrelation of volatiles and refractories in a cometary nucleus;
— study of the development of cometary activity and the processes in the surface layer of the nucleus and the inner coma (dust/gas interaction);
— global characterisation of asteroids, including the determination of dynamic properties, surface morphology and composition.

Direct evidence of the constitution of cometary volatiles is particularly difficult to obtain, as the constituents observable from Earth and even during the flybys of Comet Halley in 1986 result from physico-chemical processes such as sublimation and interactions with solar radiation and the solar wind. What we know today about cometary material from those earlier missions and ground-based observations does, however, demonstrate the low degree of evolution of cometary material and hence its tremendous potential for providing unique information about the make-up and early evolution of the solar nebula.

The study of cometary material presents a major challenge because of the very characteristics that make it a unique repository of information about the formation of the Solar System, namely its high volatiles and organic-material contents. A fundamental question that the Rosetta mission has to address is, to what extent can the

For further information, see http://sci.esa.int/rosetta

Table 4.3.1. The Rosetta Orbiter payload.

Acronym	*Objective*	*Principal Investigator*
Remote Sensing		
OSIRIS	Multi-colour imaging NAC (Narrow Angle Camera) 2.35×2.35° WAC (Wide Angle Camera) 12×12° (250-1000 nm)	H.U. Keller, MPI fur Aeronomie, Katlenburg-Lindau, Germany
ALICE	UV spectroscopy (70-205 nm)	A. Stern, Southwest Research Institute, Boulder, Colorado, USA
VIRTIS	VIS/IR mapping spectroscopy (0.25-5 μm)	A. Coradini, IASFC-CNR, Rome, Italy
MIRO	Microwave spectroscopy (1.3 & 0.5 mm)	S. Gulkis, NASA-JPL, Pasadena, CA, USA
Composition Analysis		
ROSINA	Neutral gas and ion mass spectroscopy. Double-focusing, 12-200 amu, m/Δm~3000. Time-of-flight, 12-350 amu, m/Δm~2500 including Neutral Dynamics Monitor	H. Balsiger, Univ. of Bern, Switzerland
COSIMA	Dust mass spectrometer (SIMS, m/Δm~2000)	J. Kissel, MPI für Extraterrestrische Physik, Garching, Germany
MIDAS	Grain morphology (Atomic Force Microscope, nm resolution)	W. Riedler, Space Research Inst., Graz, Austria
Nucleus Large-scale Structure		
CONSERT	Radio sounding, nucleus tomography	W. Kofman, LPG, Grenoble, France
Dust Flux, Dust Mass Distribution		
GIADA	Dust velocity and impact momentum measurement, contamination monitor	L. Colangeli, Oss. Astronomico di CapodiMonte Naples, Italy
Comet Plasma Environment, Solar Wind Interaction		
RPC	Langmuir probe, ion and electron sensor, flux-gate magnetometer, ion composition analyser, mutual impedance probe	A. Eriksson, Swedish Inst. of Space Physics, Uppsala, Sweden; J. Burch, Southwest Research Inst., San Antonio, Texas, USA; K-H. Glassmeier, TU Braunschweig, Germany; R. Lundin, Swedish Inst. of Space Physics, Kiruna, Sweden; J.G. Trotignon, LPCE/CNRS, Orleans, France; C. Carr, Imperial College London, UK
RSI	Radio science experiment	M. Pätzold, Univ. of Cologne, Germany

material accessible for analysis be considered representative of the bulk of the material constituting the comet, and of the early nebular condensates that constituted the cometesimals 4.57×10^9 years ago? This representativeness issue has to be addressed by first determining the global characteristics of the nucleus, namely its mass, density and state of rotation, which can provide us with clues as to the relationship between the comet's outer layers and the underlying material.

The dust and gas activity observed around comets, as well as its rapid response to insolation, guarantees the presence of volatiles at or very close to the surface in active areas. Analysing material from these areas will therefore provide information on both the volatiles and the refractory constituents of the nucleus. The selection of an appropriate site for the surface-science investigations should be relatively

Table 4.3.2. The Rosetta Lander payload.

Acronym	*Instrument*	*Principal Investigator*
APXS	Alpha-p-X-ray Spectrometer	R. Rieder, MPI Chemistry, Mainz, D
SD^2	Sample Acquisition System	A. Ercoli-Finzi, Polytecnico, Milano, I
COSAC	Gas Chromatograph/Mass Spectrometer	H. Rosenbauer, MPAe, Lindau, D
PTOLEMY	Evolved gas analyser	I. Wright, Open Univ., UK
CIVA ROLIS	Rosetta Lander imaging system	J.P. Bibring, IAS, Orsay, F; S. Mottola, DLR Berlin, D
SESAME	Surface Electrical and Acoustic Monitoring Experiment, Dust Impact Monitor	D. Möhlmann, DLR Cologne, D; H. Laakso, FMI, SF; I. Apathy, KFKI, H
MUPUS	Multi-Purpose Sensor for Surface and Sub-surface Science	T. Spohn, Univ. of Münster, D
ROMAP	RoLand Magnetometer and Plasma Monitor	U. Auster, DLR Berlin, D; I. Apathy, KFKI, H
CONSERT	Comet nucleus sounding	W. Kofman, LPG, Grenoble, F

straightforward, given the mission's extensive remote-sensing observation phase and the Rosetta Orbiter advanced instrumentation that covers a broad range of wavelengths.

The dust-emission processes are induced by very low density gas outflows and thus should preserve the fragile texture of cometary grains. These grains can be collected at low velocities (a few tens of m/s) by the spacecraft after short travel times (of the order of minutes). This will minimise alterations induced by any interaction with solar radiation. Similarly, gas analysed in jets or very close to the surface should yield reliable information on the volatile content of the cometary material in each source region.

Science operations

Rosetta is a Principal Investigator (PI)-type mission, i.e. the individual Experiment Teams are responsible for defining the science operations timelines for their individual instruments (Tables 4.3.1 & 4.3.2). These requests will be coordinated and merged into the Science Operations Plans by the Rosetta Science Operations Centre (RSOC), in ESA's Research and Scientific Support Department in ESTEC, Noordwijk, The Netherlands. For key mission phases (commissioning, nucleus rendezvous, lander delivery), RSOC will be collocated with the Rosetta Mission Operations Centre (RMOC) in the European Space Operations Centre (ESOC), in Darmstadt, Germany (Figure 4.3.1). ESOC will operate and control the spacecraft throughout the mission, working through the Agency's 35 m Deep Space Antenna at New Norcia in Western Australia (Figure 4.3.2).

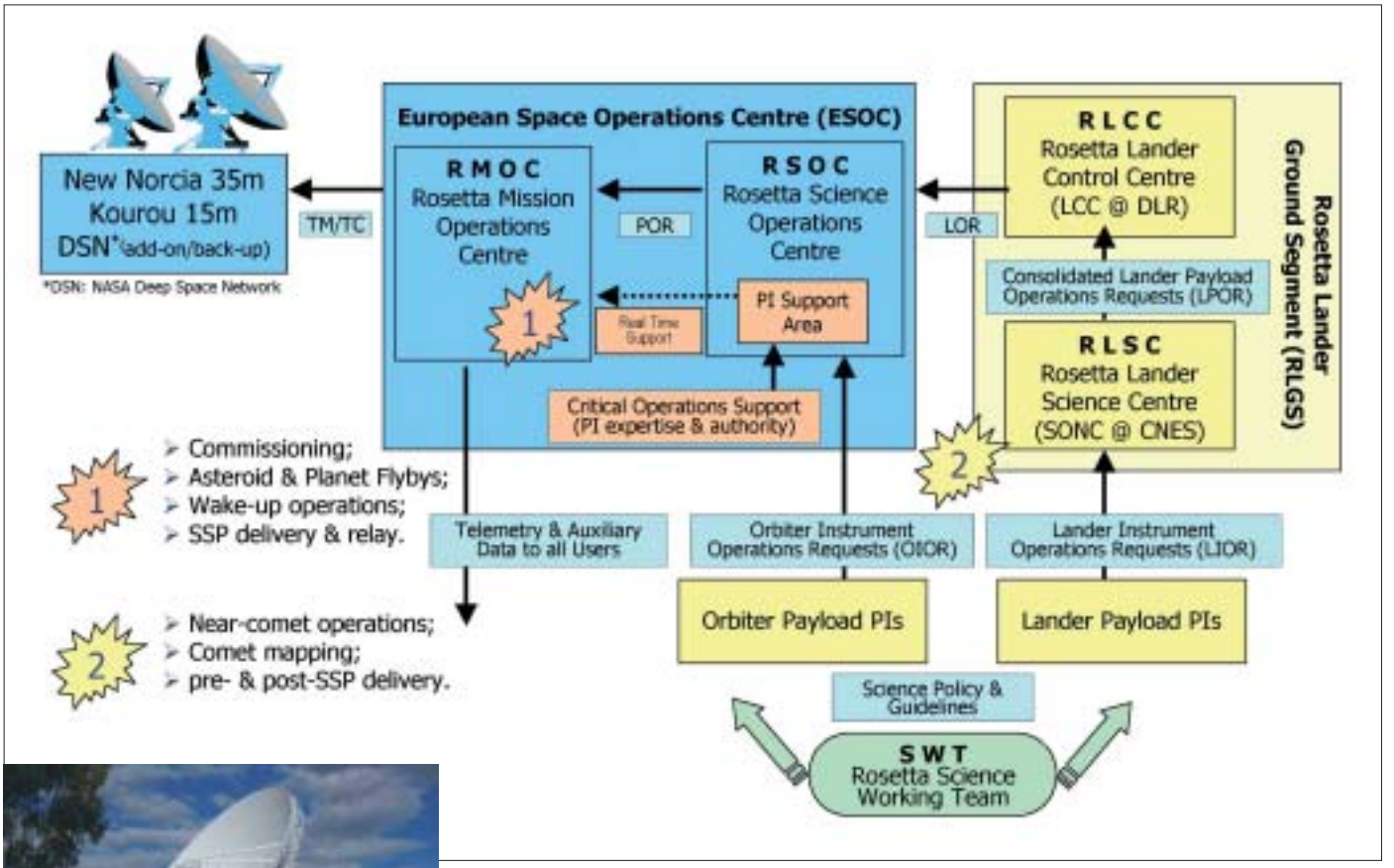

Figure 4.3.1 (above). The elements of the Rosetta Ground Segment.
Figure 4.3.2 (left). ESA's 35 m Deep Space Antenna at New Norcia, Western Australia.

The Rosetta Science Data Archive will be prepared by RSOC in collaboration with the Primitive Bodies Node of the Planetary Data System at the University of Maryland.

Five Interdisciplinary Scientists have been nominated for a limited period to support the mission's implementation:

— M. Fulchignoni, DESPA, Observatoire de Paris, France, to develop physico-chemical models of the possible target asteroids in order to provide the Rosetta Project and the Rosetta Science Working Team with a reference data set;
— P. Weissman, NASA-JPL, Pasadena, California, USA, to provide thermo-physical modelling of the cometary nucleus and of the inner coma of comets;
— R. Schulz, ESA Research and Scientific Support Department, to liaise with the astronomical community and to derive a basic characterisation of the target comet from ground-based observations;
— E. Grün, MPI für Kernphysik, Heidelberg, Germany and M. Fulle, Trieste Astronomical Observatory, Italy, to provide empirical 'engineering models' for the nucleus dust environment in order to establish a reference data set for the Rosetta Project and the Rosetta Science Teams.

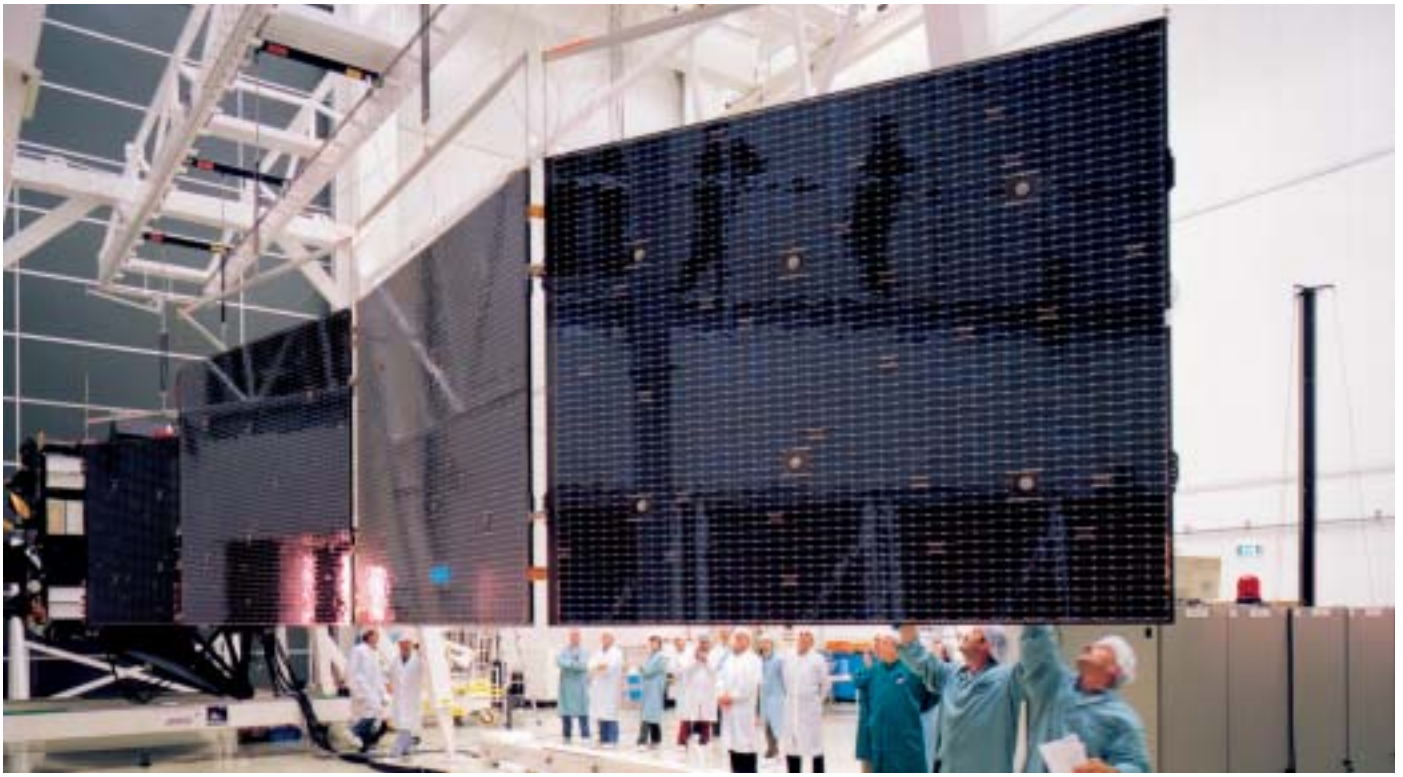

Figure 4.3.3. The Rosetta Proto-Flight Model during solar array deployment test at ESTEC.

Table 4.3.3. Rosetta spacecraft characteristics.

Spacecraft
3-axis stabilisation
Highly autonomous (two star trackers, Sun sensors, navigation cameras)
Three laser gyro packages
S/X-band up and downlink
Data transmission rates: 5-20 kbit/s (depending on geocentric distance)
Solid State Mass Memory: 25 Gbit
Solar Arrays (LILT-cells, low intensity, low temperature cells) to provide 400 W @ 5.2 AU
Size: box shaped, 2.5×2.5×2 m, all instruments body-mounted
Launch mass: ~3000 kg
Dry mass: ~1600 kg
Propellant: bipropellant monomethyl hydrazine (MMH), nitrogen tetroxide (NTO)
Mission lifetime: 11 years

Status

The Proto-Flight Model (PFM) spacecraft was assembled at Alenia Spazio, Torino, Italy. After initial testing it was shipped to ESTEC's Test Centre, where it underwent an extensive environmental test programme. These tests were completed in August 2002 and the spacecraft was shipped to Kourou in September. The 20-day launch window will open on 13 January 2003. The spacecraft will then be operated from ESOC. Commissioning of spacecraft and payload will be completed by April 2003.

4.4 Mars Express

Introduction

Mars Express, which comprises an orbiter and the small Beagle-2 lander in memory of Darwin's ship, will be launched in May/June 2003 by a Russian Soyuz-Fregat rocket from Baikonour Cosmodrome. The mission will recover some of the lost scientific objectives of both the Russion Mars-96 mission and the earlier ESA Intermarsnet study.

Scientific objectives

The scientific objectives for the Orbiter include global high-resolution photogeology at 10 m resolution and super-resolution imaging at 2 m/pixel of selected areas, global mineralogical mapping at 100 m resolution, global atmospheric circulation and mapping of the atmospheric composition, subsurface structure at km-scale down to the permafrost, surface-atmosphere interactions and interaction of the upper atmosphere with the interplanetary medium. For Beagle-2, the scientific goals include geology, geochemistry, meteorology and exobiology (i.e. search for signatures of life) of the landing site (Table 4.4.1). The scientific payloads of both craft are listed in Table 4.4.2. Current design estimates allow for an Orbiter scientific payload of about 106 kg and 60 kg total lander mass (at launch), compatible with the approved mission scenario. The Beagle-2 small lander concept, dedicated to geochemistry and exobiology with a number of robotic devices, was selected owing to its innovative scientific goals. Beagle-2 will deploy a sophisticated robotic-sampling arm, which can manipulate different types of tools and retrieve samples to be analysed by the geochemical instruments mounted on the lander platform. One of the tools to be deployed by the arm is a 'mole' capable of subsurface sampling to reach soil unaffected by solar-UV radiation.

Mission sequence

A Soyuz-Fregat launcher will inject a total of about 1100 kg into Mars transfer orbit in early June 2003, which is the most favourable launch opportunity to Mars in terms of mass in the near future. The Orbiter is 3-axis stabilised (Figure 4.4.1) and will be placed in an elliptical martian orbit (250 x 10 142 km) at 86.35° inclination and 6.75 h period, which is optimised for communications with Beagle-2 and the NASA landers of 2003 and 2005. Beagle-2 (Figure 4.4.2) will be independently targeted via its hyperbolic arrival trajectory, enter and descend through the atmosphere in about

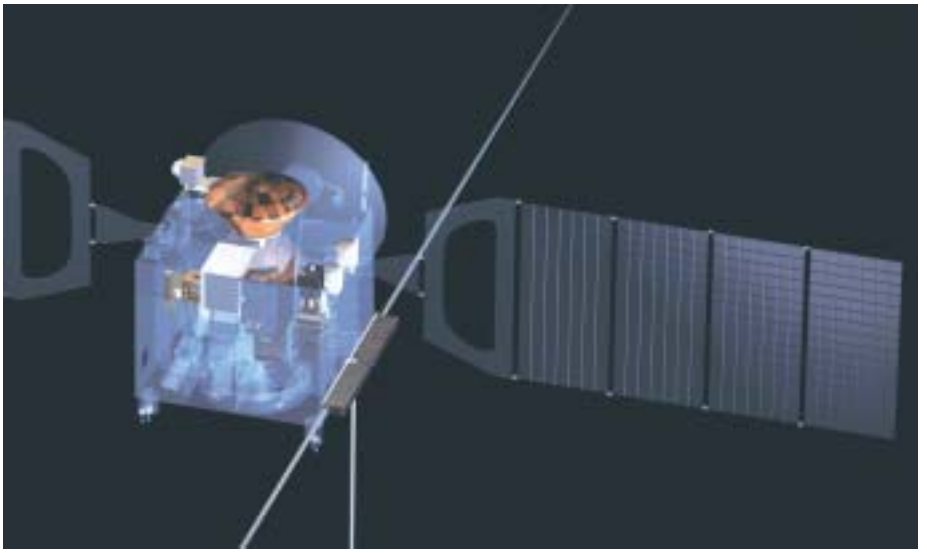

Figure 4.4.1. Mars Express configuration before arrival at Mars.

For further information, see http://sci.esa.int/marsexpress http://www.beagle2.com

Table 4.4.1. The scientific objectives of Mars Express.

Orbiter
- Global high-resolution (10 m) photogeology
- Super-resolution imaging at 2 m pix^{-1} of selected areas
- Global mineralogical mapping at 100 m resolution
- Global atmospheric circulation and mapping of composition
- Subsurface structure at km-scale down to the permafrost
- Surface-atmosphere interactions
- Interaction of the upper atmosphere with the solar wind

Lander
- Geology of landing site
- Organic and inorganic chemistry
- Exobiology (search for life signatures)
- Meteorology

Table 4.4.2. The Mars Express scientific experiments.

Expt. Code	*Instrument*	*Principal Investigator*	*Participating Countries*
Orbiter			
HRSC	Super/High-Resolution Stereo Colour Imager	G. Neukum	D, F, RU, US, FIN, I, UK
OMEGA	IR Mineralogical Mapping Spectrometer	J.P. Bibring	F, I, RU
PFS	Atmospheric Fourier Spectrometer	V. Formisano	I, RU, PL, D, F, E, US
MARSIS	Subsurface-Sounding Radar/Altimeter	G. Picardi & J. Plaut	I, US, D, CH, UK, DK
ASPERA	Energetic Neutral Atoms Analyzer	R. Lundin & S. Barabash	S, D, UK, F, FIN, I, US, RU
SPICAM	UV and IR Atmospheric Spectrometer	J.L. Bertaux	F, B, RU, US
MaRS	Radio Science Experiment	M. Paetzold	D, F, US, A
MARESS	Lander Communications Relay	E. Flamini	I
Lander			
Beagle-2	Suite of imaging instruments, organic and inorganic chemical analysis, robotic sampling devices and meteo sensors	C. Pillinger	UK, D, F, HK, CH

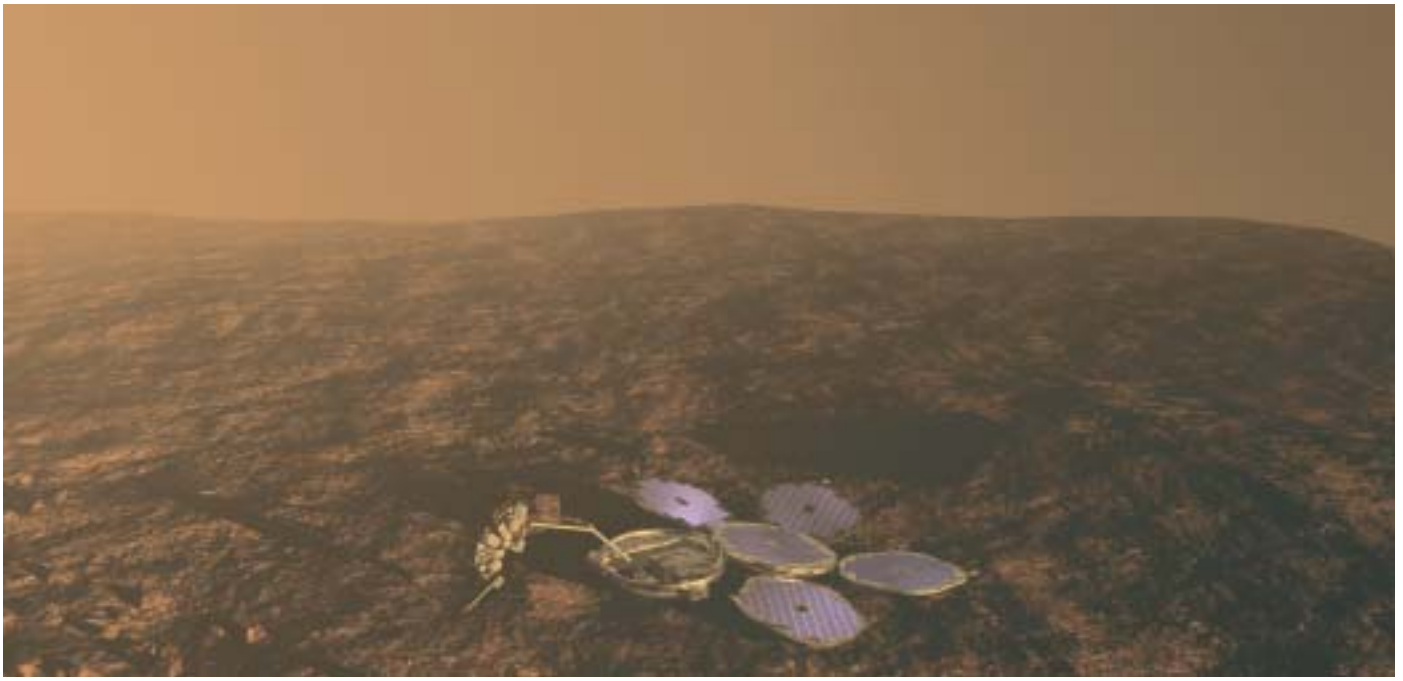

Figure 4.4.2. Beagle-2 deployed on the martian surface.

Table 4.4.3. Mars Express Interdisciplinary Scientists.

Type	*Name*	*Field*
Orbiter	K. Maezawa ISAS, Japan	Space environment and coordination between Mars Express and Nozomi
Orbiter	F. Forget Laboratoire de Météorologie Dynamique du CNRS, Université P. & M. Curie Paris, F	Atmosphere and surface-atmosphere interactions
Orbiter	G.G. Ori Int. Research School of Planetary Sciences, Università d'Annunzio, Pescara, I	Geological evolution
Orbiter	T.C. Duxbury JPL, USA	Geodesy and cartography
Lander	R. Amils CAB-Centro de Astrobiologia Torrejon de Ardoz, E	Astrobiology
Lander	E.K. Gibson NASA Johnson Space Center Houston, TX, USA	Geochemistry

5 min, and land with an impact velocity < 40 m/s and an error landing ellipse of 100 x 20 km. The selected landing site is in the Isisdis Planitia area (10.6°N, 270°W). The nominal mission lifetime of one martian year (687 days) for the Orbiter investigations, following Mars orbit insertion, will be extended by another martian year for lander relay communications and to complete global coverage. Beagle-2's lifetime will be about 6 months.

ESA is providing the launcher, the Orbiter and the operations, while Beagle-2 will be delivered by a UK-led consortium of space organisations. The Orbiter instruments, selected in June 1998 from proposals in response to an international Announcement of Opportunity, are being provided by scientific institutions through their own funding. The Mars Express mission is now in Phase-C/D, with Astrium Space in Toulouse, F, as Prime Contractor and involving a large number of European companies. As the Flight Model instruments are delivered for the assembly, integration and test (AIT) of all spacecraft subsystems, to be ready for launch in May 2003, the scientific teams are shifting from hardware and calibration activities to operations planning. AIT activities began in mid-2001 at Alenia Spazio in Torino, I. The launch window has been updated and is now spread over 30 days, opening on 23 May 2003. The cruise phase to Mars will last about 6 months.

International collaboration, either through participation in instrument hardware or scientific data analysis, is very much valued to diversify the scope and enhance the scientific return of the mission. This includes NASA's major contribution to the subsurface-sounding radar. Arriving at Mars at the very end of 2003, Mars Express will be followed by Japan's Nozomi a few days later. Both missions are highly complementary in terms of orbits and scientific investigations; Nozomi in its highly elliptic equatorial orbit will focus on the upper atmosphere and the interaction of the solar wind with the ionosphere. Close cooperation, including scientific data exchange and analysis, is foreseen by the Nozomi and Mars Express teams.

4.5 Herschel

Introduction

The Herschel Space Observatory (previously known as FIRST) is a multi-user observatory mission that will provide observation opportunities for the entire astronomical community in the relatively poorly explored 57-670 µm part of the far-IR and sub-mm ranges. Herschel (Figure 4.5.1) is the fourth of the Cornerstone missions in ESA Horizon 2000 science plan.

Scientific objectives

Herschel is the only space facility dedicated to the sub-mm and far-IR part of the spectrum. It has the potential for discovering the earliest epoch proto-galaxies, revealing the cosmologically evolving AGN/starburst symbiosis, and unravelling the mechanisms involved in the formation of stars and planetary system bodies. A major strength of Herschel is its photometric mapping capability for performing unbiased surveys related to galaxy and star formation. Redshifted ultraluminous IRAS galaxies (with SEDs that 'peak' in the 50-100 µm range in their rest frames) as well as class 0 proto-stars and pre-stellar objects peak in the Herschel prime band. Herschel is also well equipped to perform spectroscopic follow-up observations to further characterise particularly interesting individual objects.

The key science objectives emphasise the formation of stars and galaxies, and their interrelation. Example observing programmes with Herschel will include:

— deep extragalactic broadband photometric surveys in the 100-600 µm Herschel prime band and related research. The main goals will be a detailed investigation of the formation and evolution of galaxy bulges and elliptical galaxies in the first third of the present age of the Universe;
— follow-up spectroscopy of especially interesting objects discovered in the survey. The far-IR/sub-mm band contains the brightest cooling lines of interstellar gas, which give very important information on the physical processes and energy production mechanisms (e.g. AGN *vs*. star formation) in galaxies;
— detailed studies of the physics and chemistry of the interstellar medium in galaxies, both locally in our own Galaxy as well as in external galaxies, by photometric and spectroscopic surveys and detailed observations. This includes implicitly the important question of how stars form out of molecular clouds in various environments;
— observational astrochemistry (of gas and dust) as a quantitative tool for understanding the stellar/interstellar lifecycle and investigating the physical and chemical processes involved in star formation and early stellar evolution in our own Galaxy. Herschel will provide unique information on most phases of this lifecycle;
— detailed high-resolution spectroscopy of a number of comets and the atmospheres of the cool outer planets and their satellites.

From experience, it is clear that the discovery potential is significant when a new capability is provided for the first time. Observations have never been performed in space in Herschel's prime band. The total absence of (even residual) atmospheric effects – enabling both a much lower background for photometry and full wavelength coverage for spectroscopy – and a cool low-emissivity telescope open up a new part of the phase-space of observations. Thus, a space facility is essential in this wavelength range and Herschel will be breaking new ground.

Telescope and science payload

In order to fully exploit the favourable conditions offered by being in space, Herschel requires a precise, stable, low background telescope, and a complement of capable scientific instruments. The Herschel telescope will be passively cooled (to maximise

For further information, see http://astro.esa.int/herschel

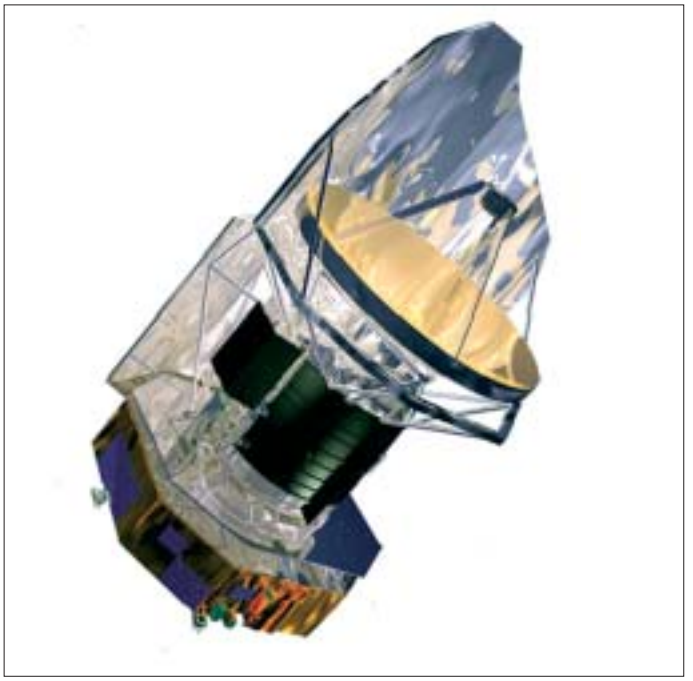

Figure 4.5.1. The Herschel satellite in orbit, showing the passively cooled telescope behind its protective sunshade, the superfluid helium cryostat containing the science instruments, and the service module. (Alcatel Space Industries)

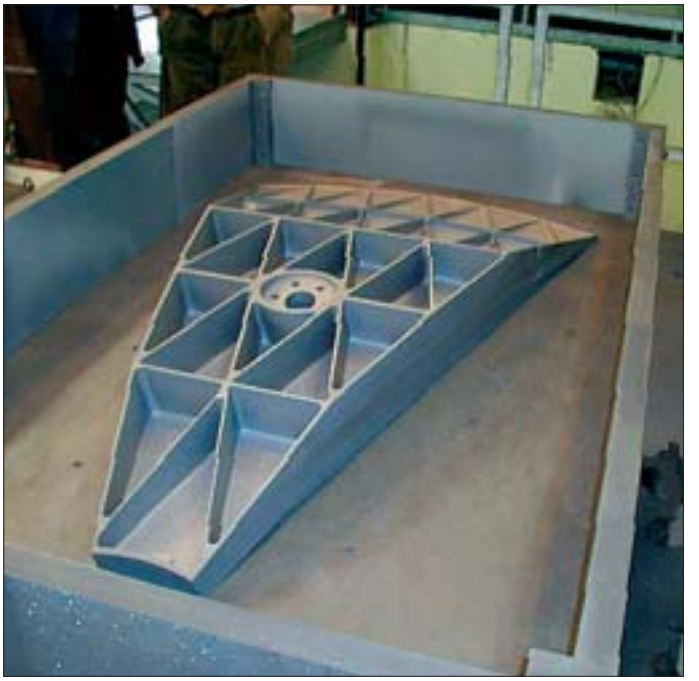

Figure 4.5.2. A full-scale SiC segment manufactured in spring 2001. The telescope primary mirror will consist of 12 such segments brazed together. (Astrium-EF)

its size) while the instrument focal plane units will be housed inside a cryostat, containing superfluid helium at a temperature below 1.7K. The telescope must have a total wavefront error (WFE) of less than 6 µm (corresponding to diffraction-limited operation at about 90 µm) during operations. It must also have a low emissivity to minimise the background signal, and the whole optical chain must be optimised for high straylight rejection. Protected by a fixed sunshade, in space the telescope will radiatively cool to an operational temperature in the vicinity of 80K.

The design is a classical Cassegrain with a 3.5 m diameter primary and an undersized secondary. The telescope will be provided by Astrium-EF (Toulouse) and constructed almost entirely of silicon carbide (SiC). It will have a primary mirror made out of 12 segments (Figure 4.5.2) brazed together to form a monolithic mirror that will be polished (much like a glass mirror) to the required accuracy, providing positive control of the overall WFE driver.

The scientific payload consists of three instruments (Table 4.5.1), which will be provided by consortia led by PIs in return for guaranteed observing time:

Photodetector Array Camera and Spectrometer (PACS)
PACS is a camera and low- to medium-resolution spectrometer for wavelengths up to about 205 µm. It employs four detector arrays, two bolometer arrays for photometry, and two photoconductor arrays for spectroscopy. PACS can be operated either as photometer, imaging a field of view (FOV) of 1.75x3.5 arcmin simultaneously in two colours, or as an integral field line spectrometer covering about 1 arcmin square on the sky.

Table 4.5.1. Herschel scientific payload.

Acronym	*Instrument*	*Principal Investigator*
PACS	camera/spectrometer, ~57-205 µm	A. Poglitsch, MPE, Garching (D)
SPIRE	camera/spectrometer, ~200-670 µm	M. Griffin, U. Cardiff (UK)
HIFI	high-res heterodyne spectrometer	Th. de Graauw, SRON, Groningen (NL)

Table 4.5.2. Principal characteristics of the Herschel mission.

Type of mission: far-IR and sub-mm observatory; 4th ESA Cornerstone mission
Science goals: star and galaxy formation, interstellar medium physics and chemistry, solar system body studies
Telescope: 3.5 m-diameter Cassegrain telescope of silicon carbide
Spacecraft: 3-axis spacecraft with superfluid helium cryostat for instrument focal plane unit cooling
Size: height 9 m x width 4.5 m, launch mass 3 t
Science data rate: 130 kbit/s average production rate
Lifetime: 3 years of routine science operations
Operational orbit: Lissajous orbit around L2
Launch: dual launch (with Planck) on Ariane-5 in early 2007

Spectral and Photometric Imaging REceiver (SPIRE)
SPIRE is a camera and low- to medium-resolution spectrometer for wavelengths longer than approximately 200 µm. It comprises an imaging photometer and a Fourier Transform Spectrometer (FTS), both of which use bolometer detector arrays. There are a total of five arrays, three dedicated for photometry and two for spectroscopy and spectrophotometry. As a photometer, it covers a large 4x8 arcmin FOV that is imaged in three colours simultaneously, and in spectroscopy a field approximately 2.6 arcmin across.

Heterodyne Instrument for the Far Infrared (HIFI)
HIFI is a heterodyne spectrometer offering very high velocity resolution spectroscopy using auto-correlator and acousto-optical spectrometers, combined with low-noise detection using superconductor-insulator-superconductor (SIS) and hot electron bolometer (HEB) mixers. HIFI covers a single pixel on the sky, and builds up images either by raster scanning or by on-the-fly mapping.

Spacecraft and in-orbit operations

The Herschel configuration shown in Figure 4.5.1 is based on the well-proven ISO cryostat technology. It is modular, consisting of the 'extended payload module' (EPLM) comprising the superfluid helium cryostat (housing the optical bench with the instrument focal-plane units) which supports the telescope, the sunshield/shade, and payload-associated equipment; and the service module (SVM), which provides the necessary infrastructure and houses the warm payload electronics. It measures some 9.3 m in height, 4.5 m in width, and has launch mass of around 3 t.

An industrial consortium led by Alcatel Space Industries (Cannes, F) as prime,

with Astrium-ED (Friedrichshafen, D) responsible for the EPLM, and Alenia Spazio (Turin, I) for the SVM, and a host of subcontractors from all over Europe, will build the spacecraft. Arianespace will provide the launch services in Kourou, French Guiana. For a summary of principal mission characteristics see Table 4.5.2.

The Ariane-5 launch vehicle, shared with ESA's cosmic microwave background-mapping Planck mission, will inject both satellites into a transfer trajectory towards the second Lagrangian point (L2) in the Sun-Earth system. They will operate independently from orbits of different amplitudes around L2, which is situated 1.5 million km from the Earth in the anti-Sun direction. It offers a stable thermal environment combined with good sky visibility. Since Herschel will be in a large orbit around L2, which has the advantage of not costing any orbit injection ΔV, its distance to the Earth will vary between 1.2-1.8 million km.

It will require about 4 months to reach the operational orbit. For the first 2 weeks after launch, while cooldown and outgassing take place, the telescope will be kept warm by heaters to prevent it acting as a cold trap for the outgassing products. It will then cool down, and it is envisaged that the opening of the cryostat door for first light will take place some 5-6 weeks after launch. Commissioning and performance verification will take place enroute towards L2. Once these crucial mission phases have been accomplished, Herschel begin routine science operations for a minimum of 3 years (until depletion of the helium), starting with a short science demonstration phase.

Science operations

Herschel will be a multi-user observatory open to the general astronomical community. It will perform routine science operations for 3 years. The observation time will be shared between guaranteed time (about one-third) 'owned' by contributors to the mission (mainly by the PI instrument consortia), and open time that will be allocated to the general community (including the guaranteed-time holders) on the basis of calls for observing time.

Herschel's scientific operations will be conducted in a novel decentralised manner. The operational ground segment comprises six elements:

— the Herschel Science Centre (HSC), provided by ESA;
— three dedicated Instrument Control Centres (ICCs), one for each instrument, provided by the respective PIs;
— the Mission Operations Centre (MOC), provided by ESA;
— the NASA Herschel Science Center (NHSC), provided by NASA.

The HSC is the interface to the science community and outside world in general, supported by the NHSC primarily for the US science community. The HSC provides information and user support related to the entire life-cycle of an observation, from calls for observing time, the proposing procedure, proposal tracking, data access and data processing, as well as general and specific information about using Herschel and its instruments.

All scientific data will be archived and made available to the data owners. After the proprietary time has expired for a given data set, the data will be available to the entire astronomical community in the same manner they were previously available only to the original owner. The accumulated experience from earlier observatory missions (particularly ISO and XMM-Newton) is being used in the implementation of the infrastructure by ESA and the PIs together. An important conclusion is to build one single system that evolves over time, rather than having separate systems for different mission phases. The first functional version of this system has already been used for instrument tests in early 2002.

Status and schedule

Following an Invitation to Tender (ITT) procedure, the industrial contract for Herschel (and Planck) for Phases B, C/D and E1 was awarded, and Phase-B began, in April 2001. The first major review, the System Requirements Review (SRR), took place in the autumn. Following the SRR, the lower level contractors are being selected. The next major step is the Preliminary Design Review (PDR), scheduled for mid-2002.

The telescope activity was started in mid-2001, and the Mid-Term Review (MTR) was successfully held in November 2001, paving the way for the Critical Design Review (CDR) in April 2002. The instrument consortia are in the process of finalising the instrument designs in order to start building the first test models. Their third formal review cycle, the Instrument Baseline Design Review (IBDR), took place in February-March 2002. The science ground segment is being developed, and will support instrument level testing beginning in 2002.

The current planning envisages a series of milestones, including instrument and telescope flight model deliveries in 2004/5, to be followed by spacecraft integration and extensive system-level ground testing, leading to the launch in early 2007.

4.6 Planck

Scientific goals

In late 1992, the COBE team announced the detection of intrinsic temperature fluctuations in the Cosmic Background Radiation Field (CBRF), observed on the sky at angular scales larger than ~10°, and at a brightness level $\Delta T/T \sim 10^{-5}$. These fluctuations have been interpreted as differential gravitational redshift of photons scattered out of an inhomogeneously dense medium, thus mapping the spectrum of density fluctuations in the Universe at a very early epoch. This long-sought result has established the Inflationary Big Bang model of the origin and evolution of the Universe as the theoretical paradigm. However, in spite of the importance of the COBE measurement, many fundamental cosmological questions remain open. In particular, the COBE resolution does not probe the size scale of the vast majority of structures that we see in the Universe today, e.g. galaxies and clusters of galaxies. The main objective of the Planck mission is to build on the pioneering work of COBE, and map the fluctuations of the CBRF with an accuracy that is set by fundamental astrophysical limits.

Mapping the fluctuations of the CBRF with high angular resolution and high sensitivity would give credible answers to such problems as: the initial conditions for structure evolution, the origin of primordial fluctuations, the existence of topological defects, and the nature and amount of dark matter. Planck will set constraints on theories of particle physics at energies greater than 10^{15} GeV, which cannot be reached by any conceivable experiment on Earth. Finally, the ability to measure to high accuracy the angular power spectrum of the CBRF fluctuations will allow the determination of fundamental cosmological parameters such as the density parameter Ω_0, the Hubble constant H_0, and the cosmological parameter (Λ), with an uncertainty of order a few percent.

The observational goal of the Planck mission is to mount a single space-based experiment to survey the majority of the sky with an angular resolution better than 10 arcmin, a sensitivity better than $\Delta T/T \sim 2\times10^{-6}$, and covering a frequency range wide enough to encompass and deconvolve all possible foreground sources of emission. The main scientific result of the mission will be a near-all-sky map of the fluctuations of the CBRF in at least three frequency channels. In addition, the sky survey will be used to study in detail the very sources of emission that 'contaminate' the cosmological signal, and will result in a wealth of information on the dust and gas in both our own Galaxy and extragalactic sources. One specific notable result will be the measurement of the Sunyaev-Zeldovich effect in many thousands of galaxy clusters, leading for example to the determination of cluster bulk velocities over scales of ~300 Mpc out to a redshift of ~1 with a velocity uncertainty of ~50 km/s.

Planck payload

The Planck payload consists of a 1.5 m-diameter offset telescope, with a focal plane shared by clusters of detectors in nine frequency bands covering the range 30-900 GHz. The lowest bands (up to ~100 GHz) consist of HEMT-based receivers actively cooled to ~20K by an H_2 sorption cooler. The higher frequency bands consist of arrays of bolometers cooled to ~100 mK; the H_2 sorption cooler provides precooling for a Joule-Thomson 4K stage, to which a dilution refrigerator is coupled. The characteristics and goal performance of the Planck instruments are shown in Table 4.6.1.

The satellite will be placed into a Lissajous orbit around the L2 point of the Earth-Sun system. At this location, the payload can be continuously pointed in the anti-Sun direction, thus minimising potentially confusing signals from thermal fluctuations and straylight entering the detectors through far sidelobes. From L2, Planck will carry out two complete surveys of the full sky, for which it requires about 14 months of observing time. The spacecraft will be spin-stabilised at 1 rpm. The viewing direction

For further information, see http://astro.esa.int/planck

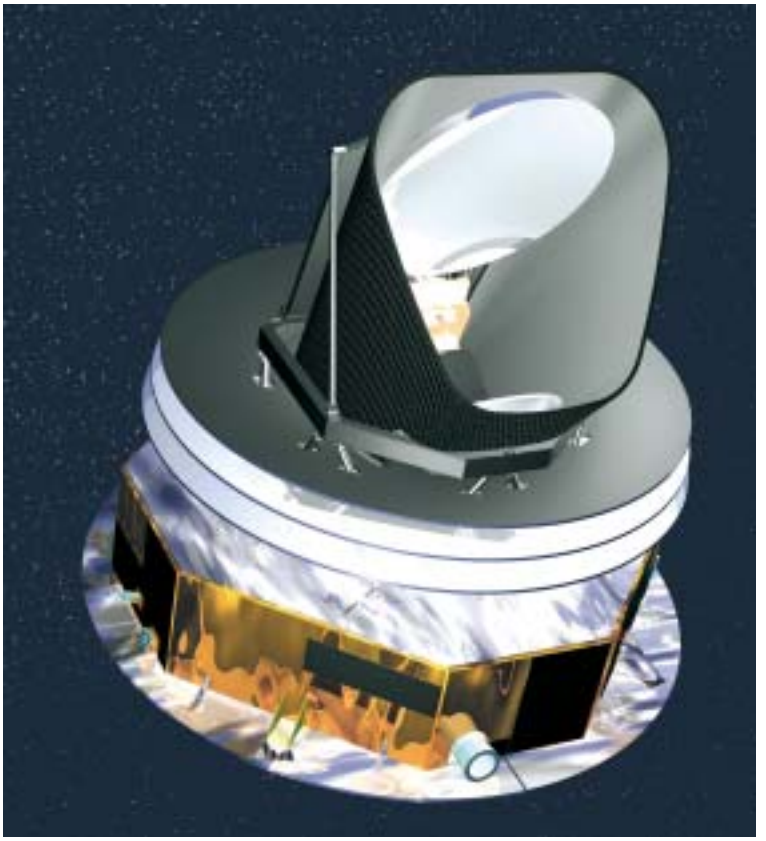

Figure 4.6.1. The current configuration of the Planck satellite, as developed by Alcatel Space (F) during Phase-B.

of the telescope will be offset by 85° from the spin axis, so that the observed sky patch will trace a large circle on the sky.

Planck is a survey-type project, developed and operated as a PI mission. The payload will be provided by two PI teams, who will also man and operate two Data Processing Centres, which will process and monitor the data during operations, and reduce the final data set into the science products of the mission. All-sky maps in the nine frequency bands will be made publicly available a year after completion of the mission, as well as a first generation set of maps of the CBRF, Sunyaev-Zeldovich effect, dust, free-free and synchrotron emission. The time series of observations (after calibration and position reconstruction) will also eventually be made available as an on-line archive.

Status

Since 1996, when Planck was selected as the third Medium-sized mission of ESA's Horizon 2000 Scientific Programme, budgetary pressures within the programme have forced a reconsideration of the original implementation plan. The current baseline scenario is to launch Planck together with ESA's Herschel Space Observatory. After launch, the two spacecraft will separate, and thereafter be operate independently.

An Invitation to Tender was issued by ESA in September 2000 to industry to present proposals for the design, construction and launch of the two spacecraft. The winning proposal was that of Alcatel Space (Cannes, France), which became ESA's Prime Contractor, and includes Alenia Spazio (Torino, Italy) as main subcontractor for the procurement of the Service Module, and Alcatel itself as responsible for the

Table 4.6.1. The target characteristics of the LFI/HFI (low/high-frequency) instruments on Planck.

Telescope	1.5 m (projected aperture) offset; shared focal plane; ε_{system}~1% Viewing direction offset 85° from spin axis									
Instrument	LFI				HFI					
Centre Frequency (GHz)	30	44	70	100	100	143	217	353	545	857
Detector Technology	HEMT radio receiver arrays				Bolometer arrays					
Detector Temperature	~20K				0.1K					
Cooling Requirements	H_2 sorption cooler				H_2 sorption + 4K J-T stage + Dilution					
Number of Detectors	4	6	12	34	4	12	12	6	8	6
Bandwidth ($\Delta\nu/\nu$)	0.2	0.2	0.2	0.2	0.25	0.25	0.25	0.25	0.25	0.25
Angular Resolution (arcmin)	33	23	14	10	10.7	8.0	5.5	5.0	5.0	5.0
Average $\Delta T/T$ per pixel (12 months, 1σ, 10^{-6} units)	1.6	2.4	3.6	4.3	1.7	2.0	4.3	14.4	147.0	6670
Sensitive to linear polarisation?	yes	yes	yes	yes	no	yes	yes	yes	no	no

Planck Payload Module. Subsystem contractors are being selected jointly by ESA and Alcatel.

Accordingly, the Phase-B (detailed design) of the Planck satellite started in May 2001, and is now nearing its end. Phase-C/D (manufacture and test) is scheduled to start before the end of 2003. At the same time, the development of the Planck instruments has nominally completed Phase-B, and they are starting manufacture, to be ready to deliver the first qualification models to ESA in mid to late 2003. The launch is foreseen for early 2007.

4.7.1 Double Star

Introduction

The collaboration between China and ESA started in 1992 when China proposed to establish a Data Centre to distribute Cluster data. Since then, several Chinese scientists have been hosted in Europe at ESA establishments and Principal Investigator institutes, and have become Co-Investigators on the Cluster mission.

In 1997, the Chinese Centre for Space Science and Applied Research (CSSAR) presented to the Cluster Science Working Team (SWT) their new two-spacecraft magnetospheric Double Star Programme (DSP; Figure 4.7.1.1) and invited the Cluster PIs to participate in the payload. Six Cluster PIs responded to this invitation and planned to provide their Cluster instrument spare Flight Models.

In September 1999, the ESA Director General was invited by the Administrator of the Chinese National Space Administration (CNSA) to discuss DSP collaboration. In March 2000, the DSP Phase-A report was presented to ESA and the Cluster SWT. The Cluster PIs reconfirmed their intention to provide their instruments and identified the support that ESA would be asked to provide. ESA confirmed its intention to participate in the collaborative programme and agreed to look at the support requested by China and at a collaboration agreement. In May 2001, the ESA Science Programme Committee approved funding for ESA's collaboration and recommended Council to approve the cooperation with China. Council did so in June 2001.

Finally, in July 2001, ESA and CNSA signed the DSP agreement of cooperation. ESA's aims in this first collaboration with China are to: provide unique opportunities for European space-plasma scientists, increase the scientific return of DSP by acquiring 4 h of data per day, support the refurbishment/rebuilding of the European instruments, coordinate the scientific operations of the European instruments on DSP, help in the pre-integration of the European instruments in Europe, help China to build two magnetically clean spacecraft, and confirm the radiation analysis model.

Scientific goals

The Double Star satellites will study the effect of the Sun on the Earth's environment. The polar spacecraft (DSP-2) will monitor the energy input from the solar wind into the polar ionosphere. The equatorial spacecraft (DSP-1) will investigate the substorm process when located in the Earth's magnetotail, as well as the entry of solar particles on the front-side of the magnetosphere. The geomagnetic substorm is a process by which energy is stored and released in the magnetosphere, resulting in serious disturbances in the Earth environment. The two DSP spacecraft, near Earth, and the four Clusters, further down the tail (Figure 4.7.1.2), will help to locate the starting point of the substorm and the physical mechanism responsible for it.

The Double Star scientific objectives are to:

— study magnetic reconnection at the magnetopause and in the magnetotail;
— understand and locate the trigger mechanism for magnetospheric storms and substorms;
— study physical processes such as particle acceleration, diffusion, injection and upflowing ions during storms;
— study temporal variations of field-aligned currents and the coupling between tail current and auroral current.

Mission and payload

DSP employs two spinning spacecraft designed, developed and operated by CNSA. The spacecraft are scheduled to be launched on two Chinese Long March-2C rockets in June 2003 and December 2003. DSP-1 will have an equatorial orbit of 550 x 63 781 km at 28.5° inclination, and DSP-2 a polar orbit of 700 x 39 000 km at 90°. The payload includes eight European instruments and eight Chinese instruments

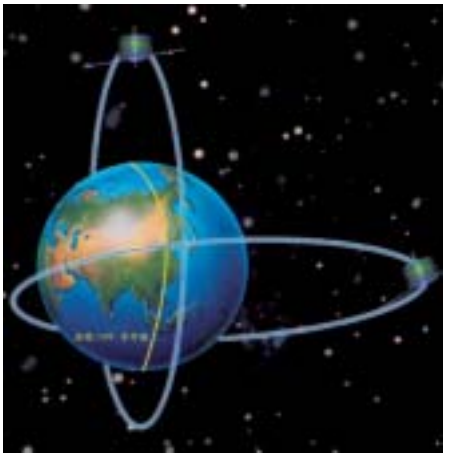

Figure 4.7.1.1. The two Double Star spacecraft visiting the magnetosphere.

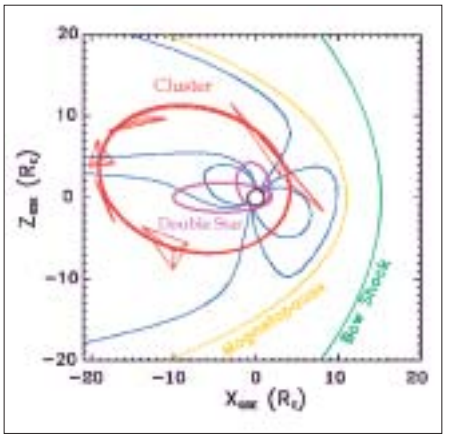

Figure 4.7.1.2. Double Star and Cluster coordinated orbits during the tail crossings.

Table 4.7.1.1. Double Star payload.

Instrument	*PI*
Equatorial satellite	
Active Spacecraft Potential Control (ASPOC)	K. Torkar, IWF, Graz, A
Fluxgate Magnetometer (FGM)	C. Carr IC, UK
Plasma Electron and Current Exp. (PEACE)	A. Fazakerley, MSSL, Dorking, UK
Hot Ion Analyser (HIA), sensor 2 of CIS	H. Reme, CESR, Toulouse, F
part of Spatio-Temporal Analysis of Field Fluct.(STAFF) + Digital Wave Processor (DWP)	N. Cornilleau/H. Alleyne, CETP, Velizy, F & Sheffield U., UK
High Energy Electron Detector (HEED)*	W. Zhang & J.B. Cao, CSSAR, China
High Energy Proton Detector (HEPD)*	J. Liang & J.B. Cao, CSSAR, China
Heavy ion detector (HID)*	Y. Zhai & J.B. Cao, CSSAR, China
Polar satellite	
Neutral Atom Imager (NUADU)	S. McKenna-Lawlor, Ireland U., IRL
Fluxgate Magnetometer (FGM)	T. Zhang, IWF, A
Plasma Electron and Current Exp. (PEACE)	A. Fazakerley, MSSL, Dorking, UK
Low Energy Ion Detector (LEID)*	Q. Ren & J.B. Cao, CSSAR,China
Low Frequency Electromagnetic Wave detector (LFEW)*	Z. Wang & J.B. Cao, CSSAR, China
High Energy Electron Detector (HEED)*	W. Zhang & J.B. Cao, CSSAR, China
High Energy Proton Detector (HEPD)*	J. Liang & J.B. Cao, CSSAR, China
Heavy ion detector (HID)*	Y. Zhai & J.B. Cao, CSSAR, China

*instrument built by China

(Table 4.7.1.1). Seven of the eight European instruments are identical to those on Cluster with one, the Neutral Atom Imager, to be newly built for DSP-2.

The Double Star Data System will coordinate payload commanding (among European instruments), acquire telemetry data by the ESA ground station and transmit these to China, distribute raw data from China to the PIs, and process instrument physical parameters for access by the user community. It is planned to reuse the software developed for the scientific operations and data distribution of the Cluster mission.

4.7.2 COROT

Introduction

COROT is a small mission for asteroseismology and planet-finding mainly funded by CNES, with substantial contributions from the ESA Science Programme, Austria, Belgium, Germany, Italy, Spain and ESA/Research and Scientific Support Division. COROT will be the third mission in the CNES small-mission programme based upon the Proteus multi-mission platform, and is due to be launched at the end of 2004. COROT is the first attempt to perform accurate asteroseismic observations, as well as to detect rocky planets. Both goals require the accuracy of space-based photometry.

Scientific payload

The payload is composed of an off-axis afocal parabolic system (two mirrors), with an f/4 telescope with a 27 cm-diameter entrance pupil and a 2.8x2.8° field of view. The camera has two separate fields of view, with two CCDs each, one for the asteroseismic observations and the other for planet-finding. The planet-finding camera includes a dispersive element (prism) that allows the collection of colour-resolved light curves. The observing programme will include the detailed asteroseismic study (with very high-frequency resolution) of a dozen of bright stars (V = 6-9), the asteroseismic study (with lower accuracy) of some hundred fainter stars, and the search for planets around a much larger number (~10 000) of fainter stars (V = 11-16.5).

ESA is financing the procurement of the telescope optics (which include an afocal dioptric telescope and a refractive objective assembly) and supporting the payload assembly, integration and verification activities. ESA's participation was approved by the Agency's Scientific Programme Committee in October 2000. In return for the ESA contribution, scientists in ESA member countries will have access to the COROT scientific data. An Announcement of Opportunity to this effect was released in early 2002.

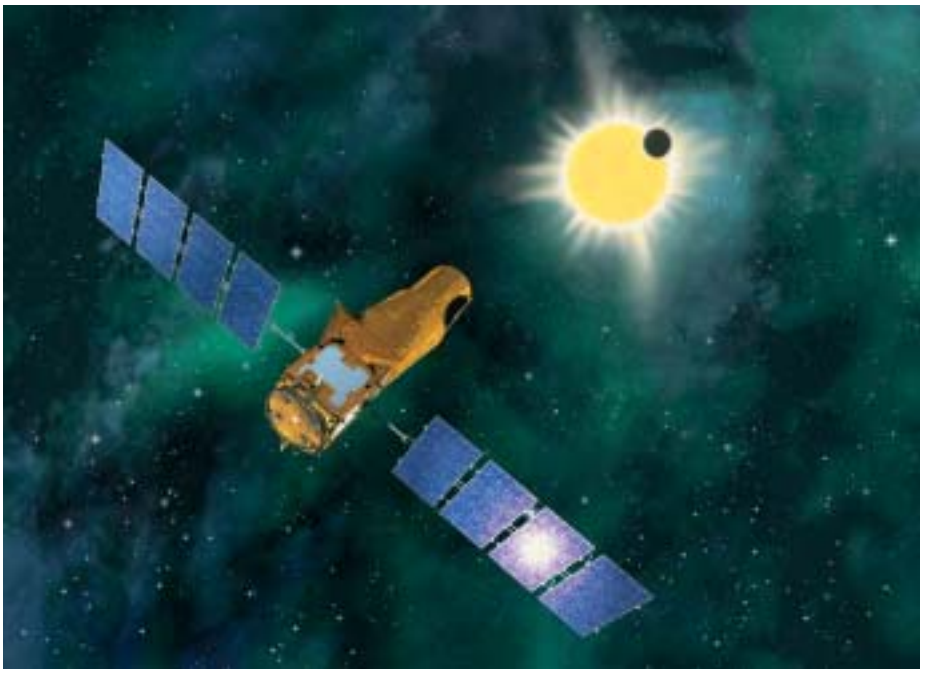

Figure 4.7.2.1. The COROT spacecraft in orbit, pointed towards a planetary transit.

For further information, see http://corot.astrsp-mrs.fr

4.7.3 Microscope

Introduction

Microscope (Microsatellite à traînée Compensée pour l'Observation du Principe d'Equivalence; Figure 4.7.3.1) is a CNES/ESA collaborative mission to test the Equivalence Principle (EP) in space to a precision of 1 part in 10^{15}. Even with the simplest experiment in space, the precision of the test can be improved by 2-3 orders of magnitude over the best ground-based and lunar laser-ranging tests. Microscope is a low-cost, room-temperature experiment in low Earth orbit with a total mission cost to CNES of about EUR15 million. ESA's share in this collaborative mission is the provision of the Field Emission Electric Propulsion (FEEP) thrusters for drag-free control of the satellite. This contribution is of particular interest to ESA, as the FEEP technology is currently foreseen to fly later on the SMART-2, LISA, GAIA, Darwin, XEUS, Hyper and GOCE missions.

Payload

The Microscope payload comprises two differential electrostatic accelerometers, one testing a pair of materials of equal composition (platinum-platinum), to provide an upper limit for systematic errors, the other testing a pair of materials of different composition (platinum-titanium) as the EP test proper. As on STEP, the test masses in the Microscope payload are concentric hollow cylinders of about 500 g each. Unlike STEP, the problem of test-mass charging is eliminated by a thin gold grounding wire. To separate the signal frequency from error sources, the spacecraft will spin at a frequency around 10^{-3} Hz.

Spacecraft and mission design

Microscope is the fourth CNES project based on the Myriade microsatellite line of products. The payload will be developed under ONERA management. OCA/CERGA (Observatoire de la Côte d'Azur/Centre d'Études et de Recherches en Géodynamique et Astrométrie) will contribute by developing the software for the error and data analysis in cooperation with ONERA.

The 3-axis 120 kg Microscope will be launched in 2006 by a Dnepr rocket (to be confirmed) into a Sun-synchronous, quasi-circular (eccentricity 10^{-2}) orbit at 700 km altitude. The drag from the residual atmosphere and solar radiation pressure will be

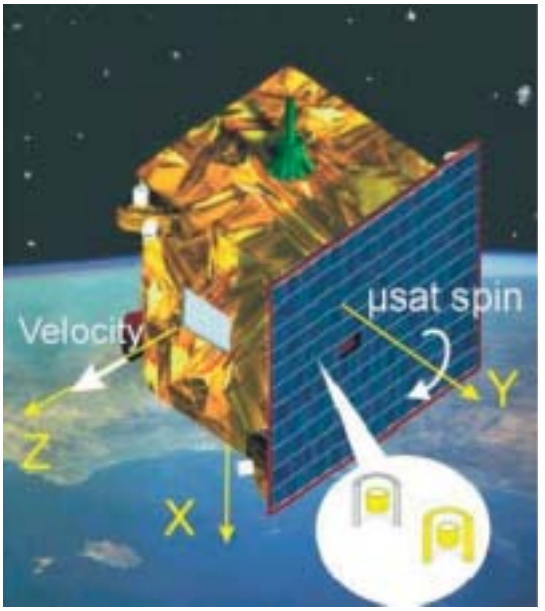

Figure 4.7.3.1. The Microscope satellite. The insert shows the orientation of the two pairs of concentric test masses.

compensated for by a system of proportional FEEP thrusters. A total of 8-12 thrusters, each with a thrust authority of 150 µN will be employed. Their noise level must not exceed 0.1 µN $Hz^{-1/2}$ at frequencies ≥ 0.1 Hz to provide the required drag-free performance of $3x10^{-10}$ m s^{-2} $Hz^{-1/2}$ in the measurement bandwidth. The FEEP thrusters also serve as actuators for fine attitude control. After the nominal mission, prolonged lifetime tests with eventually degrading FEEP thrusters are proposed to maximise the in-orbit operational experience with this novel electric propulsion system on its first space flight.

FEEP technology

FEEP thrusters operate by accelerating ions in an electric field. The ions are generated by exposing a free surface of liquid metal (caesium or indium) to an electrostatic field. The shape of this liquid surface is then modified into liquid cones by the counteracting forces of surface tension and electric field stress. At the apex of these cones, field ion emission takes place either along a knife-edge slit with a width of about 1.5 µm (caesium) or at a tungsten needle with a tip radius of 2-15 µm (indium). With an applied voltage of 5-10 kV, the ions are ejected at a velocity range of 60-100 km/s, depending on the propellant and the applied voltage. The mass flow is very low, so the developed thrust is in the desired µN regime. By smoothly varying the applied voltage, the thrust can be correspondingly controlled, as desired, all the way down to fractions of a µN. The complete FEEP thruster subsystem for Microscope requires about 38 W to develop the necessary thrust. The total propellant mass required for the nominal 1-year mission is only about 20 g per thruster. For Microscope, the caesium-type FEEPs by Alta, Italy have been selected.

Status

A joint CNES/ESA Announcement of Opportunity (AO) was released in December 2001 with the aim of Europeanising the payload. Two proposals were received by European institutes and, after careful review by ESA's advisory bodies and the Microscope Project Team, accepted by the Scientific Programme Committee in May 2002. CNES is currently performing the Phase-A study of the Microscope mission; the Phase-A Review will be held in December 2002. The payload has already passed this review and is now in its detailed design phase.

A contract for the procurement of the complete FEEP micropropulsion system has been awarded to Alta, Italy. The final configuration of the thrusters is now being studied and will be frozen at the time of the Microscope Phase-A Review. During the development phase, a 1-year endurance test of a flight-representative thruster will be carried out. The date for the final delivery of the propulsion system is set for late 2005.

5. Missions under Definition

5.1 BepiColombo

Introduction

As the inner end-member of the planetary system, Mercury plays an important role in constraining and testing dynamical and compositional theories of planetary formation. A better knowledge of the terrestrial planets is the key to understanding how conditions to support life have been met in the Solar System and how the habitability of Earth will evolve.

Terrestrial objects orbiting other stars are not accessible and the Solar System is the only laboratory where we can test models that will prove or disprove that such bodies may exist elsewhere in the Galaxy. The exploration of the Solar System and *in situ* planetary investigations can also provide the 'ground truth' to astrophysicists who ponder the appearance and signature of life in other planetary systems, or who study such questions as structure and dynamics of planetary atmospheres, surfaces of solid and fluid planets, generation of magnetic fields, stellar/galactic wind coupling with gaseous/plasma environments, magnetic confinement and reconnection in stellar and planetary environments, and acceleration of charged particles.

The main scientific objectives of BepiColombo are:

Scientific objectives

— formation and evolution of terrestrial planets in a close stellar environment;
— rotational state and interior structure;
— planetary magnetic field;
— morphology, geology, cratering and surface composition;
— volatile deposits in the polar regions;
— composition and dynamics of exosphere;
— structure and dynamics of magnetosphere.

Taking advantage of the proximity of the Sun, BepiColombo will address a number of additional goals in the following fields:

— radioscience (gravitation and fundamental science);
— influence of solar wind variability on Mercury's atmosphere and magnetosphere;
— interplanetary medium at close heliocentric distances.

Mission elements

It was concluded from the system and technology study in 1998-1999 that the scientific objectives could be fulfilled in an optimum way by distributing the instruments over three spacecraft elements, namely: the Mercury Planetary Orbiter (MPO), the Mercury Magnetospheric Orbiter (MMO) and the Mercury Surface Element (MSE).

MPO is a nadir-pointing platform that orbits the planet at altitudes between 400 km and 1500 km. It is mostly, but not exclusively, dedicated to remote sensing and allows for an almost uniform coverage of the surface. Its dual X- and Ka-band telemetry subsystem not only guarantees a yearly data return larger than 1 Tbit, but also provides a facility for radioscience measurements with unprecedented accuracy (Figures 5.1.1 and 5.1.2).

MMO is a spinner in an eccentric orbit and carries field and particle instruments. Japan has informed ESA about its intent to contribute MMO (Figures 5.1.2 and 5.1.3)

The nominal scenario of BepiColombo included an MSE to perform a detailed exploration of the landing site and make measurements that would serve as ground truth for the observations performed by the orbiters. This element is extremely desirable but its existence is threatened owing to the budgetary constraints that have been recently imposed on ESA's scientific programme. It is acknowledged that the decision of launching BepiColombo without MSE should not be taken lightly, because such an opportunity might not turn up again in the foreseeable future. It is

For further information, see http://sci.esa.int/home/bepicolombo

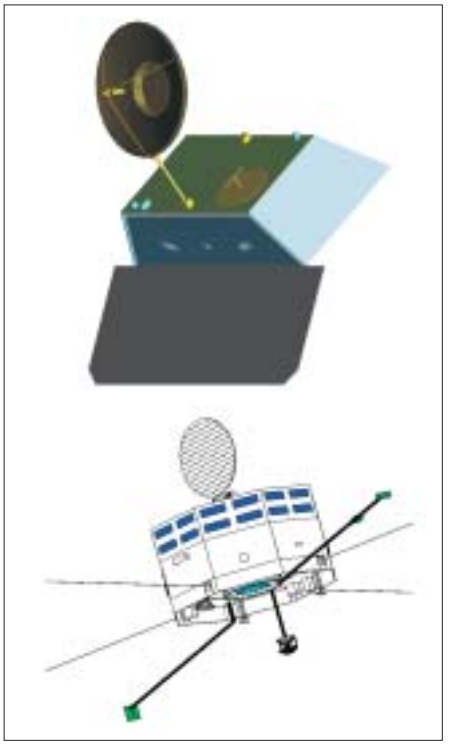

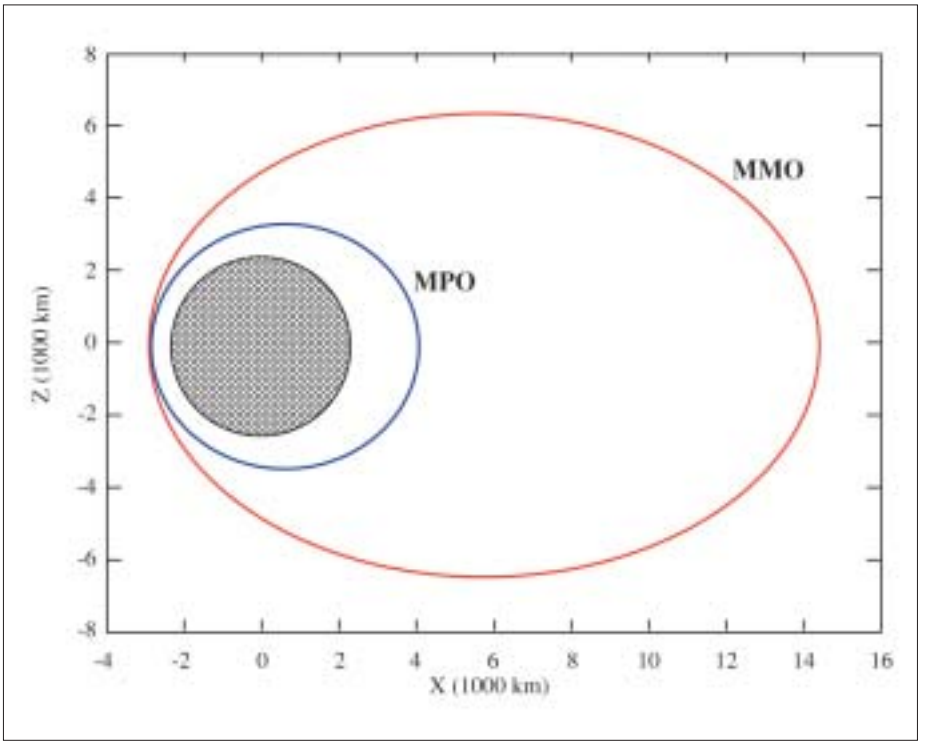

Figure 5.1.1 (top). The BepiColombo planetary orbiter (MPO).

Figure 5.1.2 (bottom). The BepiColombo magnetospheric orbiter (MMO).

Figure 5.1.3. Orbits of the planetary (MPO) and magnetospheric (MMO) elements in relation to Mercury's size.

hoped, however, that an enlarged cooperative approach, involving Japan and other countries, will reinstate the mission in its integrality.

Orbit

The method for transporting the spacecraft elements to their destinations results from a trade-off between mission cost and launch flexibility. It combines ion propulsion, chemical propulsion and gravity assists. The spacecraft approach their destination after two Venus and two Mercury flybys. The use of Solar Electric Propulsion reduces the duration of the interplanetary cruise to about 2.5 years. Additional flybys of the Moon and Earth enable a significant increase of the launch mass but increase the duration of the transfer to Mercury by a year. At Mercury, the spacecraft composite separates from the Solar Electric Propulsion Module. A Chemical Propulsion Module produces the required thrust for Mercury capture, and MMO orbit insertion and, possibly, MSE landing.

Status

Two competitive definition studies are being carried out by two industrial consortia led by Alenia Spazio (Torino, I) and Astrium GmbH (Friedrichshafen, D), based on the separate launches of MPO and MMO with two Soyuz-Fregat launchers in 2011-2012. Separate, but coordinated Announcements of Opportunity for the MPO and MMO payload instruments will be issued by ESA and ISAS in spring 2003, respectively.

5.2 GAIA

Introduction

After a detailed concept and technology study since 1998, the GAIA mission was selected as a confirmed mission within ESA's scientific programme in October 2000, with a launch date 'not later than 2012'.

Scientific goals

GAIA will rely on the proven principles of ESA's Hipparcos mission to solve one of the most difficult yet deeply fundamental challenges in modern astronomy: to create an extraordinarily precise 3-D map of about 10^9 stars throughout our Galaxy and beyond. In the process, it will map their motions, which encode the origin and evolution of the Galaxy. Through comprehensive photometric classification, it will provide the detailed physical properties of each star observed: characterising their luminosity, temperature, gravity and elemental composition. This massive stellar census will provide the basic observational data to tackle an enormous range of important problems related to the origin, structure and evolutionary history of our Galaxy – the equivalent 'humane genome project' for astronomy.

GAIA will achieve this by repeatedly measuring the positions of all objects down to V = 20 mag. Onboard object detection will ensure that variable stars, supernovae, burst sources, microlensed events and minor planets will all be detected and catalogued to this faint limit. Final accuracies of 10 microarcsec at 15 mag, comparable to the diameter of a human hair at a distance of 1000 km, will provide distances accurate to 10% as far as the Galactic Centre, 30 000 light years away. Stellar motions will be measured even in the Andromeda Galaxy.

GAIA's expected scientific harvest is of almost inconceivable extent and implication. Its main goal is to clarify the origin and history of our Galaxy, by providing tests of the various formation theories, and of star formation and evolution. This is possible since low-mass stars live for much longer than the present age of the

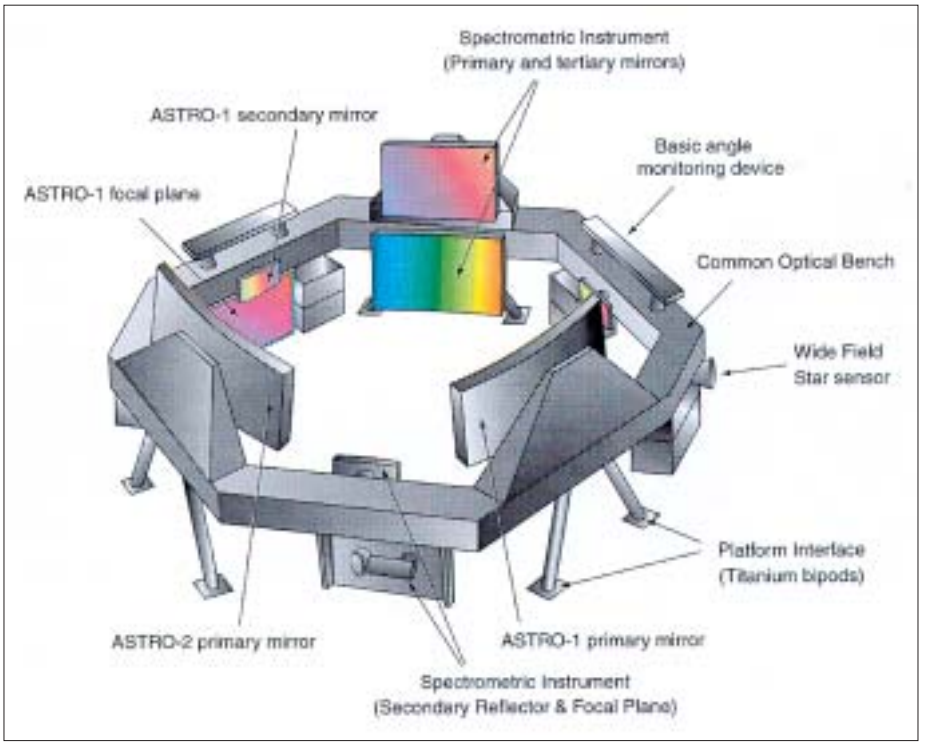

Figure 5.2.1. The GAIA payload comprises two astrometric viewing directions, and the radial velocity/spectroscopic instrument, suspended on a common stable platform. The instrument scans the sky by spinning about an axis perpendicular to the supporting ring structure.

For further information, see http://astro.estec.esa.nl/GAIA

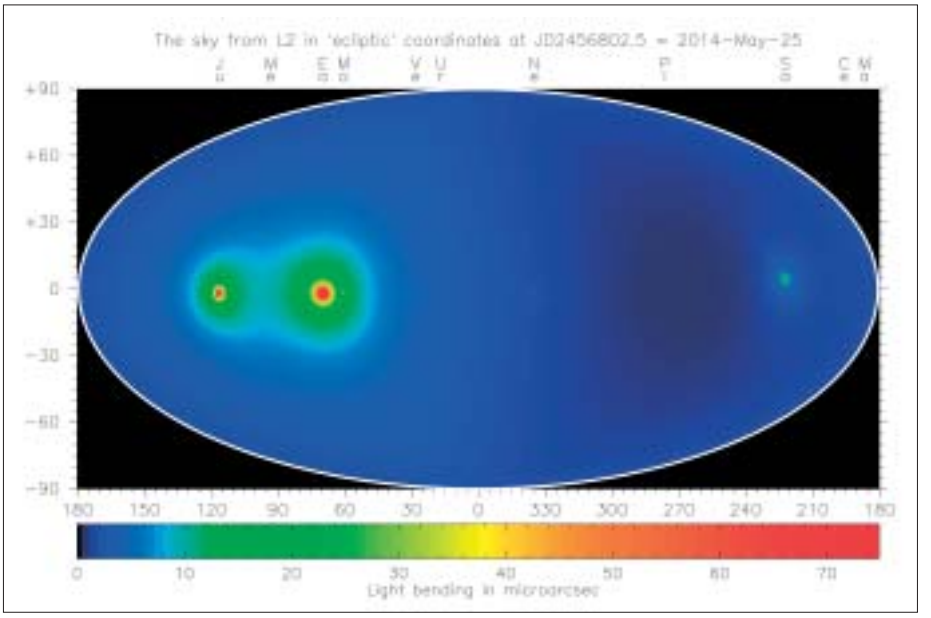

Figure 5.2.2. The amplitude of the relativistic light bending terms due to the presence of the various Solar System objects, as seen by GAIA from its L2 orbit. The sky is shown in ecliptic coordinates, and the dominant effect of the Sun's gravitational field has been suppressed. At the epoch simulated (May 2014), the effects of Jupiter, the Earth, Moon and Saturn can be clearly seen. All planets as well as other Solar System objects, including the four Galilean moons of Jupiter, and the most massive minor planets, will have a measurable effect on the GAIA observations. (courtesy J. de Bruijne).

Universe, and therefore retain in their atmospheres a fossil record of their detailed origin. The GAIA results will precisely identify relics of tidally-disrupted accretion debris, probe the distribution of dark matter, establish the luminosity function for pre-main sequence stars, detect and categorise rapid evolutionary stellar phases, place unprecedented constraints on the age, internal structure and evolution of all stellar types, establish a rigorous distance scale framework throughout the Galaxy and beyond, and classify star formation and kinematical and dynamical behaviour within the Local Group of galaxies.

GAIA will pinpoint exotic objects in colossal and almost unimaginable numbers: many thousands of extra-solar planets will be discovered, and their detailed orbits and masses determined; tens of thousands of brown dwarfs and white dwarfs will be identified; some 100 000 extragalactic supernovae will be discovered and details passed to ground-based observers for follow-up observations; Solar System studies will receive a massive impetus through the detection of many tens of thousands of new minor planets; inner Trojans and even new trans-neptunian objects, including Plutinos, may be discovered. GAIA will follow the bending of star light by the Sun and major planets, over the entire celestial sphere, and therefore directly observe the structure of space-time – the accuracy of its measurement of General Relativistic light bending may reveal the long-sought scalar correction to its tensor form. The PPN parameters gamma and beta will be determined with unprecedented precision. New constraints on the rate of change of the gravitational constant, and on gravitational wave energy over a certain frequency range, will be obtained.

The spacecraft

GAIA will carry the demonstrated Hipparcos principles into orders-of-magnitude improvement in terms of accuracy, number of objects, and limiting magnitude, by combining them with state-of-the-art technology. GAIA will be a continuously scanning spacecraft, accurately measuring 1-D coordinates along great circles, and in two simultaneous fields of view, separated by a well-defined and well-known angle (these 1-D coordinates are then converted into the astrometric parameters in a global

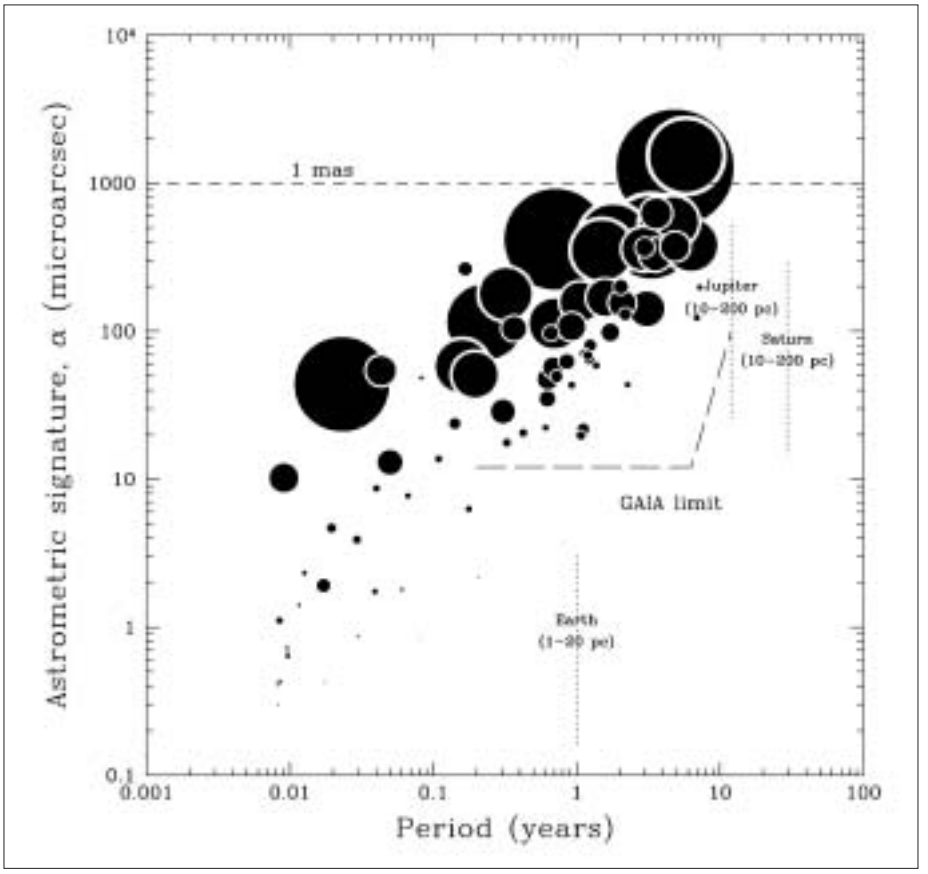

Figure 5.2.3. Astrometric detection of planets by GAIA. The 'astrometric signature' induced on the parent star is shown for the known planetary systems as a function of orbital period. Circles are shown with a radius proportional to planetary mass. Astrometry at the milliarcsec level has negligible power in detecting these systems, while the situation changes dramatically for microarcsec measurements. The positions of the innermost short-period planet (b) and outermost longest period planet (d) in the Ups And triple system are indicated. Short-period systems to which radial velocity measurements are sensitive are difficult to detect astrometrically, while the longest period systems will be straightforward for microarcsec positional measurements. Effects of Earth, Jupiter, and Saturn are shown at the distances indicated.

data analysis, in which distances and proper motions 'fall out' of the processing, as does information on double and multiple systems, photometry, variability, metric, planetary systems, etc.). The payload is based on a large CCD focal plane assembly, with passive thermal control and a natural short-term (3 h) instrument stability due to the sunshield, the selected orbit and a robust payload design.

The telescopes are of moderate size, with no specific design or manufacturing complexity. The system fits within a dual-launch Ariane-5 configuration, without deployment of any payload elements. The study identifies a Lissajous orbit at L2 as the preferred operational orbit, from where about 1 Mbit/s is returned to the single ground station throughout the 5-year mission. The 10 microarcsec accuracy is evaluated through a comprehensive accuracy assessment programme; this remarkable accuracy is possible partly by virtue of the (unusual) instrumental self-calibration achieved through the data analysis on-ground. This ensures that final accuracies essentially reflect the photon noise limit for localisation accuracy, exactly as achieved with Hipparcos.

One of the objectives of the Concept and Technology Study was to identify the areas of technology where further development is required before moving into Phase-B, scheduled to start in early 2005. About 15 well-identified key technology areas were identified, including the CCD/focal plane development, silicon carbide mirrors, onboard data handling and antenna design. Some of these activities are now underway, and should lead to full confidence in the required technology by the end of 2004.

Table 5.2.1. GAIA vs. Hipparcos capabilities.

	Hipparcos	*GAIA*
Magnitude limit	12	20 mag
Completeness	7.3 - 9.0	~ 20 mag
Bright limit	~ 0	~ 3-7 mag
Number of objects	120 000	26 million to V = 15
		250 million to V = 18
		1000 million to V = 20
Effective distance limit	1 kpc	1 Mpc
Quasars	none	~ 500 000
Galaxies	none	10^6 - 10^7
Accuracy	~ 1 milliarcsec	4 marcsec at V = 10
		10 marcsec at V = 15
		200 marcsec at V = 20
Broadband photometry	2-colour	4-colour to V = 20
Medium band photometry	none	11-colour to V = 20
Radial velocity	none	1-10 km/s to V = 16-17
Observing programme	pre-selected	onboard and unbiased

Scientific organisation

During 2001, a scientific organisation structure was put in place for the period until the start of Phase-B. About 200 European scientists have expressed an interest in working on various preparatory aspects of GAIA, ranging from the instrument design, through to the data processing, the treatment of specific objects (such as variable and multiple stars), and the optimisation of the photometric and radial velocity instruments. A group of about 12 scientists forms the GAIA Science Team, charged with advising ESA on all aspects of the scientific development and conduct of GAIA, and chaired by the ESA Project Scientist.

About 20 working groups, under the direction of leaders and coordinated by the science team, are responsible for the study and development of the various scientific aspects of the mission. Considerable progress has been made in many areas during the last 2 years. One very challenging task is to design the medium-band photometric system capable of classifying and physically characterising the 10^9 objects observed: for example, determining their temperatures, surface gravity, reddening and metallicity. Dedicated workshops were held in Vilnius and Barcelona during 2001. One working group is charged with the optimisation and development of the radial velocity instrument, where the challenge is to establish the characteristics of an instrument optimally designed to determine radial velocities for as many objects as possible (down to 17-18 mag), and to derive spectral characteristics at the same time. The relativity working group has made considerable progress in defining the principles underlying the derivation of a reference system deeply affected by gravitational light bending where, for example, effects due to the Sun, Jupiter the other planets and even the more massive minor planets, will be observable at the microarcsec level. One group is assessing the observability and detectability of Solar

System objects, including Near-Earth Objects; another is assessing the detectability of transients events such as microlensing, supernova and gamma ray bursts.

A key activity where much early effort has been devoted is to establish the feasibility of the GAIA data analysis procedure. The task is large and daunting: over its 5-year mission, GAIA will deliver some 100 TBytes of data, and will require processing power of order 10^{20} floating-point operations. Given that the data are effectively 'tangled' in time and position on the sphere, the data analysis problem is extremely challenging, even taking realistic assumptions about data processing capabilities extrapolated 10 years into the future. A prototype system has been set up, which is capable of ingesting a realistic but simplified telemetry stream, detecting and matching up observations of the same objects observed days, weeks or months apart, and subjecting them to an iterative adjustment in which the stellar parameters, satellite attitude and calibration parameters are estimated. The present study aims at the solution of simulated observations of about a million stars distributed over the celestial sphere. Successful completion of this work in May 2002 provides considerable confidence in the feasibility of the GAIA data processing, and provides a processing platform for further developments.

Rediscussion of the science programme

Following the ESA Ministerial Meeting in November 2001, the scientific programme is being rediscussed and all approved programmes, including GAIA, have been directed to respond to the new financial profile by investigating cost-cutting measures. This exercise was completed in mid-2002. The main opportunity for GAIA was to explore whether the mission is consistent with launch on a Soyuz launch vehicle, rather than the Ariane-5 vehicle assumed for the concept study phase.

The problem to be tackled was whether the payload could be redesigned for the smaller fairing diameter, of order 3.8 m, compared with 4.5 m for Ariane-5. Specific industrial studies evaluated these possibilities and a revised design, now accepted as the new baseline, has been completed: the new instrument layout fits into the Soyuz launcher, has led to a significant reduction in the cost of GAIA, and retains all of the original astrometric and photometric target accuracies. In this concept, the earliest launch date for GAIA, from a technical development point of view, remains at mid-2010.

5.3 LISA

Scientific goals

Gravitational waves are a necessary consequence of Einstein's theory of General Relativity. They cause a shrinking and stretching of space-time and therefore modify the distance between freely falling test masses. Their strength can be expressed in terms of the 'strain', the relative change in distance caused by a gravitational wave. In contrast to the familiar electromagnetic waves, they are by nature quadrupole waves.

Predicted in 1916 by Einstein and proved in the late 1950s to be observable, there is no direct evidence for their existence, although there is indirect evidence: the orbital period of the Hulse-Taylor binary pulsar (PSR1913+16) is decaying owing to the loss of orbital energy to gravitational waves at exactly the rate predicted by General Relativity. Efforts to detect gravitational waves in the high-frequency range (from 10 Hz to the kHz range) on the ground with bar detectors and small interferometers have been made since the 1960s. The construction of several large ground-based interferometers with increased sensitivity is now well underway. One is already fully operational (TAMA, in Japan), others are in their final stages of construction (LIGO, an US project with two sites in Hanford, Washington and Livingston, Louisiana; GEO600, a British-German collaboration, near Hannover, D) or are well advanced (VIRGO, an Italian-French project near Pisa, I). Full operation of most of the first-generation ground-based detectors is expected within a few years.

The primary objective of the LISA (Laser Interferometer Space Antenna) mission is the detection and observation of gravitational waves from massive black holes (MBHs) and galactic binaries in the frequency range 10^{-4}-10^{-1} Hz (Figure 5.3.1). This low-frequency range is inaccessible to ground-based interferometers owing to the background of local gravitational noise and because ground-based interferometers are limited in length to a few kilometres.

Ground-based interferometers can, in principle, observe the bursts of gravitational radiation emitted by galactic binaries during the final stages (lasting minutes or seconds) of coalescence when the frequencies are high and both the amplitudes and the frequencies increase quickly with time. However, the improvement of theoretical knowledge over the last few years has shown that the signal-to-noise ratio, though

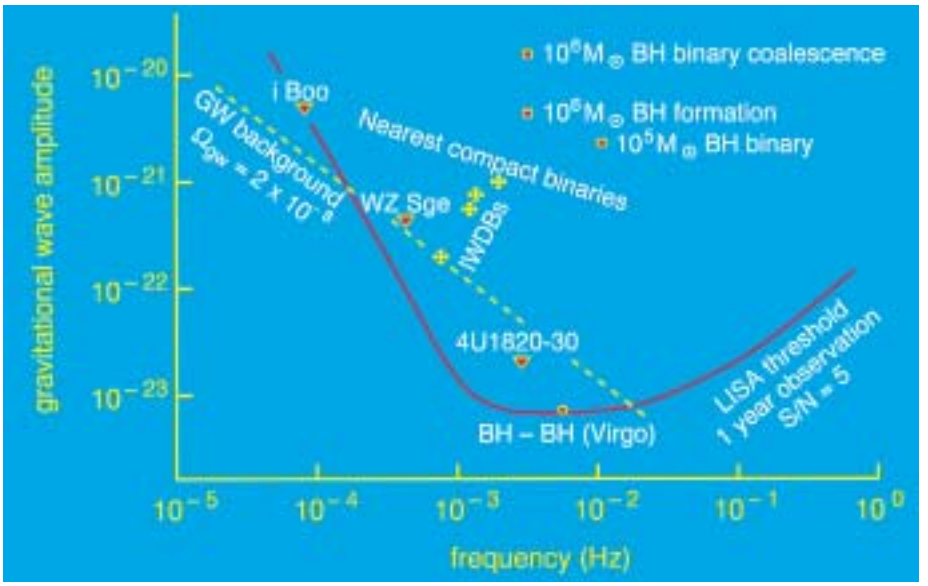

Figure 5.3.1. The target sensitivity curve of LISA and the strengths of expected gravitational-wave sources.

For further information, see http://sci.esa.int/lisa/

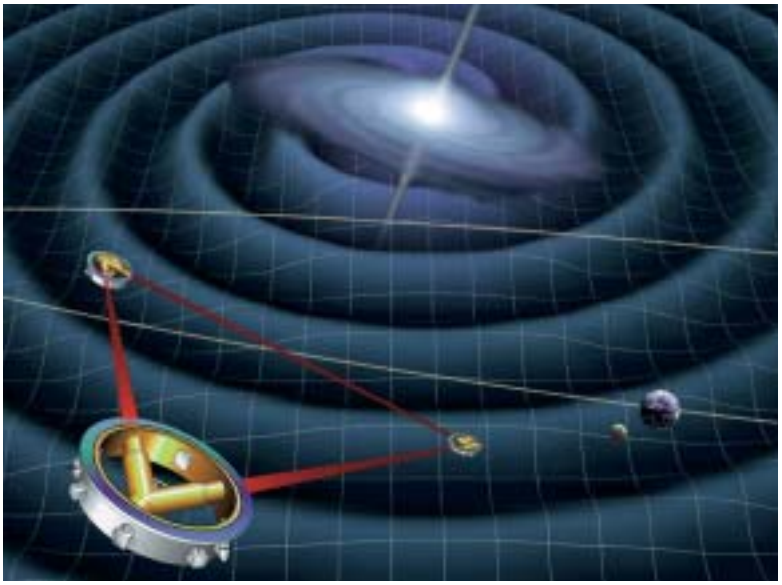

Figure 5.3.2. Orbital configuration of the three LISA spacecraft.

still slightly uncertain, is expected to be marginal for first-generation detectors. Only second-generation detectors, to be commissioned after 2005, are expected to achieve reliable detection of those important astrophysical sources. Coalescences of MBHs are detectable only in space because of the very low frequencies involved.

In the low-frequency band of LISA, sources are well known and signals are stable over long periods (many months to thousands of years). LISA will detect signals from numerous sources with signal-to-noise ratios of 50-1000 for MBHs, which will allow determination of the internal parameters of their sources, such as position and orientation. LISA will complement the operation of the second-generation ground-based interferometers, giving a full coverage of the frequency spectrum from 0.1 mHz to the kHz region.

Configuration

The LISA mission comprises three identical spacecraft positioned 5 million kilometres apart as an equilateral triangle. LISA is basically a giant Michelson interferometer with a third arm to give independent information on the two polarisations of gravitational waves and for redundancy. The separation (the armlength of the interferometer) determines the frequency range in which observations can be made. The centre of the triangular formation is in the plane of the ecliptic, 1 AU from the Sun and trailing the Earth by approximately 20°. The plane of the triangle is inclined at 60° with respect to the ecliptic, which means that the triangular formation is maintained throughout the year, with the triangle appearing to counter-rotate about the centre of the formation once per year (Figure 5.3.2).

The position of the formation at 20° behind the Earth is a result of a trade-off between minimising the gravitational disturbances from the Earth-Moon system and the communications needs. Futher away would further reduce the disturbances, but a larger distance would require larger antennas or higher transmitter power.

While LISA can be described as a Michelson interferometer, the implementation is somewhat different from a ground-based interferometer. The laser light going out from the centre spacecraft to the other corners is not directly reflected back because very little light would be received. In an analogy with a radio-frequency transponder,

Figure 5.3.3. Cutaway view of one of the three identical LISA spacecraft. The main structure is a ring with a diameter of 1.8 m and a height of 0.48 m. The top of the spacecraft is covered by a solar cell array, removed here to allow a view of the Y-shaped payload.

the laser on the distant spacecraft is instead phase-locked to the incoming light, providing a return beam of full intensity. The transponded light from the far spacecraft is received by the centre spacecraft and superposed with the onboard laser light that serves as the local oscillator in a heterodyne detection. As this intertwines laser frequency noise with a potential gravitational wave signal, the signal from the other arm is used to take out the laser frequency noise and obtain the pure gravitational wave signal.

Even at a distance of 50 million kilometres from Earth, the remaining gravitational disturbances of the Earth, Moon and the large planets are enough to cause relative velocities of the spacecraft of up to 20 m/s. In the course of a year, the separation changes by many thousands of kilometres. The relative velocity causes the transponded light to be Doppler-shifted by up to 20 MHz. The resulting signal is well outside the LISA detection band and can be removed by onboard data processing.

Each spacecraft has a launch mass of about 460 kg (including contingency), which includes the payload, ion drive, all propellants and the spacecraft adapter. All three spacecraft can be launched by a single Delta-II 7925H. The three will separate and use their ion drives to reach their operational orbits after 13 months. There, the propulsion modules will be jettisoned and the attitude and drag-free control left to μN thrusters.

Each spacecraft carries two 30 cm steerable high-gain antennas for communication with the Earth. Using the 34 m antennas of the Deep Space Network (DSN) and 5 W transmitter power, data can be transmitted in the X-band at 7 kbit/s. Data are transmitted for 8 h every 2 days and stored onboard in a solid-state mass memory of 1 Gb capacity during times of no communication. Only one spacecraft is used to transmit data to Earth; the other two transmit their data to the 'master spacecraft' via the laser link between the three. Nevertheless, all three spacecraft are identical which not only reduces the cost but also increases the redundancy because each could become the master spacecraft. The nominal mission lifetime is 2 years once the spacecraft reached their operational orbits.

Payload

Each spacecraft contains two optical assemblies (Figure 5.3.3), pointing towards an identical assembly on the other two spacecraft. In this way, the spacecraft form two independent Michelson interferometers, providing redundancy. A 1 W infrared laser beam (1064 nm wavelength) is transmitted to the partner spacecraft via a 30 cm aperture f/1 Cassegrain telescope. The same telescope is used to focus the very weak beam (a few pW) coming from the other spacecraft and to direct the light to a sensitive photodetector (a quadrant photodiode), where it is superimposed with a fraction of the original local light. At the heart of each assembly is a vacuum enclosure containing a free-flying polished platinum-gold 40 mm cube – the proof mass – which serves as an optical reference ('mirror') for the light beams. A passing gravitational wave will change the length of the optical path between the proof masses of one arm of the interferometer relative to the other arm. The fluctuations in distance are measured to a precision of 40 pm (averaged over 1 s) which, when combined with the large separation between the spacecraft, allows LISA to detect gravitational wave strains down to a level of order $\Delta\lambda/\lambda = 10^{-23}$ in 1 year of observation with a signal-to-noise ratio of 5.

The spacecraft serves mainly to shield the proof masses from the adverse effects of solar radiation pressure so that the test masses follow a purely gravitational orbit. Although the position of the spacecraft does not enter directly into the measurement, it is nevertheless necessary to keep all spacecraft moderately accurately centred on their respective proof masses to reduce spurious local noise forces. This is achieved by the drag-free control system consisting of an accelerometer (or inertial sensor) and a system of µN thrusters.

Capacitive sensing in three dimensions is used to measure the displacements of the proof masses relative to the spacecraft. These position signals are used in a feedback loop to command Field Emission Electric Propulsion (FEEP) thrusters so that the spacecraft follows its proof masses precisely. As a reference point for the drag-free system, one or the other mass (or any point in between) can be chosen. The FEEP thrusters are also used to control the attitude of the spacecraft relative to the incoming optical wavefronts using signals derived from the quadrant photodiodes.

Although the spacecraft shields its proof masses from non-gravitational forces, cosmic rays and solar flare particles can cause a significant charging of the proof masses. As charges will cause non-gravitational forces on the proof masses, a discharging system of a fibre-coupled UV light source will operate at regular intervals.

As the three-spacecraft constellation orbits the Sun in the course of a year, the observed gravitational waves are Doppler-shifted by the orbital motion and amplitude modulated by the non-isotropic antenna pattern of the detector. This allows us to determine the direction of the source and to assess some of its characteristics, e.g. its orientation if the signal is periodic and has a sufficiently large signal-to-noise ratio. Depending on the strength of the source, a precision for determining the position of up to 1 arcmin can be achieved.

Status

LISA is envisaged as an ESA/NASA collaborative project, selected as an ESA cornerstone mission and included in NASA's strategic plan with a nominal launch in 2011. In the collaboration, NASA provides the launch vehicle, ground segment, mission and science operations, and about 50% of the payload. ESA contributes the three spacecraft, including the ion drives and FEEP thrusters. The remaining 50% of the payload is provided by European institutes.

5.4 NGST

Introduction

NASA, ESA and the Canadian Space Agency (CSA) have since 1996 collaborated on the definition of a worthy successor to the Hubble Space Telescope (HST): the Next Generation Space Telescope (NGST).

NGST will be a passively cooled, 6 m-class telescope, optimised for diffraction-limited performance in the near-IR (1-5 µm) region, but with extensions to either side into the visible (0.6-1 µm) and mid-IR (5-28 µm) regions. The large aperture and shift to the IR embodied by NGST is first and foremost driven scientifically by the desire to follow the contents of the faint extragalactic Universe back in time and redshift to the epoch of 'First Light' and the ignition of the very first stars. Nonetheless, like its predecessor, NGST will be a general-purpose observatory and carry a suite of astronomical instruments capable of addressing a very broad spectrum of outstanding problems in galactic and extragalactic astronomy. In contrast to HST, however, NGST will be placed into a Sun-Earth L2 halo orbit and will not be serviceable after launch.

In November 2000, the Science Programme Committee approved ESA's participation in NGST as a Flexi-mission. This level of participation will secure ESA a ~15% partnership in the NGST observatory as well as a continuation of its present participation in HST to the end of that observatory's operational life (expected in 2010). Through the concerted efforts of NASA, ESA and CSA, the NGST project has matured dramatically since its inception. The project is now poised to enter its design and construction phase.

Scientific payload

The science case for the mission has been documented in quantitative detail by a joint *ad hoc* Science Working Group (ASWG) and the blueprints for an observatory architecture capable of meeting the derived scientific requirements were drawn up during 1999-2000. On the NASA side, two competing prime contractors have been

Figure 5.4.1. NGST concept. (Ball/TRW)

For further information, see http://rssd.esa.int/NGST

Figure 5.4.2. Simulated deep NGST image. (STScI)

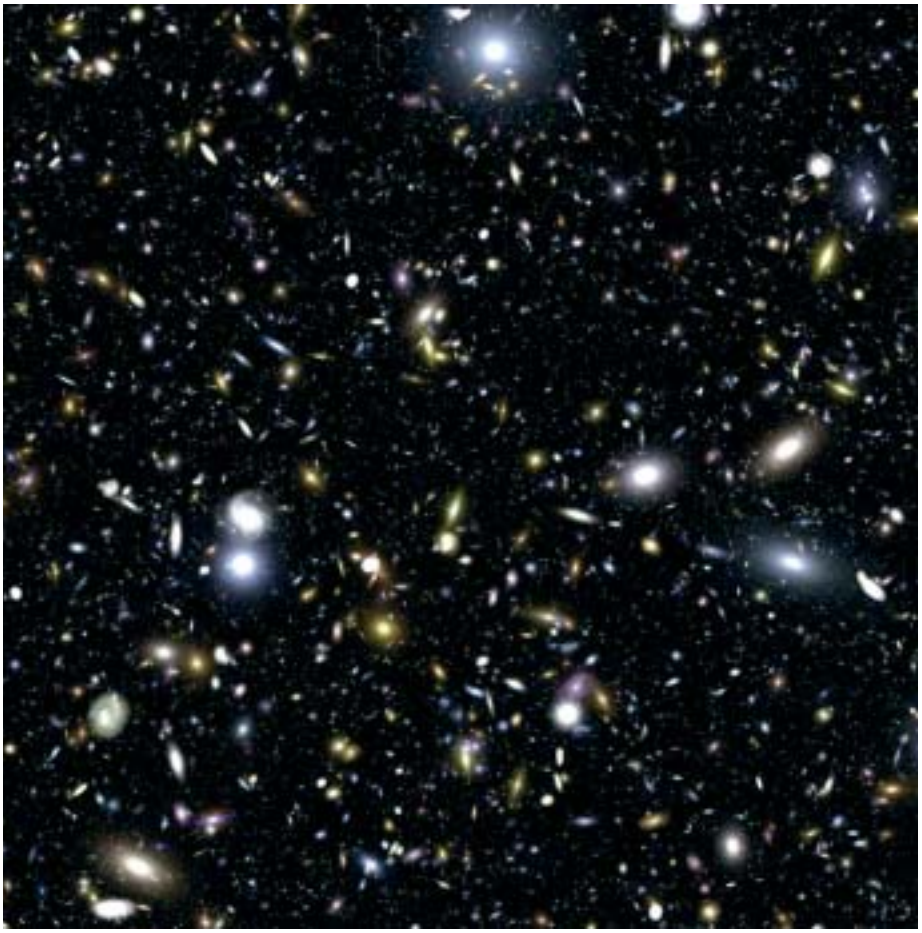

appointed to carry out definition studies of the observatory, one of which will soon be selected to build the observatory.

NGST will carry three instruments:

— NIRCam: a near-IR Wide Field Camera covering 0.6-5 µm;
— NIRSpec: a near-IR Multi Object Spectrograph covering 1-5 µm;
— MIRI: a mid-IR combined Camera/Spectrograph covering 5-28 µm.

The NGST telescope proper and its associated instruments are to be cooled in bulk to ~30-50K, a temperature determined by the operating temperature of the candidate InSb and HgCdTe detector arrays covering the prime near-IR 1-5 µm range. Cooling will be passive by placing the observatory at L2 and keeping the telescope proper and its instrumentation in perpetual shadow by a large deployable sunshade. The three-mirror NGST telescope is specified to yield diffraction-limited performance at wavelengths above 2 µm in the near-IR. In order to fit into the shrouds of suitable launchers (EELV, Atlas or Ariane-5), the 6 m primary mirror needs to be segmented and (along with the secondary mirror) deployable in orbit. Fine pointing will be achieved by deflecting the beam by a fast-steering mirror controlled by a Fine Guidance Sensor (to be provided by Canada) in the telescope focal plane.

The 0.6 µm visible wavelength limit of the NGST observatory allows the use of gold as the reflecting coating in the telescope and instruments. For reasons of cost, diffraction-limited performance will not be obtained at wavelengths in the region of overlap with HST below 2 µm. Nonetheless, depending on the character of the residual aberrations, NGST's image quality may still exceed that of the less-than-half smaller HST in terms of resolving power.

The performance at longer wavelengths in the mid-IR is a slightly more complex story. The primary source of stray light in the mid-IR is thermal radiation emitted by the backside of the NGST sunshield and scattered off the largely unbaffled telescope. Provided the temperature of the sunshield can be kept below ~110K and the dust contamination of the NGST optics can be kept sufficiently low, the intensity of this stray light contribution can be kept below that of the Zodiacal light at wavelengths shorter than ~10 µm. The NGST specifications are designed to assure such 'sky-limited' performance throughout the core 1-5 µm region and out to at least 10 µm.

The NGST telescope will be fully diffraction-limited throughout the mid-IR. However, the candidate Si:As detector arrays needed to reach wavelengths beyond 5 µm require an operating temperature of ~8K, which is significantly below the ~30-50K ambient environment of the telescope and instrument module. Active cooling is therefore called for as part of the mid-IR instrument. The present baseline is to use a solid hydrogen cryostat.

Although observations beyond 10 µm will not be sky-limited and subject to thermal self-emission from NGST, the sheer size and location of the telescope ensures that it will perform in a manner vastly superior to anything that can be done from the ground at these wavelengths. The extreme long wavelength cut-off of the NGST observatory is expected to fall just short of ~30 µm, a limit dictated by the sensitivity cut-off of the baseline Si:As detectors.

ESA contributions

ESA's contributions to NGST will follow closely the HST model, and consist of three main elements: scientific instrumentation, non-instrument flight hardware and contributions to operations.

For the first item, ESA will provide the Near-IR Multi-Object Spectrometer. In addition, through special contributions from its member states, Europe will make a 50% contribution to the Mid-IR Camera/Spectrograph to be developed jointly by NASA and ESA. ESA is also pursuing the option of providing the cryostat for the Mid-IR instrument. These instrument contributions are presently undergoing detailed definition studies in industry. As of May 2002, the negotiations with NASA on ESA's contributions to non-instrument flight hardware and operations are still in progress.

Through its participation in NGST, ESA will secure for astronomers from its member states full access to the NGST observatory on identical terms to those enjoyed today on HST: they will have representation on all advisory bodies of the project and win observing time on NGST through a joint peer review process, backed by a guarantee of a minimum ESA share of 15%.

5.5 Solar Orbiter

Introduction

Our understanding of the solar corona, the associated solar wind and the 3-D heliosphere has advanced significantly as a result of missions such as Helios, Ulysses, Yohkoh and SOHO. We have reached the point, however, where further *in situ* measurements, much closer to the Sun, together with high-resolution imaging and spectroscopy from a near-Sun and out-of-ecliptic perspective, are needed to bring about major breakthroughs in solar and heliospheric physics. ESA's Solar Orbiter, selected in 2000 as a Flexi-mission, will provide these observations by means of a novel orbital design and state-of the-art instruments. The key mission goals for Solar Orbiter are to:

— explore the uncharted innermost regions of the Solar System;
— study the Sun from close by (45 solar radii, or 0.21 AU);
— swing by the Sun, tuned to its rotation, and examine the solar surface and the space above from a quasi-heliosynchronous vantage point;
— provide images of the Sun's polar regions from heliographic latitudes as high as 38°.

The scientific objectives of Solar Orbiter are to:
— determine *in situ* the properties and dynamics of plasma, fields and particles in the near-Sun heliosphere;
— investigate the fine-scale structure and dynamics of the Sun's magnetised atmosphere, using close-up, high-resolution remote sensing;
— identify the links between activity on the Sun's surface and the resulting evolution of the corona and inner heliosphere;
— observe and fully characterise the Sun's polar regions and equatorial corona from high latitudes.

The near-Sun interplanetary measurements, together with simultaneous remote sensing observations of the Sun, will disentangle spatial and temporal variations. These observations will be carried out during the quasi-heliosynchronous part of the orbit, around perihelion. At these times, the Orbiter will have approximately the same angular velocity as the solar surface, making it 'heliostationary'. This will allow the characteristics of the solar wind and energetic particles measured at the Orbiter to be directly linked with the plasma conditions in their source regions on the Sun.

By approaching as close as 45 solar radii, Solar Orbiter will view the solar atmosphere with unprecedented spatial resolution (35 km pixel size, equivalent to 0.05 arcsec from Earth). Over extended periods, Solar Orbiter will deliver images and measurements of the Sun's polar regions and the surface not visible from Earth.

Science payload

Solar Orbiter will achieve these wide-ranging goals via a suite of sophisticated instruments. The model payload includes two instrument packages, optimised to meet the solar and heliospheric science objectives:

— *heliospheric in situ instruments:* solar wind analyser, radio and plasma wave analyser, magnetometer, energetic particle detectors, interplanetary dust detector, neutral particle detector, solar neutron detector.
— *solar remote-sensing instruments:* extreme ultraviolet (EUV) full-Sun and high-resolution imager, high-resolution EUV spectrometer, high-resolution visible-light telescope and magnetograph, EUV and visible-light coronagraph, radiometer.

For further information, see http://sci.esa.int/home/solarorbiter/

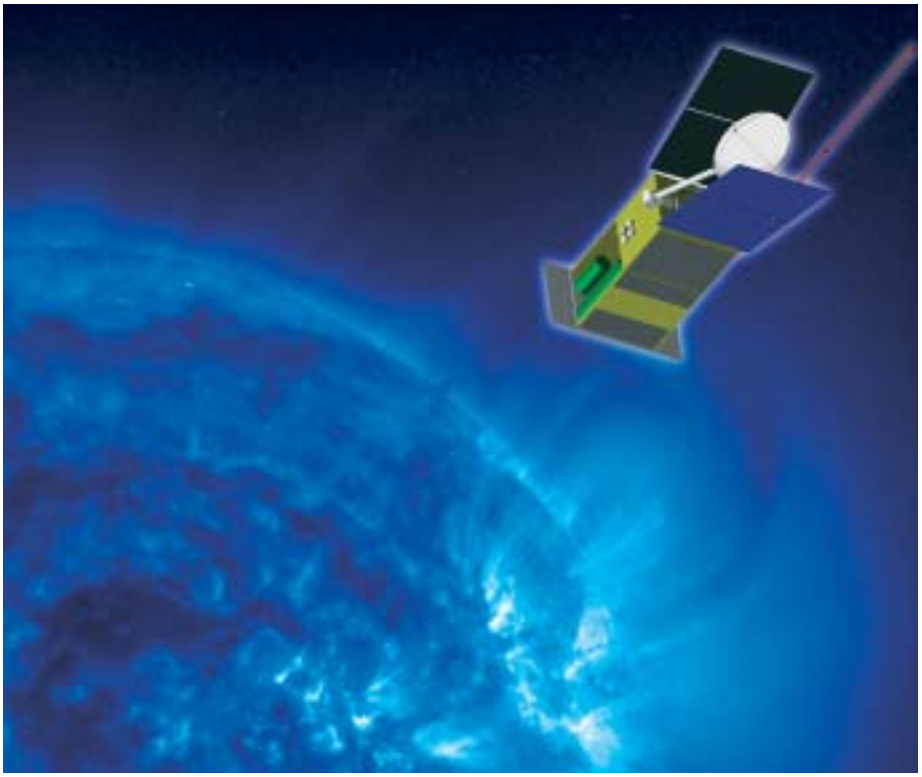

Fig. 5.5.1. Artist's impression of the Solar Orbiter spacecraft near perihelion.

Owing to the Orbiter's proximity to the Sun, many of these instruments can be smaller than similar instrumentation deployed in Earth orbit. Two Solar Orbiter Payload Working Groups (one for *in situ* instruments and one for remote-sensing instruments) will be established to arrive at a detailed definition of the model payload, and to identify necessary payload technology developments.

As currently envisaged, Solar Orbiter will employ solar electric propulsion in conjunction with multiple planetary swingbys to reach an initial operational orbit (perihelion distance 0.21 AU, equal to 45 solar radii; aphelion distance 0.89 AU) in only 2 years. The orbital period will be 149 days. Within the nominal 5-year mission phase, the Orbiter will perform several swingby manoeuvres at Venus, in order to increase the inclination of the orbital plane to 30° with respect to the solar equator. During an extended mission phase of about 2 years, the inclination will be further increased to 38°. The spacecraft will be 3-axis stabilised and always Sun-pointed. Given the extreme thermal conditions at 45 solar radii (equivalent to 23 solar constants), the thermal design of the spacecraft has been considered in detail during the Assessment Study phase, and viable solutions have been identified. Telemetry will be handled via X-band low-gain antennas, and by a 2-axis steerable Ka-band high-gain antenna. The total mass of Solar Orbiter will be compatible with a Soyuz-Fregat launch from Baikonur.

In order to carry out this ambitious mission within the constraints of a Flexi-mission, it is envisaged that Solar Orbiter could utilise technology developed for the BepiColombo mission to Mercury. Furthermore, given the high level of international interest in Solar Orbiter, a collaborative mission in the framework of the International Living With a Star (ILWS) programme is also being explored.

5.6 Eddington

Introduction

Eddington has two primary science goals: to produce the data on stellar oscillations necessary to understand stellar structure and evolution, and to detect and characterise habitable planets around other stars. These goals will be achieved through extremely sensitive, continuous photometric monitoring of a very large number of stars, at an accuracy level that requires space-based observations.

Science goals

Stellar structure and evolution

Eddington will produce the data necessary for a detailed understanding of the interior structure of stars and the physical processes that govern their evolution, providing the empirical basis for developing the theory of stellar evolution to the stage where it can be used with confidence to address some of the major issues in modern astrophysics (such as 'how old is the Universe? Or an individual Galaxy? Or an individual stellar aggregate? Or how do galaxies evolve?'). The tool for this will be stellar seismology ('asteroseismology'): the study of the resonant oscillation frequencies of stars of different masses, ages and chemical compositions. Oscillations probe the interior of stars, yielding data on the interior structure that cannot be obtained by classical observations. The primary data product of Eddington will thus be long, accurate photometric time series of a large number of stars, spanning a wide range in age, mass and chemical composition. The techniques will yield quantitative measurements of (for example) stellar ages and the sizes of convective cores to few-percent accuracy (limited by the uncertainties about the underlying physics rather than by the data). These accuracies are far superior to the levels usual in astronomy, and will yield a detailed understanding of the physical processes that govern stellar evolution and a quantitative determination of the interior structure of stars in different stages of evolution, e.g. of stars that ultimately become Type-II supernovae and major contributors to the chemical evolution of galaxies.

Habitable planets

Eddington will detect terrestrial planets around other stars, in particular planets orbiting in the 'habitable zone' and thus in principle able to sustain life. Habitable planets are defined as planets with a rocky surface (implying a size similar to the Earth) and with temperatures compatible with the presence of liquid water ($0°C < T < 100°C$). The tool will be the search for photometric dips caused by the transit of a planet in front of its parent star. Again, the primary data product will be long, accurate stellar photometric time series. In addition to finding a significant number of habitable planets, Eddington will discover large numbers of giant planets and of smaller planets outside the habitable zone, hence providing unique physical information on their properties and yielding a large database for investigations into the origin of planetary systems.

Additional science goals

The Eddington data will allow several other scientific programmes to be carried out in stellar physics and fields such as detection and light curves of supernovae, low surface brightness galactic halos, and photometric variability of quasars.

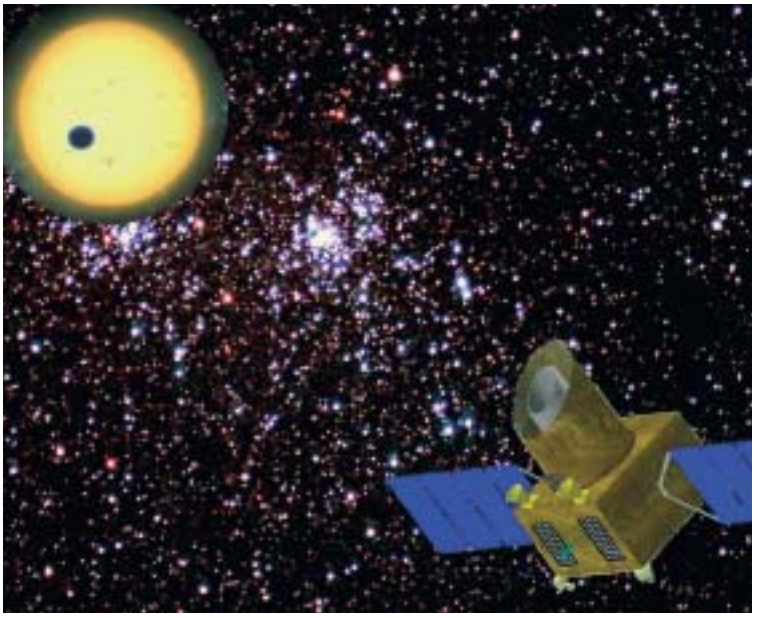

Figure 5.6.1. Eddington and its main scientific objectives: the model spacecraft and payload resulting from the assessment study performed in 2000 are shown against the background of the rich stellar cluster NGC 869 (one of the candidate targets for asteroseismic observations) and of an artist's impression (approximately to scale) of the observed transit of the giant planet HD209458b in front of its parent star.

For further information, see http://sci.esa.int/home/eddington

Payload

The Eddington payload is a wide-field, high-accuracy optical photometer, mounted on a 3-axis stabilised platform, and it is characterised by its simplicity and robustness. A model payload was defined during the initial assessment study performed in the spring of 2000, based on a lightweight 1.2 m-diameter optical telescope with a fully unvignetted 3° field of view, using a telescope based on an innovative compact two-mirror, three-reflection design. The baseline focal plane is equipped with a mosaic CCD camera covering the field of view. Detailed industrial studies are under way, which will lead to a more detailed definition of the payload. These studies are exploring innovative approaches to the problem of wide-field, high-accuracy photometry, including the use of multiple, parallel smaller aperture telescopes and the use of active pixel sensors for the focal plane.

Observing programme

Eddington will determine the interior structure of stars spanning the H-R diagram, with different ages and chemical composition. Its payload is therefore designed to reach sufficiently faint magnitudes (as faint as V = 11 for low-mass stars, and V = 13 for higher-mass stars) allowing for the rarer and fainter stellar types in crucial stages of evolution to be studied. Two years of observations dedicated mainly to asteroseismic science are foreseen, with each observing run lasting 1-2 months (to achieve sufficient resolution in the oscillation frequencies). Asteroseismic data will be collected on some 50 000 stars. While the observing programme will be the subject of an open Announcement of Opportunity (with some usual allowance for guaranteed time observers), a baseline observing programme will include several of the nearby open clusters (where homogeneous samples of stars of the same age and chemical composition, but spanning a range of masses, are available), as well as several individual stellar fields. For the planet-finding phase, a single, long duration (> 3 yr) observation of a single rich stellar field is foreseen, to ensure the detection of multiple (> 3) transits for planets with the same orbital period as our Earth. The long duration observation on a single field in the planet-finding phase will also provide lower time resolution asteroseismic data, especially valuable for the seismological investigation of long-period oscillating stars. Also, several periodic transits of short-period planets and individual transits of longer-period planets will be found in the 1-2 months of asteroseismic observations, allowing study of a significantly larger number of stars. During the 5-year mission (including the stars monitored for transits during the asteroseismic observations), some 500 000 stars will be searched for planetary transits, with an accuracy sufficient to yield a significant crop of habitable planets, as well as large number of higher mass and hotter planets.

Conclusions

The Eddington mission will enable us bring to maturity one of the cornerstones of modern astrophysics (the theory of stellar structure and evolution), by supplying solid experimental foundations, i.e. quantitative data that will, for the first time, allow direct testing of its assumptions, models and theories. At the same time, it will lead to the discovery of other planetary systems, with terrestrial planets in the habitable zone, in principle able to sustain life, and to the detection of a large number of planets spanning a wide range of characteristics, thereby allowing a statistical study of the properties of planetary systems as a function of stellar parameters. Eddington will thus supply the data needed for a complete theory of planetary system formation. In both fields (stellar structure, and evolution and exo-planet studies), the European scientific community has a leading role and a tradition of strong expertise. The Eddington mission represents a unique opportunity to bring this lead to full fruition.

5.7 STEP

Introduction

The Satellite Test of the Equivalence Principle (STEP) is a NASA/ESA collaborative project to test the Equivalence Principle (EP) to a precision of 1 part in 10^{18}, an improvement of five orders of magnitude over present knowledge. In this collaboration, ESA will procure the Service Module and a Rockot launch vehicle, while NASA will procure the dewar and the ground segment and will be responsible for overall project management, integration, testing and pre-launch, mission and science operations. The payload sharing ratio is 50/50. The European payload elements are assumed to be nationally-funded. STEP will be launched in February 2006 into a Sun-synchronous, circular orbit at 550 km altitude.

Scientific significance

The Equivalence Principle postulates the equivalence between inertial and gravitational mass or, stated differently, that bodies of different mass and/or composition fall with the same acceleration in a gravitational field. This contention cannot be proved – it can only be tested to higher and higher precision. The most precise ground-based and lunar-laser ranging tests today have achieved a precision of a few parts in 10^{13}. Experiments on the ground are limited at this level because of unshieldable seismic noise and the weak driving acceleration.

Einstein generalised the Equivalence Principle and made it the foundation of his theory of General Relativity. A violation of the Equivalence Principle at some level would either require a modification of Einstein's theory or constitute the discovery of a new force. There are, in fact, good reasons to believe that General Relativity is not the ultimate theory of gravity.

Gravitation, electromagnetism and the weak and strong interactions are the four known fundamental forces of Nature. Einstein's theory of gravity, General Relativity, is a 'classical', non-quantum field theory of curved spacetime, constituting an as-yet unchallenged description of gravitational interactions at macroscopic scales. The other three interactions are dealt with by a quantum field theory called the 'Standard Model' of particle physics, which accurately describes physics at short distances where quantum effects play a crucial role. But, at present, no realistic theory of quantum gravity exists. This fact is the most fundamental motivation for pursuing our quest into the nature of gravity. The Standard Model successfully accounts for all existing non-gravitational particle data. However, just as in the case of General Relativity, it is not a fully satisfactory theory. Its complicated structure lacks an underlying rationale. Even worse, it suffers from unresolved problems concerning the violation of the charge conjugation parity symmetry between matter and antimatter and the various unexplained mass scales. Purported solutions of these shortcomings typically involve new interactions that could manifest themselves as apparent violations of the Equivalence Principle.

The truly outstanding problem remains the construction of a consistent quantum theory of gravity, a necessary ingredient for a complete and unified description of all particle interactions. Superstring theories – in which elementary particles would no longer appear as pointlike – are the only known candidates for such a grand construction. They systematically require the existence of spinless partners of the graviton: dilatons and axion-like particles. The dilaton, in particular, could remain nearly massless and induce EP violations at a level that, albeit tiny, may well be within STEP's reach (Figure 5.7.1).

There is further compelling evidence for the possible existence of two kinds of EP violation in the range 10^{-16} to 10^{-17}. One is a consequence of a possible variation with time of the fine structure constant (claimed by some researchers); the other is a consequence of 'little' string theory.

STEP will probe a very large and otherwise inaccessible domain in the parameter

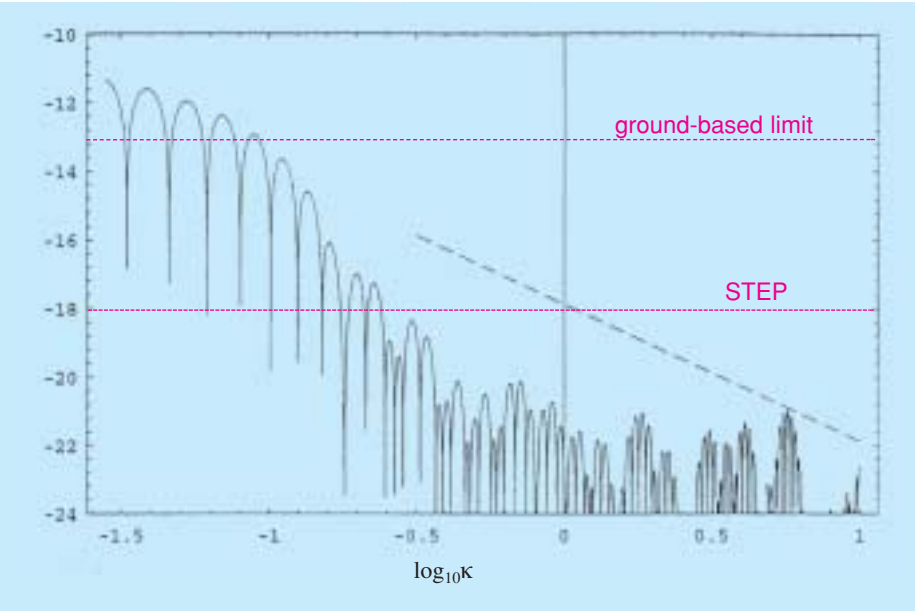

Figure 5.7.1. Level of EP violation (when comparing uranium with a light element) in a class of string-inspired theoretical models. The solid line represents the exponent of the Eötvös ratio (essentially the difference of the ratios of the gravitational and inertial mass of two test bodies) as a function of $\log_{10}\kappa$ (κ is the curvature of the string-loop induced function $\ln(B^{-1}(\Phi))$ near a minimum Φ_m; values in the range $0.1<\kappa<10$ are most reasonable). The dashed line represents an analytical estimate.

space of new interactions of the types outlined above. Whatever its outcome, STEP will advance our knowledge of the fundamental laws of physics: a null result would remain, for years to come, a severe constraint on current and future theories; a positive result would constitute the discovery of a new fundamental force of Nature.

Payload

The STEP Project is the modern version of Galileo's famous free-fall experiment in which he (is said to have) dropped two weights from the Leaning Tower of Pisa to demonstrate that they fall at the same rate. In STEP, the test masses are placed inside a satellite in low-Earth orbit, where they 'fall around the Earth' (Figure 5.7.2). In this way, the test masses never strike the ground, and any difference in the rate of fall can build up over a long time period. In Earth orbit, the signal is periodic and the experiment can be repeated several thousand times during the mission lifetime.

The test masses are freely-floating hollow cylinders centred on each other to eliminate any disturbances from the Earth's gravity gradient (Figure 5.7.3). Any differential motion of these two test masses is sensed by coils coupled to Superconducting Quantum Interference Device (SQUID) magnetometers, forming a superconducting differential accelerometer. The SQUIDs can detect any differential motion of the two test masses in a pair with a sensitivity of 10^{-15} m. In the STEP experiment, the sensor is optimised for maximum acceleration sensitivity and can detect a relative acceleration of 10^{-15} m s^{-2} in 1 s. The differential accelerometer produces an electrical output exactly proportional to the difference in acceleration of the two masses. The test masses do not actually move: they remain centred on each other throughout the orbit. The signal of any EP violation is the electrical force required to hold the test masses centred. To sample a variety of test-mass materials, STEP carries four such differential accelerometers. The payload chamber is accommodated inside a superfluid helium dewar that cools the payload to 1.8K. At several hundred kilometres altitude, the density of the Earth's atmosphere is sufficient to brake the satellite so that the test masses would soon strike the walls of the experiment chamber. The satellite must therefore compensate for the braking by

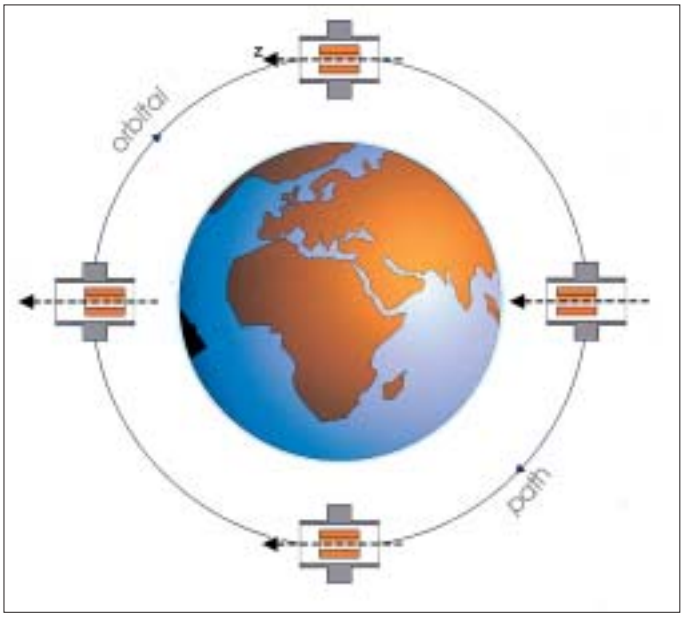

Figure 5.7.2. Relative motion of two concentric cylindrical test masses in the case of an EP violation. The masses are constrained to 1-D motion. In this example, the inner test mass falls faster towards the Earth. The EP violation signal is periodic at orbital frequency. STEP carries four pairs of concentric test masses inside a quartz block.

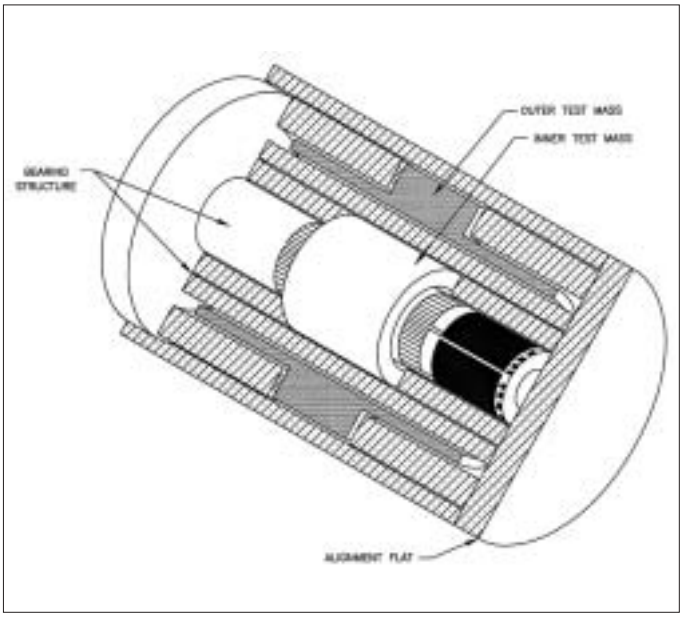

Figure 5.7.3. One of the four differential accelerometers of the EP experiment.

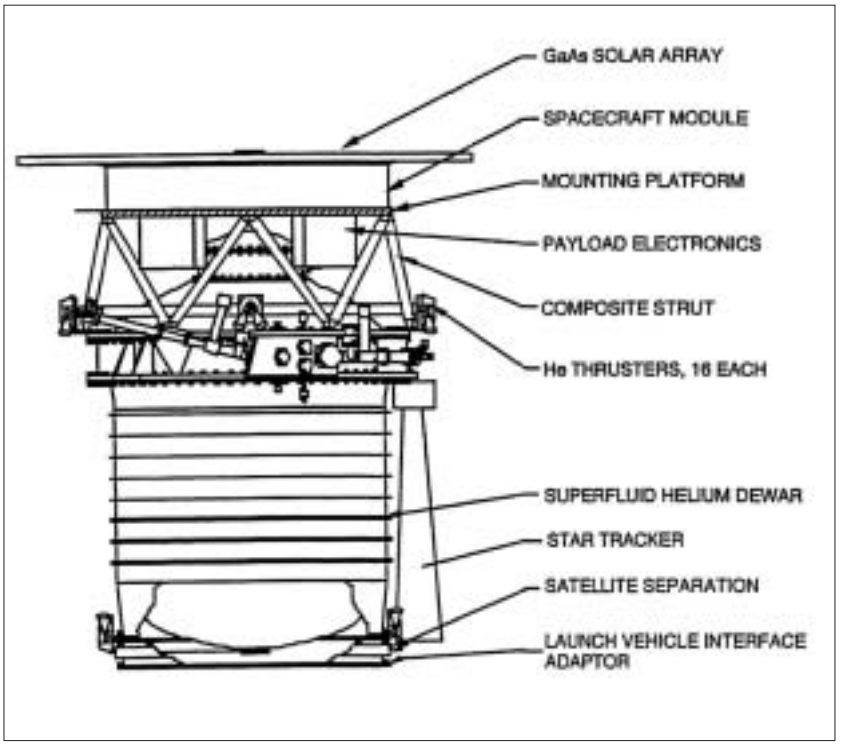

Figure 5.7.4. The STEP spacecraft, comprising the Service Module mounted on top of the Payload Module (the dewar accommodating the STEP experiment).

employing a combination of proportional thrusters so that the test masses inside are free-floating and can follow a purely gravitational orbit.

Spacecraft and mission design

The STEP spacecraft (Figure 5.7.4) is 3-axis stabilised. It has an octagonal shape, a height of 2.2 m and a launch mass of 1150 kg (including adapter ring and 20% system margin). It consists of the Service Module, providing the conventional functions, and the Payload Module, essentially the dewar housing the experiment. Mounted on top of the Service Module is a GaAs solar array, providing 300 W of power and, at the same time, shielding the spacecraft from insolation.

The drag-free system employs the payload accelerometers as sensors (augmented by two star trackers as an absolute reference) and uses as actuators 16 proportional thrusters with helium, vented from the superfluid helium dewar, as propellant. The 'drag-free system' does not make the spacecraft completely drag-free: it only attenuates the disturbances to a tolerable level (10^{-13} m s^{-2} rms) over a finite frequency range (10^{-5} Hz measurement bandwidth). In essence, the drag-free system operates by measuring the common-mode motion of the accelerometer test masses and uses these measurements in a feedback loop to command the thrusters to make the spacecraft follow the test masses.

To achieve a highly stable thermal environment for the STEP experiment, eclipses must be completely avoided. This is possible by selecting a Sun-synchronous orbit with an altitude in the range 325 km to about 1000 km. For STEP, for which a circular orbit at 550 km altitude was selected, a Sun-synchronous orbit is achieved in a near-polar orbit with an inclination of 97.6°. STEP has two annual launch windows, the first opens on 9 February for an orbit with the ascending node at 06.00 h, the second opens on 10 August for an orbit with the ascending node at 18.00 h. In both cases, the eclipse-free time is 8.7 months; a launch after 9 February or 10 August simply means that the eclipse-free time is reduced. STEP needs a minimum of 6 months operational lifetime plus about a month for initial setup and calibration. STEP is planned for launch by a European Rockot vehicle from the Plesetsk Cosmodrome (67°N, 40°E) in mid-February 2006. During flight, the spacecraft rotates about its long axis at a small multiple of the orbital frequency in order to spectrally shift the science signal from orbit-fixed systematic error sources.

Status

From July 1999 to April 2000, ESA carried out an industrial study of the Service Module at Phase-A level. This was followed by a Pre-Phase-B study in January - July 2002. An industrial study on drag-free control and algorithm design ran from April 2001 to July 2002. On the US side, STEP was selected for a Phase-A Concept Study in NASA's Small Explorer (SMEX) programme. This study was carried out May - November 2001. ESA's share in the Project (Service Module, launch vehicle) was provisionally approved by the SPC in December 2001, subject to later approval by NASA.

Note added in proof: on 2 July 2002, NASA announced the non-selection of STEP as a SMEX.

5.8 SMART-2

Introduction

SMART-2 is primarily intended to demonstrate the key technologies for the ESA/NASA collaborative LISA cornerstone mission. To this end, SMART-2 will accommodate a LISA Technology Package (LTP), provided by European institutes and industry, and probably also a Disturbance Reduction System (DRS) that is very similar to the LTP and has the same goals but is provided by US institutes and industry. The LTP and the DRS can be accommodated on a single spacecraft.

Currently under discussion is the possibility of also using SMART-2 for validating some technologies for the Darwin cornerstone mission, namely formation flying and metrology. The accommodation of the Darwin Technology Package (DTP) would require a minimum of two spacecraft for SMART-2; this option is referred to as 'SMART-2 Plus'.

Missions goals

The mission goals for the LTP can be summarised as:

— demonstrating drag-free and attitude control in a spacecraft with two proof masses in order to isolate the masses from inertial disturbances. The aim is to demonstrate the drag-free system with a performance on the order of 10^{-14} m s^{-2} /√Hz in the bandwidth 10^{-3}-10^{-1} Hz. The LISA requirement in the same band is 10^{-15} m s^{-2} /√Hz;

— demonstrating the feasibility of performing laser interferometry in the required low-frequency regime with a performance as close as possible to 10^{-12} m/√Hz in the frequency band 10^{-3}-10^{-1} Hz, as required for the LISA mission;

— assessing the longevity and reliability of the capacitive sensors, thrusters, lasers and optics in the space environment.

The mission goals for the DTP can be summarised as:

— deployment and acquisition tests: The two spacecraft are injected from the transfer configuration into a sphere of several kilometre diameter, acquire each other and move into the position required for observation;

— observation mode: the two spacecraft control the pointing position with a precision ranging from centimetres down to millimetres;

— reconfiguration mode: a set-up sequence that includes moving to a new baseline and a new pointing direction.

LISA Technology Package

The LTP represents one arm of the LISA interferometer, in which the distance between the two proof masses is reduced from 5 million km to 20 cm. As in LISA, the proof masses fulfil a double role: they serve as optical references (mirrors) for the interferometer and as inertial references for the drag-free control system.

The LTP drag-free control system consists of an accelerometer (or inertial sensor), a propulsion system and a control loop. The two identical proof masses (46 mm cubes) are housed in individual vacuum cans. Capacitive sensing in three dimensions measures the displacement of the cubes with respect to their housing. These position signals are used in a feedback loop to command µN proportional thrusters to enable the spacecraft to remain centred on the proof mass. Field Emission Electric Propulsion (FEEP) thrusters will be used.

Although the proof masses are shielded from non-gravitational forces by the spacecraft, cosmic rays and solar flare particles can significantly charge them, leading to electrostatic forces. A system of fibre-coupled UV lamps will discharge the proof masses at regular intervals.

Using two proof masses, the reference point for the drag-free system can be chosen to be on each of the two masses or at any point between. Having two also allows verification of the performance of the drag-free control loop with the second proof

mass by sensing its movements relative to the spacecraft (or the first proof mass) while the spacecraft follows the first proof mass.

The position of the proof masses with respect to the spacecraft or each other is measured by an interferometric system that is capable of pm precision in the frequency band 10^{-3}-10^{-1} Hz. The outcome of ongoing technology development contracts will decide upon the exact realisation of the interferometric measurement system. The remaining temperature fluctuations aboard the spacecraft require the use of materials with very small coefficients of thermal expansion. As the dynamic range needed is comparatively large (up to 10 mm), a heterodyne interferometer is favoured.

Disturbance Reduction System

The Disturbance Reduction System (DRS) is a NASA-supplied system with the same mission goals as LTP but using slightly different technology. Its exact design will be determined by studies but the baseline foresees two inertial sensors and an interferometric readout similar to that planned for LTP. The thrusters for the drag-free control system will be different from the FEEPs: DRS is based on colloidal thrusters that use ionised droplets of a colloid accelerated in an electrical field to provide propulsion.

Darwin Technology Package

The Darwin Technology Package (DTP) includes the propulsion system for the two spacecraft (FEEPs), the guidance and navigation package, the attitude and orbital control software, a radio-frequency (RF) metrology system and the main metrology system. The latter includes a high-precision metrology laser/delay line system with a fringe tracker. For Darwin, two levels of tests are foreseen: a coarse control to cm-level using RF sensors, and an intermediate control to µm-level using laser sensing.

The delay line/fringe tracker module is intended to verify the need for positional tracking through the science telescopes, using a separate channel on the Darwin mission. The nulling interferometer technology needed for Darwin is not part of the DTP but is instead validated separately on the ground, first using laboratory breadboards and later by deploying a working instrument on the European Southern Observatory's Very Large Telescope Interferometer in Chile.

Launch and orbit

The projected launch vehicle will be an Ariane ASAP to deliver SMART-2 into a geostationary transfer orbit. From there, it will use its own propulsion module to reach its operational orbit around the L1 point about 1.5 million km from Earth. The exact orbital parameters are subject to a trade-off: a larger orbit (about 750 000 km radius) allows a 'free injection' strategy, saving propellant and mass; a tighter orbit (about 120 000 km radius) facilitates communications with Earth. The orbit is chosen so that it fulfils the requirements of both the DTP and the much more stringent ones of the LTP in respect of thermal stability and gravitational disturbances. The DTP needs about 6 months for in-orbit evaluation, LTP and DRS about 3 months each. The total mission duration is approximately 1.5 years, which includes reaching the operational orbit, initial set-up and calibration.

Status

Two parallel system-level industrial studies were finished in July 2002. These definition studies investigated four different mission scenarios:

— two spacecraft, each accommodating a DTP. One carries the LTP, the other NASA's DRS, or, more likely, one spacecraft carries both the LTP and DRS;
— as above but without the DRS;
— one spacecraft, accommodating the LTP and DRS;
— one spacecraft, accommodating the LTP.

A decision which of these scenarios will be implemented is expected in late 2002.

5.9 Venus Express

Introduction

Venus Express, an orbiter to study the atmosphere, plasma environment and surface of Venus, was proposed to ESA in response to the March 2001 Call for Ideas for reuse of the Mars Express platform. A strict schedule was imposed, aiming at a launch date in 2005, with a strong recommendation to include instruments already available, in particular as flight-spare units from Mars Express and Rosetta. A Mission Definition Study was conducted during mid-July to mid-October 2001. Venus Express was eventually recommended for selection by the science programme advisory committees on the strength of its excellent scientific value. On 11 July 2002, although the payload funding was still not fully in place, the Scientific Programme Committee (SPC) unanimously approved the start of work on Venus Express, as the prospects for reaching an agreement on payload funding by 15 October were sound. Industrial and payload activities began in mid-July. Venus Express will be put forward for confirmation at the SPC meeting in November 2002.

Mission overview

Venus Express is to be launched from Baikonur Cosmodrome by a Soyuz-Fregat in November 2005 on a direct transfer trajectory to Venus lasting about 150 days. It will then be inserted into a highly elliptical 5-day orbit around Venus with pericentre at 400 km altitude (250 km under study). The spacecraft will be transferred to its operational quasi-polar orbit (18 h and 24 h orbits are under consideration) by lowering the apocentre to an altitude in the range 52 000-66 000 km. A nominal mission duration of about 2 Venusian days (480 Earth days) is foreseen.

Scientific goals

The fundamental mysteries of Venus relate to the global atmospheric circulation, the atmospheric chemical composition and its variations, the surface-atmosphere physical and chemical interactions including volcanism, the physics and chemistry of the cloud layer, the thermal balance and the role of trace gases in the greenhouse effect, the origin and evolution of the atmosphere, and the plasma environment and its interaction with the solar wind. The key issues of the history of venusian volcanism, the global tectonic structure and important characteristics of the planet's surface are also unresolved. Resolving these issues is of crucial importance for comparative planetology and for understanding the long-term evolution of climatic processes on Earth-like planets.

The above problems will be efficiently addressed by an orbiter equipped with a suite of remote sensing and *in situ* instruments. Venus Express will provide a breakthrough by fully exploiting the near-IR atmospheric windows over the night side, discovered in the 1980s, through which radiation from the lower atmosphere and even the surface escapes to space. Thus, a combination of spectrometers, spectro-imagers and imagers covering the UV to thermal-IR range, along with instruments such as a radar and a plasma analyser, can sound the entire atmosphere from the

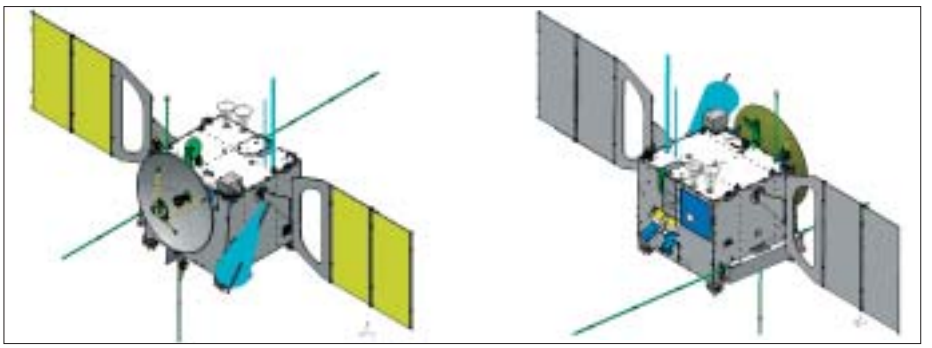

Figure 5.9.1. The Venus Express mission reuses the Mars Express spacecraft platform.

Table 5.9.1. The Venus Express scientific payload.

Code	*Technique*	*PI & Co-PI*
ASPERA	Plasma analyser. Energetic neutral atom imager	PI: S. Barabash (IRF-Kiruna, Sweden) Co-PI: J.-A. Sauvaud (CESR/CNRS, Toulouse, France)
MAG	Magnetometer	PI: T. Zhang (IFW, Graz, Austria)
PFS	High-resolution IR Fourier spectrometer	PI: V. Formisano (IFSI- Frascati, Italy)
SPICAV	UV & IR atmospheric spectrometer for solar/stellar occultations and nadir observations	PI: J.-L. Bertaux (SA/CNRS, Verrières-le-Buisson, France) Co-PI: O. Korablev (IKI, Moscow, Russia) Co-PI: P. Simon (BIRA-IASB, Brussels, Belgium)
SOIR	High-resolution solar occultation channel	Co-PI: D. Nevejans (BIRA-IASB, Brussels, Belgium)
VeRa	Radio occultation instrument	PI: B. Häusler (Universität der Bundeswehr, München, Germany) Co-PI: M. Pätzold (Univ. Köln, Germany)
VENSIS	Surface, subsurface and ionosphere sounding radar	PI: G. Piccardi (Info-Com, Univ. di Roma, Italy) Co-PI: J. Plaut (JPL, USA)
VIRTIS	UV-visible-IR imaging and high-resolution spectrometer	Co-PI: P. Drossart (CNRS/LESIA & Observatoire de Paris, France) Co-PI: G. Piccioni (IASF-CNR, Roma, Italy)
VMC	Wide-angle Venus Monitoring Camera	PI: W. Markiewicz (MPAe, Katlenburg-Lindau, Germany)

surface to 200 km altitude, and address specific surface questions complementing the Magellan investigations. This mission will also tackle open questions on the plasma environment, focusing on non-thermal atmospheric escape. This issue will be addressed via traditional *in situ* measurements as well as by innovative energetic neutral atom-imaging techniques.

Scientific payload

In order to deliver a mission within 3 years, the Venus Express payload comprises mainly existing flight spare units developed for previous missions. The scientific payload (Table 5.9.1) consists of six instruments directly derived from Mars Express and Rosetta flight spare units. In addition, there is a magnetometer and a high-resolution solar occultation IR channel as part of SPICAV. During the Mission Definition Study, it was found scientifically reasonable and technically feasible to replace the standard Mars Express engineering Video Monitoring Camera by a scientific instrument, the Venus Monitoring Camera (VMC).

The spacecraft

The Venus Express spacecraft (Figure 5.9.1) is derived from the Mars Express bus, with modifications to handle the hotter thermal environment at Venus. It is based on a box-like bus of 1.7x1.7x1.4 m. The X-band telemetry rate will vary according to the Earth distance; it is expected that a downlink of at least 500 Mbit per day will be supported. An S-band downlink channel is also provided for radio science investigations. A variable telecommand rate of 7.8-2000 bit/s is foreseen.

The modifications to cope with the harsher thermal conditions, including adaptation of the instruments' thermal accommodation, were identified during the industrial study phase and present no particular challenge.

The development programme will directly integrate and test the Flight Model instruments on the Proto-Flight Model spacecraft. Instrument Flight Model delivery is planned for early 2004.

6. Missions under Study

6.1 Darwin

Introduction

The Darwin Infra Red Space Interferometer was studied by ESA between 1997 and 2000. The study, carried out by Alcatel Space Division in Cannes, France focused on developing a system to achieve two main scientific objectives:

— the detection and characterisation of Earth-like planets orbiting other stars;
— the imaging of astrophysical objects with unprecedented spatial resolution.

The most challenging of these objectives is the recording of IR spectra of terrestrial exo-planets that could detect signs of biological activity at distances of up to 20 pc. In order to do this, the Darwin project is constructed around the new technique of 'nulling interferometry', which exploits the wave nature of light to extinguish the light from a bright object (the central star in this case) at the same time as the light from a nearby source (the planet) is enhanced. The IR was selected because the contrast between a planet and its star is higher in that wavelength region.

The scientific case

The last 6 years have seen the detection of planets beyond our Solar System finally becoming a fait accompli. The technique used so far has been indirect. It relies on measuring the reflex motion of the parent star with respect to the common centre of mass of the star-planet system, perturbing three (in principle) measurable variables:

— the radial velocity (a small periodic Doppler shift in the radial velocity of the absorption lines in the stellar spectrum which needs to be measured over a relatively long period of time – typically at least three times the planetary orbital period);
— the astrometric position;
— the arrival times of electromagnetic radiation.

The last measurable was detected first. In the timing of radio signals from a number of pulsars, several Earth-size planets have been detected. These objects have presumably been formed out of the debris of the supernova explosion, giving rise to the pulsar, and will very likely not figure in astrobiological considerations.

The first detection of a proper planet using the radial velocity method was reported in 1995 and several groups have altogether put more than 78 planets (as of April 2002) onto the map of our immediate neighborhood. Most of the Sun-type stars brighter than ~ 8 mag (about 3000 objects) are now being monitored by one or another of about ten different programmes initiated after the first successes.

It appears unlikely, however, that this method could be used to infer the presence of Earth-type planets. The lower limit to the planetary mass is more plausibly about the same as that of the planet Uranus (but at significantly smaller orbital distances – the orbital period of Uranus is about 85 years).

The planets found with the radial velocity method are more akin to Jupiter than Earth. This is due to the selection effect that biases searches for the objects causing the greatest radial velocity deflection and with short orbital periods. As time passes, longer and longer periods are being picked up, and there are now a number of confirmed planets in orbits with periods of a few years. A few of the objects could perhaps be even more closely related to the Brown Dwarfs. Because of the dependence on the actual inclination of the planet's orbit, the radial velocity method provides only the minimum mass and orbital radius, and there is no way to determine its actual size or composition. Since all objects are detected indirectly, a question raised at times is if the detected object could be a star in an orbit seen face on. A number of facts speak against such a hypothesis:

For further information, see http://sci.esa.int/home/darwin

— a plot of the number of detected objects versus $M \sin(i)$ peaks at $M \sin(i) < 1\ M_{\mathrm{Jup}}$. An unknown process would have to bias our detection towards picking up systems seen only face on.
— one planet, HD 209458b, has been found to transit its star (see below). This object is definitely in an edge-on orbit and its mass can be shown to be below $1\ M_{\mathrm{Jup}}$. It is thus a bona fide planet.

In the case of the observed occultation, the planet orbits the star HD 209458 every 3.52 days at a distance of about 0.05 AU. The occultation lasts about 2.5 h and, from this observation, the inclination is found to be 87.1°. Its mass has been determined to be $0.63\ M_{\mathrm{Jup}}$ and the radius $1.27\ R_{\mathrm{Jup}}$.

Technology

The main problem involved in the direct detection of an exo-planet of a size comparable to Earth and located at a similar distance from its star is mainly one involving contrast and dynamical range. The central star outshines the planet in the visual wavelength range by a factor of at least 10^9. This problem is alleviated by going to the mid-IR, where the planet's thermal emission peaks. Even at these wavelengths, the contrast is more than a factor of 10^6. The star and planet will be very near each other on the sky, and we need to devise a way of extinguishing the light from the star. Different coronagraphic methods (in space) have been evaluated, and although they can detect the exoplanet in some cases, these methods do not lend themselves to a large enough search space (unless the telescope is extremely large). Lately it has been suggested to fly coronographic systems operating in the visual wavelength range in space. A 5-10 m diameter monolithic telescope could then suffice. Apart from the obvious problems with very large space telescopes, it remains to be evaluated if one can detect unambiguous biomarkers in the visual region of the spectrum, however. A further complication is that the wavefronts detected need to be corrected to within 0.1 nm (r.m.s.) which is currently not possible for large optical systems in space or on the ground.

Two other methods are 'nulling interferometry' and 'densified pupil'. Of these, nulling interferometry was selected for the Darwin study because of its relative simplicity and maturity (at the time). It can be described by considering two apertures, separated by a baseline. One points the two telescopes towards the same star, and connects the light output of the two units. If one then makes the optical path lengths of both apertures the same, the amplitudes of the electromagnetic radiation will interfere. This is interferometry in the classical sense, producing a set of dark and bright fringes. If we instead now make the light from one of the telescopes arrive at the site of beam combination with an added phase shift of π, the light along the optical axis will instead interfere destructively (the dark fringe appear 'on top' of the star). At the same time, waves arriving from a small angle, θ, away will interfere constructively. This separation will depend on the distance between the two telescopes. If we now assume that we have a star orbited by a planet at an angle θ away, we can extinguish the light from the primary and isolate the planetary light. The contrast between the star and planet is now restricted to light leaks from the 'central null' – due to imperfections in the optics and jitter of mechanical components. By using more telescopes it is possible to create a more complex transmission pattern. The actual pattern depends on the number of apertures, and the geometrical configuration. In the Darwin configuration we have six telescopes in a hexagonal pattern, and with all telescopes equidistant from a central beam combiner. Then the pattern is roughly doughnut-shaped. It is now possible to 'tune' the array to each individual star that is observed, such that the transmission ring is on top of the

habitable zone (see below). The signal also needs to be modulated, in order to separate out an eventual planetary signal from any background (such as exo-zodiacal light – dust in the target system radiating as a blackbody at ~ 300K) or to discriminate between different combinations of planets in the observed system. This can be performed either by the rotation of the array of telescopes, switching between different combinations of apertures or by a combination of both. The latter option is chosen as the baseline for Darwin.

Biomarkers

A major goal of the mission is not only to detect terrestrial exoplanets but also to investigate if the conditions on the planet would allow life as we know it to exist and, indeed, if it already exists. Although extremely difficult, it has been found, however, that the simultaneous detection of water and molecular oxygen at a temperature of about 300K is a clear indication of life as we know it (Figure 6.1.1). This is because oxygen is one of the most reactive substances there is. If all life on the Earth were removed, all of the free oxygen in the Earth's atmosphere would disappear in the geologically short time of 4 million years. The atmosphere of the Earth is out of equilibrium, caused by life. Before that, our biosphere was dominated by oxygen-generating species. The atmosphere of the early Earth was out of equilibrium with methane.

The criterion on temperature defines a habitable zone around each star. Strictly speaking, the surface temperature of a planet will depend not only on the energy input from the primary, but also on the atmospheric pressure and composition. Earth, for instance, would be significantly colder without its greenhouse effect. Since we have no *a priori* idea about the presence and/or composition of any atmospheres, we have to use this criterion with care.

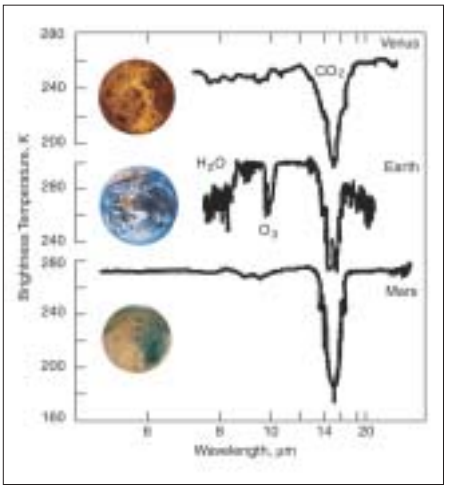

Figure 6.1.1. Thermal-IR spectra (λ = 5-18 μm) of the three terrestrial planets in our Solar System that are in the habitable zone (0.8-1.7 AU). Earth is obviously different from the others in that it shows strong signatures of ozone and water. This indicates the presence of life as we know it on our planet, but not on the two others. Darwin will carry out this analysis for Earth-like planets out to a distance of 25 pc.

Model mission

The current mission scenario is a model that can fulfil the scientific objectives, but it does not incorporate international collaboration. It consist of six 1.5 m-aperture telescopes, which transmit their input beams to a beam-combiner satellite. The individual telescopes, each mounted on a separate spacecraft, are held with the required precision in their relative positions by a metrology system, which includes laser metrology, radio-frequency goniometry and the tracking of interferometric fringes from a bright guide star. In the case of planet-finding, this is not going to be a problem, since the search for exo-planets will be carried out around relatively nearby

(and thus relatively bright) stars. The primary in each system can thus be used as a guide star for both pointing and fringe tracking for the adjustment of positions. Adjustment of path lengths and the required phase delay is then introduced in the beam combiner satellite, where detection is also carried out. The system operates at wavelengths of ~ 5-20 µm, and thus requires passive cooling of all optical components to below 40K to reduce the thermal background. Because of this, all power-generating functions (computing, transmitting of data to Earth, laser metrology) is carried out from a non-cooled communications satellite. All eight spacecraft are deployed and flown in formation around the L2 Sun-Earth Lagrangian point. In the planet-finding mode, Darwin uses baselines of 40-250 m. Launch is foreseen with an Ariane-5.

A separate beam-combiner table on the central spacecraft is used for 'normal' Michelson interferometry in an imaging mode. Baselines up to 1 km are foreseen. In this mode, objects such as star-forming regions, Active Galactic Nuclei, the core of our own Galaxy, black holes and very early galaxy formation will be studied at unprecedented spatial resolution.

Development

An ambitious technology programme has started to develop the required items such as the nulling interferometry, metrology and formation flying. Development of optical components such as polarisers, beam splitters and achromatic phase-shifters is also being initiated. More then 30 different technology studies have begun or will before 2003. A number are technology developments for other missions but take Darwin's requirements into account. A significant fraction of this technology has also broad uses in other areas of human activity such as telecommunication, Earth observation and signal processing. A number – mainly connected with formation-flying – such as propulsion, guidance, navigation and metrology need to be evaluated on a test-flight, and their technology development is thus accelerated. Such a space test of selected key technologies is foreseen on the SMART-2 precursor mission in 2006.

Collaboration with the European Southern Observatory to validate nulling from the ground, and to carry out required precursor observations, is also being started in the Ground-based European Nulling Interferometry Experiment (GENIE). It derives from the breadboarding activities in the technology programme where laboratory evaluation of nulling interferometry to the required precision is being carried out. The required precursor science is the observation of every target star in order to determine the actual level of zodiacal dust. Darwin would not be able to discern an Earth-like planet in a reasonable time for zodiacal dust levels above 500 times those of our Solar System.

International

It is foreseen to carry out Darwin – and selected items of the precursor activities – in an international scenario. There are close exchanges with the NASA Terrestrial Planet Finder (TPF) study, and Darwin is laying the foundation for a jointly executed mission in the timeframe of 2014.

Conclusion

It has been demonstrated – technologically, industrially and scientifically – that a dedicated mission to find and study, in detail, Earth-like planets orbiting nearby stars can be carried out in an international collaboration and within a reasonable time (2014). The scientific goals – including imaging at spatial scales hitherto unprecedented in the thermal-IR region – are of the highest order and warrant a significant effort. Further, the technology in need of development in order to carry out this mission is broadly useful, both for other space missions and unrelated human activity.

6.2 XEUS

Introduction

The X-ray Evolving Universe Spectroscopy Mission (XEUS) is under study as part of ESA's long-term Horizons 2000 science programme. A key goal of this mission is nothing less than the study of the hot matter and unseen dark matter when the Universe was very young, by spectroscopic investigations of the first massive black holes. These are believed to have formed when the Universe was only a small fraction of its current age and they may have played a crucial role in the formation of the first galaxies. XEUS will have sufficient sensitivity to derive their masses, spins and distances by observing X-ray intensity variations and emission lines that have been broadened and distorted by the effects of strong gravity close to the event horizon. By studying how black hole masses and spin rates evolve with cosmic time, astronomers will be able to investigate how they grow and the role they play in the evolution of the galaxies, such as our own. One of the most surprising discoveries of the past decade is that the stuff that we are made off ('normal' matter) makes up only about 5% of the content of the Universe. Most of Universe is made up of mysterious dark matter and dark energy that are not explained by our current understanding of fundamental physics. Most of the normal matter in the Universe is trapped in a dark matter 'cosmic web' as a hot tenuous intergalactic medium. XEUS will have sufficient sensitivity to characterise the mass, temperature and density of this material using X-ray absorption line spectroscopy. As well as allowing the nature of the dark matter to be probed, these studies will allow the cosmic history of common elements such as C, O, Ne and Fe to be investigated. Another key science goal for XEUS is to study the formation of the first gravitationally bound, dark matter-dominated systems (small groups of galaxies) and investigate how they evolved into the massive clusters of galaxies that we see today.

Spacecraft

XEUS will be a long-term X-ray observatory consisting of separate detector and mirror spacecraft flying in formation and separated by the 50 m-focal length of the optics (Figure 6.2.1). XEUS will be launched by an Ariane-5 some time after 2012 and have an initial mirror diameter of 4.5 m, limited by the Ariane's shroud diameter. XEUS requires a revolutionary extension of the technology devised for the X-ray

Figure 6.2.1. XEUS observing the deep Universe. The detector spacecraft (foreground) maintains its position at the focus of the X-ray mirrors 50 m away to within 1 mm. The eight sets of thrusters, one at each corner of the box-shaped detector spacecraft, are used to maintain alignment and for orbital manoeuvring. The radiator used to cool the cryogenic instruments is on the upper surface. The cylindrical mirror spacecraft slowly rotates to minimise the thermal gradients across the highly sensitive mirror surfaces.

For further information, see http://sci.esa.int/xeus/

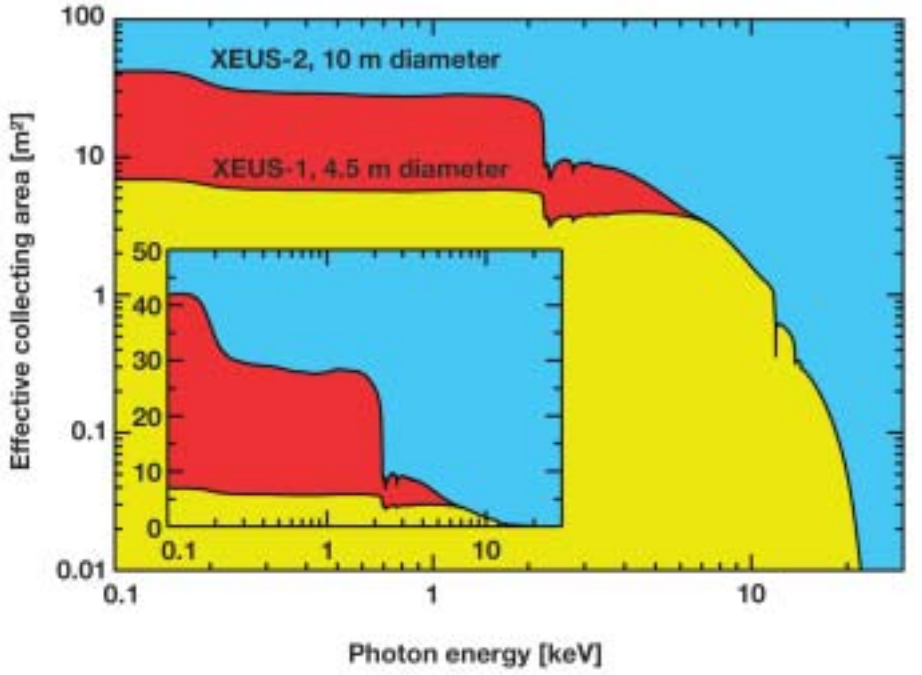

Figure 6.2.2. The XEUS mirror effective area at different energies. Directly after launch, XEUS will have a mirror diameter of 4.5 m (XEUS-1). XEUS-2, extended with additional mirror modules by a visit to the ISS, would have a diameter of 10 m and a considerably larger effective area below 5 keV. The inset shows, on a linear scale, the dramatic increase in effective area from XEUS-1 to XEUS-2.

telescopes on XMM-Newton. X-rays are focused by glancing them off the inside faces of bucket-shaped mirrors. In order to increase the effective area, each of XMM-Newton's three 0.7 m-diameter mirror modules consists of 58 individual mirrors. XEUS will need around 500 mirrors. In order to achieve the much bigger size and sharper vision required, the mirrors will be divided into segments, or 'petals'. Each petal will be individually calibrated and aligned in orbit to provide a spatial resolution of 2-5 arcsec (half-energy width). Narrow and wide field imagers will provide fields of view of 1 arcmin and 5 arcmin and energy resolutions of 500-1000 and 20 at 1 keV, respectively. It is likely that the narrow-field imager will be a cryogenic detector such as an array of bolometers or super-conducting tunnelling junctions, and the wide-field device will be based on advanced semiconductor technology. The detector spacecraft will have a sophisticated attitude and orbit control system, manoeuvring itself to remain at the focus of the optics. After using most of its fuel, the detector spacecraft will dock with the mirror spacecraft and the mated pair will transfer to the same orbit as the International Space Station (ISS). The mirror spacecraft will then dock with the ISS and additional mirror segments that have been previously transported to the ISS will be robotically attached around the outside of the spacecraft. This increases the mirror diameter to 10 m and the effective area at 1 keV from 6 m^2 to 30 m^2 (Figure 6.2.2). The dramatic increase in sensitivity associated with this expansion means that once the mirror spacecraft has left the ISS to be joined by a new detector spacecraft, complete with the latest generation of detectors, the study of the early X-ray Universe can begin in earnest. The 0.1-2.5 keV limiting sensitivity of XEUS will then be $4x10^{-18}$ erg cm^{-2} s^{-1}, approximately 200 times better than ESA's current X-ray observatory, XMM-Newton, and comparable to those of the next generation of ground- and space-based observatories, such as ALMA and NGST.

6.3 Lobster-ISS

Introduction

The X-ray sky is highly variable and unpredictable. A new X-ray source may suddenly appear in the sky, out-shine its contemporaries and then disappear a few days later. Sometimes an 'old favourite' will surprise everyone by behaving in a totally new and unexpected way. A highly sensitive X-ray mission such as ESA'' XMM-Newton observes only a small region of sky at any one time and could easily miss such unpredictable events. This is where an all-sky X-ray monitor like Lobster-ISS can play a vital role. By alerting astronomers to important events occurring anywhere in the sky, powerful observatories can be rapidly repointed to take advantage of new opportunities. The importance of this capability was recognised as early as the 1960's and the sensitivity of all-sky monitors has steadily improved. Currently, astronomers benefit from the all-sky monitor on NASA's RXTE satellite and from the Wide Field Cameras (WFCs) on the Italian/Dutch BeppoSAX satellite. Even though the WFCs have large, rather than all-sky, fields of view, their ability to provide accurate source positions rapidly played a crucial role in the discovery of X-ray afterglows to gamma-ray bursts. This discovery led to the confirmation that gamma-ray bursts occur in the distant Universe and are one of the most energetic events known. These instruments will be followed in 2004 by the MAXI all-sky X-ray monitor on the Japanese Experiment Module on the International Space Station (ISS). MAXI will offer around a factor 10 improvement in sensitivity, compared to RXTE.

Scientific goals

ESA is proposing to fly an even more sensitive (by another factor of 10) all-sky monitor on the ISS in around 2009, called Lobster-ISS. The proposal was submitted to ESA's Directorate of Science in response to the call for Flexi-Mission proposals (F2 and F3) issued in October 1999. In this call, proposals based on the utilisation of Columbus and other ISS elements were invited. The PI is G.W. Fraser, Univ. Leicester, UK, with Co-Is from the Los Alamos National Laboratory (US), NASA Goddard (US), Inst. of Astronomy Cambridge (UK), Univ. Southampton (UK), Univ. Melbourne (Australia) and Univ. Helsinki (FIN). Lobster-ISS will use a novel form of micro-channel plate X-ray optics developed under the ESA Technology Research

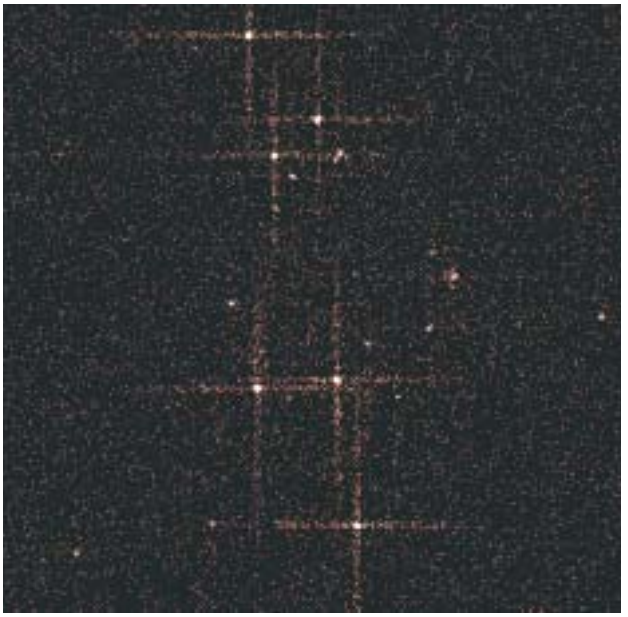

Figure 6.3.1. A simulated image of a 10x10° region of the Large Magellanic Cloud as observed by Lobster-ISS in 1 day. A total of 22 X-ray sources are clearly detected. The distinctive crosses are a characteristic of the lobster-eye X-ray optics, which focus approximately half the photons into the four arms and the rest into the central point source.

For further information, see http://www.src.le.ac.uk/lobster/

Figure 6.3.2. Lobster-ISS mounted on the zenith-pointing platform of the Columbus EPF. The main truss of the ISS runs along the top left of the image and ESA's Columbus module is visible at the lower right. Lobster-ISS consists of six individual telescope modules, each pointing in different directions to provide an instantaneous field of view of 162x22.5° (one of the modules is partially hidden behind the star tracker).

Programme to provide this unprecedented sensitivity. It will be the first true imaging X-ray all-sky monitor and it will be able to locate X-ray sources to within 1 arcmin to allow the rapid identification of new transient sources. Lobster-ISS will produce a catalogue of 200 000 X-ray sources every 2 months which will be rapidly made available to the astronomical community via the Internet. As well as providing an alert facility, the high sensitivity will allow many topics to be studied using Lobster-ISS data alone. These include the long-term variability of active galactic nuclei and stars, the mysterious and difficult to study X-ray flashes, and the highly topical X-ray afterglows of gamma-ray bursts. Figure 6.3.1 shows a Lobster-ISS image of part of the Large Magellanic Cloud obtained in a 1-day simulated observation. All the bright X-ray binaries, supersoft sources and supernova remnants are visible and their intensities and overall spectra could be monitored on a daily basis. The advantage of this type of optics for an X-ray all-sky monitor is its extraordinarily large field of view. This is achieved by accurately bending the thousands of tiny glass pores that make up each micro-channel plate by exactly the right amount to focus incident X-rays like a telescope. This is where the name comes from, since this is similar to how the eye of a crustacean works.

In order to provide the best possible view of the sky, the optimum location for Lobster-ISS is on the zenith pointing of the External Payload Facility (EPF) on ESA's Columbus module (Figure 6.3.2). An initial ESA feasibility study showed that Lobster-ISS could be comfortably accommodated on the standard ISS Express Palette Adaptor. The ISS orbits the Earth keeping its main axis parallel to the local horizon. This is a great advantage for an all-sky monitor since it means that the field of view will automatically scan most of the sky during every 90 min ISS orbit. A 12-month ESA Phase-A study is expected to start later in 2002. This will concentrate on the overall instrument design, ISS accommodation, robotic handling and end-to-end operations.

6.4 EUSO-ISS

Introduction

The Earth is being continuously bombarded by high-energy cosmic rays. While cosmic rays with energies up to 10^{15} eV almost certainly originate from comparatively well-understood objects in our Galaxy, such as the expanding shocks of exploded stars, understanding the origin of the highest energies (> $5x10^{19}$ eV) is one of the great challenges in astrophysics. Although these extreme energy cosmic rays (EECRs), believed to be probably mostly protons, are very rare (only around 1/km^2 per century!) they are the most energetic particles known in the Universe, with energies 10^8 times greater than produced by Fermilab's Tevatron – the world's most powerful particle accelerator. Because they are so rare, only about 30 such events have been detected using different ground-based air shower detectors in the past 30 years. There has been no convincing identification of any of these events with a likely astronomical source.

Scientific goals

At such extreme energies, cosmic ray protons interact with the cosmic microwave background that permeates space, and the distance that an EECR can travel is limited to our galactic neighbourhood. Intriguingly, all the astronomical objects that could conceivably produce EECRs, such as massive black holes, colliding galaxies or gamma-ray bursts, are all much further away than this. This has led to the idea that the decay of topological defects, or other massive relics of the Big Bang, may instead produce EECRs. If this is indeed the case, then it implies the existence of 'new physics'. These paradoxes are at the heart of the ambitious EUSO mission to study EECRs from space by using the Earth's atmosphere as a giant cosmic ray detector. EUSO will observe the flash of fluorescence light and the reflected Cerenkov light produced when an EECR interacts with the atmosphere (Figure 6.4.1). Direct imaging of the light track and its intensity variations will allow the sky position of the event,

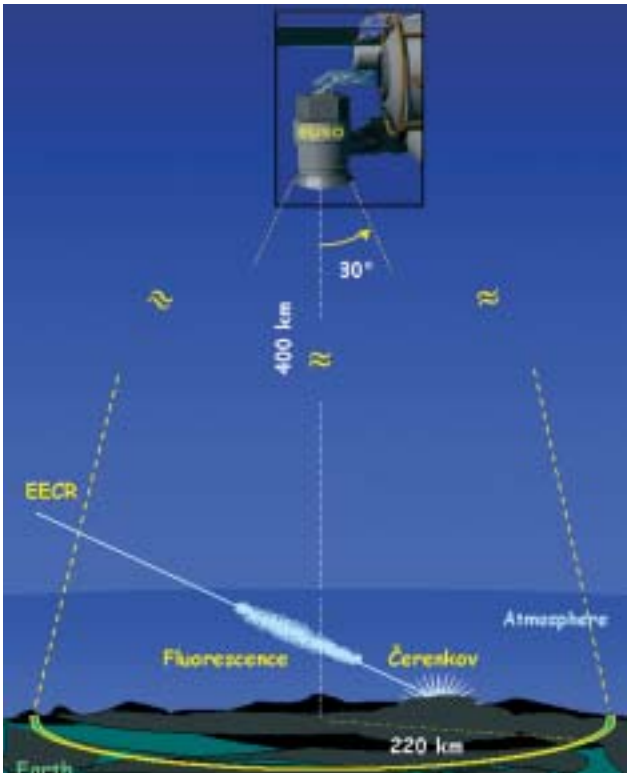

Figure 6.4.1. The EUSO method of operation. EUSO will observe downwards from the International Space Station at a height of 400 km with a wide 60° field of view and detect the fluorescent and reflected Cerenkov radiation produced when an Extreme Energy Cosmic Ray interacts with the Earth's atmosphere.

For further information, see http://www.ifcai.pa.cnr.it/~EUSO/

Figure 6.4.2. EUSO is the cylindrical structure attached to the left side of ESA's Columbus External Payload Facility. From this location, EUSO will have an unobstructed nadir view.

Table 6.4.1. The EUSO consortium.

France	APC-Paris; LAPP-Annecy; ISN-Grenoble; CERS-Toulouse; LPTHE; LAPTH; College de France; Observatoire de Paris
Italy	CNR-IASF Palermo; CNR-ISAO Bologna; Univ/INFN at Catania, Firenze, Genova, Palermo, Roma, Torino, Trieste; Osservatori Astronomici/INAF at Arcetri and Catania. Istituto Naz. Ottica-Firenze; CARSO
Portugal	LNP-Lisbon
UK	Univ. Leeds
Germany	MPIfR-Bonn
Japan	Riken; ICRR/Univ. Tokyo; KEK; NASDA; Univ. Saitama, Aoyama, Kinki, Seikei, Konan
USA	NASA Marshall, Alabama Univ. Huntsville; UCLA, Los Angeles; Univ. California at Berkeley; Vanderbilt Univ.; Univ. Tennessee; Univ. Texas at Austin

as well as the overall energy, to be reconstructed. In the same way that Lobster-ISS will benefit from the scanning offered by its zenith location, EUSO will take advantage of the continuous nadir pointing provided by the lowest location of the Columbus External Payload Facility. By looking down from here with a 60° field of view, EUSO will detect around 1000 events per year, allowing a sensitive search for the objects producing EECR.

Protons are not the only type of extreme energy particle that will be observed by EUSO. Many models for the production of EECR indicate that large numbers of neutrinos should also be produced. Since neutrinos propagate, on average, much deeper into the atmosphere than protons before interacting, EUSO will be able to distinguish between the two types of particles by selecting on interaction depth and so potentially opening up the new field of high-energy neutrino astronomy Since most sources of EECRs are expected to be transparent to their own neutrinos, these particles would allow us to observe deep inside a source to view the particle acceleration mechanism directly.

Status

The EUSO proposal was submitted to ESA in response to the same call for Flexi-Mission proposals (F2 and F3) as Lobster-ISS. The PI is L. Scarsi from IASF-CNR, Palermo (I), who leads a large consortium of astronomers, cosmic-ray and particle physicists (Table 6.4.1). EUSO will consist of a UV telescope with a large collecting area and field of view using a lightweight double Fresnel lens system, a highly segmented focal surface detector array and sophisticated onboard image processing. The image processing will provide sensitive discrimination between EECRs and other sources of UV radiation, such as lightening, meteoroids, aurorae and man-made illumination. EUSO will need a large carrier such as ESA's Automated Transfer Vehicle, with its Integrated Cargo Carrier, owing to its 2.5 m-diameter and 4 m-length cylindrical dimensions. Following an initial feasibility study, the best way of accommodating such a large and heavy payload on the ISS is one of the key topics of the 12-month ESA Phase-A study, which began in March 2002 at Alenia Spazio (I).

6.5 Hyper

Introduction

Atomic quantum sensors are a major breakthrough in the technology of time and frequency standards as well as ultra-precise sensing and monitoring of accelerations and rotations. They apply a new kind of optics based on matter waves. Today, atomic clocks are the standard for time and frequency measurement at the highest precisions. Inertial and rotational sensors using atom interferometers have a similar potential for replacing state-of-the-art sensors in other fields. Hyper (hyper-precision cold atom interferometry in space) is designed to realise two different types of sensors based on atom interferometers, each optimised for a specific scientific objective: a Mach-Zehnder interferometer to measure rotations and accelerations, and a Ramsey-Bordé interferometer to measure frequencies.

In a Mach-Zehnder interferometer, slowly drifting atoms are coherently split, redirected and recombined such that the atomic trajectories enclose a surface as large as possible. Beam splitting is achieved by atom-light interaction. During each interaction sequence, the atoms cross two counter-propagating laser beams. An atom absorbs a photon out of one laser beam and is stimulated by the other laser beam to re-emit the photon. In this way, twice the recoil of a photon is transferred coherently to the atomic wave (rather than atoms), such that the atomic wave is either equally split, deflected or recombined. The Mach-Zehnder interferometer senses both rotations and accelerations in only one particular direction. Two interferometers with counter-propagating atoms are required in order to discriminate between both kinds of motion. This combination of two interferometers is called an Atomic Sagnac Unit (ASU).

Unlike the Mach-Zehnder interferometer, the Ramsey-Bordé-configuration is designed to measure frequencies. It is based on atoms at rest which are split by a temporal sequence of four laser pulses retroreflected on one mirror such that two atom interferometers are formed. The frequency sensitivity is due to the asymmetry of the beam splitting. The part of the matter wave that is split off is excited and experiences the recoil shift, while the other part remains unaffected. In the two interferometers, the frequency shifts have opposite signs because the roles of the ground and excited states are reversed.

Scientific objectives

The primary scientific objectives of the Hyper mission are

— to test General Relativity by mapping for the first time the spatial (latitudinal) structure (magnitude and sign) of the gravitomagnetic (frame-dragging or Lense-Thirring) effect of the Earth with about 10% precision;
— independently from Quantum Electrodynamics (QED) theories, to determine the fine structure constant α by measuring the ratio of Planck's constant to the atomic mass one to two orders of magnitude more precise than present knowledge.

As a secondary objective, Hyper will investigate matter-wave decoherence to set an upper bound for quantum gravity models.

Atom interferometry also allows us test the Equivalence Principle with quantum particles by comparing the free fall of two distinct atomic species (rubidium and caesium). This measurement complements the Microscope and STEP missions, which will investigate the free-fall of macroscopic objects. Hyper's atom interferometer should reach an accuracy of about one part in 10^{16}. The mass and power constraints imposed by the satellite make it difficult to pursue both the measurement of the Lense-Thirring effect and a test of the Equivalence Principle. The test of the Equivalence Principle is therefore considered as an alternative objective.

Hyper carries four cold atom interferometers that can be operated either in the

For further information, see http://sci.esa.int/home/hyper

Mach-Zehnder mode or in the Ramsey-Bordé mode. For the measurement of the gravitomagnetic effect of the Earth, the four atom interferometers are used in the Mach-Zehnder mode. For the measurement of the fine structure constant, they are used in the Ramsey-Bordé mode. In space, the drift velocity of the atoms can be reduced to 20 cm/s, which gives 3 s of drift time in a 60 cm enclosure. The temperature of the atoms is 1K, corresponding to a thermal velocity of ~1 cm/s.

Spacecraft and payload

The Payload Module, with a mass of 240 kg and 200 W power consumption, consists essentially of the Optical Bench, carrying the:

— optical elements for coherent atom manipulation;
— high-precision star tracker (200 mm-diameter Cassegrain telescope, pointing accuracy 6×10^{-9} rad at 1 Hz readout frequency;
— two drag-free proof masses.

the Atom Preparation Bench, carrying the

— four atom interferometers based on caesium or rubidium accommodated in two magnetically-shielded vacuum chambers;
— optics for atom preparation and detection.

the Laser Bench, carrying the

— laser for atom interferometry, preparation (e.g. trapping, cooling) and detection of the atoms;
— high-precision microwave synthesiser for the hyperfine transitions of caesium or rubidium.

The Payload Module, a cylinder of 0.9 m diameter and 1.3 m height, is accommodated in the centre of the box-shaped Service Module. Together, they are the spacecraft, which has a launch mass of 767 kg. Hyper will be launched by a Rockot from Plesetsk Cosmodrome into a 700 km altitude, circular, Sun-synchronous orbit. Drag-free performance to a level of 10^{-9} m/s^{-2} at 0.3-3 Hz is achieved by a drag-free control system, comprising two drag-free proof masses and their capacitive sensors and 16 proportional Field Emission Electric Propulsion (FEEP) thrusters mounted externally, each with a thrust authority of 150 µN. Nominal mission lifetime is 2 years.

Status

Hyper was proposed to ESA in January 2000, in response to ESA's Call for Mission Proposals for the second and third Flexi-missions (F2/F3). It was selected for a study at assessment level, carried out from March - July 2000 by the Concurrent Design Facility Team at ESTEC. In its evaluation of the study, the Fundamental Physics Advisory Group (FPAG) concluded that 'Hyper is a mission in a completely new field of space science and has, therefore, not quite reached the technical maturity of other extensively studied projects. Also, the field of cold atoms and matter-wave interferometry is developing rapidly and thus the FPAG recommends not to select Hyper for a flight mission at this time (as one of the F2/F3 missions) but to continue studies of the Hyper mission and to initiate technology development in areas relevant for Hyper. The FPAG specifically recommends that ESA funds a follow-on study in 2001 with technical input from ESTEC and that ESA includes support for the relevant technical developments in the TRP/CTP programme from 2002 onwards.' The Space Science Advisory Committee and Scientific Programme Committee also adopted that view and, therefore, the FPAG recommendation is now being implemented by ESA. The Hyper industrial study is being carried out from June 2002 to January 2003.

Acronyms

AAT	Anglo-Australian Telescope
ACR	Anomalous Cosmic Rays
ACS	Advanced Camera for Surveys (HST)
ADS	Astrophysics Data System (NASA)
AFM	Atomic Force Microscope
AGB	Asymptotic Giant Branch
AGN	Active Galactic Nuclei
AGU	American Geophysical Union
AIV	Assembly, Integration & Verification
ALICE	Rosetta Orbiter UV imaging spectrometer
ALMA	Atacama Large Millimetre Array
AMIE	Asteroid Moon micro-Imager Experiment (SMART-1)
AO	Announcement of Opportunity
APXS	Alpha-Proton-X-ray Spectrometer (Rosetta)
ASI	Italian Space Agency
ASIC	Application Specific Integrated Circuit
ASPOC	Active Spacecraft Potential Control (Cluster)
ASU	Atomic Sagnac Unit
AU	Astronomical Unit
BeppoSAX	Satellite per Astronomia in raggi X (Italy/The Netherlands)
BiSON	Birmingham Solar Oscillations Network
BLR	Broad Line Region
c	speed of light
CADC	Canadian Astronomical Data Centre
CBRF	Cosmic Background Radiation Field
CCD	Charge Coupled Device
CDF	common data format
CDMS	Cluster Data Management System
CDR	critical design review
CDS	Coronal Diagnostics Spectrometer (SOHO)
CDS	Command & Data Subsystem
CDS	Centre de Données astronomiques de Strasbourg
CdTe	cadmium telluride
CELIAS	Charge, Element and Isotope Analysis System (SOHO)
CEPHAG	Centre d'Etude des Phenomenes Aleatoires et Geophysiques (France)
CERN	Centre Européen de Recherches Nucléaires (France)
CESR	Centre d'Etude Spatial des Rayonnements (France)
CFHT	Canadian-French-Hawaiian Telescope
CGRO	Compton Gamma Ray Observatory (NASA)
CIR	Corotating Interaction Region
CIS	Cluster Ion Spectrometry
CIVA	Comet Infrared and Visible Analyser (Rosetta)
CMB	Cosmic Microwave Background
CMD	colour magnitude diagram
CME	Coronal Mass Ejection
CMOS	Complementary Metal Oxide Semiconductor
CNES	Centre National d'Etudes Spatiales
CNR	Consiglio Nazionale della Ricercha (Italy)
CNRS	Centre National de la Recherche Scientifique (France)
CNSA	China National Space Administration
Co-I	Co-Investigator
COBE	Cosmic Background Explorer (NASA)
COMPTEL	Compton Telescope (CGRO)
CONSERT	Comet Nucleus Sounding Experiment by Radiowave Transmission (Rosetta)
COPUOS	Committee for the Peaceful Use of Outer Space (United Nations)
COROT	COnvection, ROtation and planetary Transits
COS	Cosmic Origins Spectrograph (HST)
COSAC	Comet Sampling and Composition Experiment (Rosetta)
COSIMA	Cometary Secondary Ion Mass Analyser (Rosetta)
COSPAR	Committee on Space Research
COSPIN	Cosmic Ray & Solar Charged Particles Investigation (Ulysses)
COSTEP	Comprehensive Measurements of the Supra-Thermal and Energetic Particles Populations (SOHO)
CP	Charge Parity
CR	Carrington Rotation
CSA	Canadian Space Agency
CSDS	Cluster Science Data System
CsI	caesium iodide
CSRC	Czech Space Research Centre
CSSAR	Centre for Space Science and Applied Research (China)
CTIO	Cerro Tololo Inter-American Observatory
CTP	Core Technology Programme
D-CIXS	Demonstration of a Compact Imaging X-ray Spectrometer (SMART-1)
D/SCI	Directorate of Scientific Programmes (ESA)
DESPA	Observatoire de Paris, Département Spatial
DISR	Descent Imager/Spectral Radiometer (Huygens)
DLR	Deutsches Zentrum für Luft- und Raumfahrt
DPC	Data Processing Centre
DROID	distributed readout architecture
DSN	Deep Space Network
DSP	Double Star Programme
DSP	Digital Signal Processor
DSRI	Danish Space Research Institute
D/TOS	Directorate of Technical and Operational Support (ESA)
DTP	Darwin Technology Package

EAS	European Astronomical Society
ECF	European Coordinating Facility
EECR	extreme energy cosmic ray
EFW	Electric Field and Wave experiment (Cluster)
EGS	European Geophysical Society
EIT	Extreme UV Imaging Telescope (SOHO)
EQM	Electrical Qualification Model
EM	Electrical Model, Engineering Model
EOF	Experiment Operations Facility (SOHO)
EP	Equivalence Principle
EPAC	energetic particle instrument (Ulysses)
EPDP	Electric Propulsion Diagnostic Package (SMART-1)
EPF	External Payload Facility (Columbus)
EPIC	European Photon Imaging Camera (XMM)
EPS	European Physical Society
ERNE	Energetic and Relativistic Nuclei and Electron experiment (SOHO)
ERO	Early Release Observation
ESA	European Space Agency
ESLAB	European Space Laboratory (former name of RSSD)
ESO	European Southern Observatory
ESOC	European Space Operations Centre, Darmstadt (Germany)
ESR	Emergency Sun Reacquisition (SOHO)
ESRIN	ESA's Documentation and Information Centre (Italy)
ESRO	European Space Research Organisation
ESTEC	European Space Research and Technology Centre, Noordwijk (The Netherlands)
EUSO	Extreme Universe Space Observatory
EUV	Extreme Ultra-Violet
Exosat	European X-ray Observatory Satellite (ESA)
FEEP	Field Emission Electric Propulsion
FES	Fine Error Sensor
FGS	Fine Guidance Sensor (HST)
FIRST	Far Infrared and Submillimetre Space Telescope (now Herschel)
FM	Flight Model
FMI	Finnish Meteorological Institute
FOC	Faint Object Camera (HST)
FOS	Faint Object Spectrograph (HST)
FOV	Field of View
FP	Fabry-Pérot
FPAG	Fundamental Physics Advisory Group
FTE	flux transfer event
FTS	Fourier Transform Spectrometer
FUV	far-ultraviolet
FWHM	Full Width at Half Maximum
GaAs	gallium arsenide
GAIA	Global Astrometric Interferometer for Astrophysics
GC	Galactic Centre
GI	Guest Investigator
GIADA	Grain Impact Analyser and Dust Accumulator (Rosetta)
GMT	Greenwich Mean Time
GONG	Global Oscillation Network Group
GR	General Relativity
GRB	Gamma Ray Burst
GSE	Ground Support Equipment
GSFC	Goddard Space Flight Center (NASA)
GSPC	Gas Scintillation Proportional Counter
GSTP	General Support & Technology Programme (ESA)
GTO	Geostationary Transfer Orbit
HASI	Huygens Atmospheric Structure Instrument
HCS	Heliospheric Current Sheet
HDF	Hubble Deep Field
HEB	Hot Electron Bolometer
HEW	Half Energy Width
HFI	High Frequency Instrument (Planck)
HGA	High-Gain Antenna
HIFI	Heterodyne Instrument for the Far-IR (Herschel)
HPGSPC	High Pressure Gas Scintillation Proportional Counter (BeppoSAX)
HPOC	Huygens Probe Operations Centre
HR	Hertzsprung-Russell
HRTS	High Resolution Telescope and Spectrograph
HSC	Herschel Science Centre
HST	Hubble Space Telescope
IAC	Instituto de Astrofisica de Canarias
IACG	Inter-Agency Consultative Group for Space Science
IAEA	International Atomic Energy Agency
IAP	Institute of Atmospheric Physics (Czech Republic)
IAS	Institut d'Astrophysique Spatiale, Orsay (France)
IAS	Istituto di Astrofisica Spaziale (Rome)
IASTP	Inter-Agency Solar-Terrestrial Physics
IAU	International Astronomical Union
IBDR	instrument baseline design review
IBIS	Integral imager
ICC	Instrument Control Centre (Herschel)
IDA	ISO Data Archive
IDC	ISO Data Centre
IDS	Interdisciplinary Scientist
IDT	Instrument Dedicated Team
IFSI	Istituto Fisica Spazio Interplanetario (Italy)
IFTS	Imaging Fourier Transform Spectrometer

IGPP	Institute of Geophysics & Planetary Physics
ILEWG	International Lunar Exploration Working Group
ILWS	International Living With a Star
IMEWG	International Mars Exploration Working Group
IMF	Initial Mass Function
IMF	Interplanetary Magnetic Field
INT	Isaac Newton Telescope
INTA	Instituto Nacional de Técnica Aerospacial (Spain)
IOA	Institute of Astronomy (Cambridge, UK)
IPAC	Infrared Processing Analysis Centre
IR	Infrared
IRAS	Infrared Astronomy Satellite
IRF-U	Institute for Space Physics-Uppsala (Sweden)
IRSI	InfraRed Space Interferometer
ISAAC	Infrared Spectrometer and Array Camera
ISAS	Institute of Space and Astronautical Science (Japan)
ISDC	Integral Science Data Centre
ISGRI	Integral Soft Gamma Ray Imager
ISL	Instrument Sonde de Langmuir
ISM	Interstellar Medium
ISO	Infrared Space Observatory (ESA)
ISOC	Integral Science Operations Centre
ISS	International Space Station
ISSI	International Space Science Institute, Bern (Switzerland)
ISTP	International Solar-Terrestrial Physics
ITT	Invitation to Tender
IUE	International Ultraviolet Explorer
IUPAP	International Union of Pure and Applied Physics
IUS	Inertial Upper Stage
JCMT	James Clark Maxwell Telescope
JEM-X	Integral X-ray monitor
JPL	Jet Propulsion Laboratory (NASA)
JSOC	Joint Science Operation Centre (Cluster)
KATE	X/Ka-band Telemetry & Telecommand Experiment (SMART-1)
KSC	Kennedy Space Center (NASA)
LAEFF	Laboratory for Space Astrophysics and Fundamental Physics
LAP	Langmuir Probe (Rosetta)
LAPP	Laboratoire d'Annecy-Le-Vieux de Physique des Particules (CNRS, France)
LASCO	Large Angle Spectroscopic Coronagraph (SOHO)
LASP	Laboratory for Astronomy and Solar Physics (NASA)
LET	Low Energy Telescope (Ulysses)
LFCTR	Laboratorio di Fisica Cosmica e Techologie Relative del CNR (Italy)
LFI	Low Frequency Instrument (Planck)
LIM	local interstellar medium
LISA	Laser Interferometer Space Antenna
LMC	Large Magellanic Cloud
LOI	Luminosity Oscillation Imager (SOHO)
LOWL	Ground-based instrument for observing solar low *p*-modes, High Altitude Observatory, USA
LPCE	Laboratoire de Physique et Chemie, de l'Environnement (France)
LPSP	Laboratoire de Physique Stellaire et Planétaire (France)
LTP	LISA Technology Package
LWS	Long Wavelength Spectrometer (ISO)
MBH	massive black hole
MCP	Microchannel Plate
MDC	Mars Dust Counter
MDI	Michelson Doppler Imager (SOHO)
Microscope	MICROSatellite à traînée Compensée pour l'Observaton du Principe d'Equivalence (CNES)
MIDAS	Micro-Imaging Dust Analysing System (Rosetta)
MIP	Mutual Impedance Probe (Rosetta)
MIRO	Microwave Instrument for the Rosetta Orbiter (Rosetta)
MMO	Mercury Magnetospheric Orbiter (BepiColombo)
MOC	Mission Operations Centre
MOS-CCD	Metal Oxide Semiconductor - Charge Coupled Device
MoU	Memorandum of Understanding
MPAE	Max-Planck-Institut für Aeronomie
MPE	Max-Planck-Institut für Extraterrestrische Physik
MPI	Max-Planck Institut (Germany)
MPIA	MPI für Astronomie
MPIK	Max-Planck-Institut für Kernphysik
MPO	Mercury Planetary Orbiter (BepiColombo)
MSE	Mercury Surface Element (BepiColombo)
MSSL	Mullard Space Science Laboratory (UK)
MTR	mid-term review
MUPUS	Multi-Purpose Sensors for Surface and Subsurface Science (Rosetta)
MUSICOS	Multi-Site Continuous Spectroscopy
NAC	Narrow Angle Camera (OSIRIS)
NASA	National Aeronautics & Space Administration (USA)
NFI	Narrow Field Instrument (BeppoSAX)
NGST	Next Generation Space Telescope
NHSC	NASA Herschel Science Centre
NICMOS	Near-Infrared Camera and Multi-Object Spectrometer (HST)
NIS	normal incidence spectrometer

NLR	Narrow Line Region
NOT	Nordic Optical Telescope
NRAO	National Radio Astronomy Observatory (USA)
NSSDC	National Space Science Data Center (at GSFC, USA)
NTT	New Technology Telescope
NVSS	NRAO/VLA Sky Survey
OHP	Observatoire de Haute-Provence
OLP	off-line processing
OM	Optical Monitor (XMM-Newton)
OMC	Optical Monitor Camera (Integral)
OSIRIS	Optical and Spectroscopic Remote Imaging System (Rosetta)
PACS	Photodetector Array Camera and Spectrometer (Herschel)
PAH	Polycyclic Aromatic Hydrocarbon
PAM	Payload Assist Module
PARCS	Primary Atomic Reference Clock in Space
pc	parsec
PCA	Proportional Counter Array
PCD	Photon Counting Detector
PDP	Project Data Base
PDR	preliminary design review
PDS	Planetary Data System
PEN	penetrator
PI	Principal Investigator
PIA	(ISO)PHOT Interactive Analysis
PLM	Payload Module
PN	Planetary Nebula
PP	Permittivity Probe (SESAME on Rosetta)
PPDB	Primary Parameter Data Base (Cluster)
ppm	parts per million
PPN	Parameterised Post-Newtonian
PROM	Programmable Read-Only Memory
PS	Project Scientist
PSE	Probe Support Equipment (Huygens)
PSF	Point Spread Function
PWA	Permitivity, Waves and Altimetry (part of HASI on Huygens)
QM	Qualification Model
QPO	Quasi Periodic Oscillations
QSO	Quasi Stellar Object
R&D	Research and Development
RAL	Rutherford Appleton Laboratory (UK)
RF	Radio Frequency
RGS	Reflection Grating Spectrometer (XMM-Newton)
RMOC	Rosetta Mission Operations Centre
ROLIS	Rosetta Lander Imaging System
ROMAP	RoLand Magnetometer & Plasma Monitor (Rosetta)
ROSINA	Rosetta Orbiter Spectrometer for Ion and Neutral Analysis (Rosetta)
RPC	Rosetta Plasma Consortium
RSI	Radio Science Investigation
RSOC	Rosetta Science Operations Centre
RXTE	Rossi X-ray Timing Explorer (NASA)
SAO	Smithsonian Astrophysical Observatory (US)
SAp/Saclay	Service d'Astrophysique (Commissariat à l'Energie Atomique; Saclay, France)
SAS	Scientific Analysis System (XMM-Newton)
SAX	Satellite per Astronomia in raggi X (Italy/The Netherlands)
SEPP	Solar Electric Primary Propulsion
SESAME	Surface Electric, Seismic and Acoustic Monitoring Experiment (Rosetta)
SiC	silicon carbide
SIS	Superconductor-Insulator-Superconductor
SLAMP	Short Large Amplitude Magnetic Pulsation
SLP	Segmented Langmuir Probe
SMART	Small Mission for Advanced Research in Technology (ESA)
SMC	Small Magellanic Cloud
SMOG	Survey of Molecular Oxygen in the Galaxy (SMART-1)
SN	Supernova
SNR	Supernova Remnant
SOC	Science Operations Centre
SOHO	Solar and Heliospheric Observatory
SOPC	Science Operations & Planning Computer
SOS	Silicon-on-Sapphire
SOT	Science Operations Team
SPC	Science Programme Committee (ESA)
SPDB	Secondary Parameter Data Base (Cluster)
SPEDE	Spacecraft Potential, Electron & Dust Experiment (SMART-1)
SPI	Integral spectrometer
SPIRE	Spectral and Photometric Imaging Receiver (Herschel)
SQUID	Superconducting Quantum Interference Device (STEP)
SRON	Space Research Organisation Netherlands
SRR	system requirements review
SSAC	Space Science Advisory Committee (ESA)
SSP	Surface Science Package (Huygens and Rosetta)
SSWG	Solar System Working Group
ST	Science Team; Space Technology (NASA)
ST-ECF	Space Telescope European Coordinating Facility
STEP	Satellite Test of the Equivalence Principle
STIS	Space Telescope Imaging Spectrograph

STJ	Superconducting Tunnel Junction
STScI	Space Telescope Science Institute
STSP	Solar Terrestrial Science Programme
SUMER	Solar UV Measurements of Emitted Radiation (SOHO)
SWAN	Solar Wind Anisotropies (SOHO)
SWS	Short Wavelength Spectrometer (ISO)
SWT	Science Working Team
TPF	Terrestrial Planet Finder (NASA)
TRACE	Transition Region & Coronal Explorer (NASA)
TRP	Technology Research Programme (ESA)
UCB	University of California Berkeley
UCLA	University of California Los Angeles
UV	Ultraviolet
UVCS	Ultraviolet Coronal Spectrometer (SOHO)
VILSPA	Villafranca Satellite Tracking Station
VIRGO	Variability of Irradiance and Gravity Oscillations (SOHO)
VIRTIS	Visible Infra Red Thermal Imaging Spectrometer (Rosetta)
VLA	Very Large Array
VLBI	Very Long Baseline Interferometry
VLT	Very Large Telescope
WAC	Wide Angle Camera (OSIRIS on Rosetta)
WEC	Wave Experiment Consortium (Cluster)
WFC	Wide-Field Camera
WFE	wavefront error
WFPC	Wide-Field Planetary Camera (HST)
WHT	William Herschel Telescope
WWW	World Wide Web
XEUS	X-ray Evolving Universe Spectroscopy mission (ESA)
XMM	X-ray Multi-Mirror Mission (ESA)